THE UNIVERSITY OF QUEENSLAND

AUSTRALIA

Mechanisms of 2,4-Dinitrochlorobenzene-induced acute inflammation in Human Papillomavirus type 16 E7 oncoprotein expressing skin

Le Son Tran

Bachelor of Biomedical Science/ Master of Genetics

A thesis submitted for the degree of Doctor of Philosophy at

The University of Queensland in 2014

The University of Queensland Diamantina Institute

Abstract

Persistent infection with oncogenic human papillomaviruses (HPV), particularly HPV16, is associated with selective expression of two virally encoded proteins (E6 and E7). One action of HPV16.E7 protein is to subvert the innate immune system through the down-regulation of IFNγ pathways, modulation of antigen presentation, and suppression of Toll-like receptor 9 protein.

K14.E7 transgenic mice, which express HPV16.E7 oncoprotein within basal keratinocytes under the control of the keratin 14 transcriptional promoter, have been extensively used as a model of HPV oncoprotein–induced immune suppression associated with human squamous cancers, in which only the *E6* and *E7* genes of the papillomavirus are expressed. It has previously been shown that skin grafts expressing HPV16.E7 oncoprotein are not spontaneously rejected when transplanted onto syngeneic animals, but they are rejected when certain components of the innate immune system are unavailable, confirming that the expression of HPV16.E7 in the epithelium results in the establishment of a local suppressive environment and the subversion of antigen-specific T cells. Therefore, successful strategies targeting HPV-associated cancer need to circumvent or disrupt the local suppressive environment.

Topical immunotherapy with immunostimulatory agents has been used clinically to treat cancerous lesions including squamous cell and basal cell carcinoma in immunocompetent and immunosuppressed patients. Topical application of 2,4-dinitrochlorobenzene (DNCB) is an effective therapy for condylomata acuminata caused by HPV infection. DNCB induced the complete clearance of HPV-associated warts in 13/15 patients. However, the use of DNCB for treatment has been discouraged because of its mutagenic potential. The aim of my doctoral research is to understand the mechanism of DNCB-induced inflammation in K14.E7 transgenic mice which has been poorly understood. I hypothesized that understanding how induction of a vigorous acute inflammatory response by DNCB can break the local immune-suppressive environment and restore the effector function of adaptive immunity might lead to more acceptable treatments for persisting HPV infection. In support of this hypothesis, the present study showed that DNCB application along with E7 specific immunization therapy was capable of inducing HPV16.E7 skin graft rejection.

Arginase, which metabolizes l-arginine to *N*-ornithine and urea, has been identified as a crucial regulator of inflammation. As inflammation decides the fate of HPV infection and arginase is an important regulator of inflammation and immunity, I investigated the

interaction between DNCB-induced inflammation and HPV16.E7 protein in the induction of arginase in K14.E7 transgenic mice. The first part of this study showed that topical DNCB application to skin expressing HPV16.E7 as a transgene induces a hyperinflammatory response, which is not seen in nontransgenic control animals. The E7-associated inflammatory response was characterized by enhanced expression of Th2 cytokines and increased infiltration of $CD11b^{+}Gr1^{int}F4/80^{+}Ly6C^{hi}Ly6G^{low}$ myeloid cells, producing arginase-1. Inhibition of arginase with an arginase-specific inhibitor, N(omega)-hydroxy-nor-L-arginine, ameliorated the DNCB-induced inflammatory response.

Furthermore, Th2 cytokines but not Th1 cytokines are induced in K14.E7 skin and these cytokines have been well-known as potent inducers of arginase-1 production in macrophages. In the second part of my study, I demonstrated that neutralization of these cytokines did not change the level of arginase activity in bone marrow-derived macrophages cultured in DNCB treated K14.E7 skin explant supernatant, suggesting that IL-4 and IL-10 might not be necessary for the induction of arginase activity in DNCB treated K14.E7 skin. Interestingly, IL-17A, an important proinflammatory cytokine, was also induced in K14.E7 mice but not in wild-type nontransgenic mice and $CD11b^{+}F4/80^{+}$ but not lymphocytes are the major producer of IL-17A in DNCB treated K14.E7 skin. Importantly, IL-17A deficient K14.E7 mice express diminished arginase activity and develop an alleviated inflammatory response to DNCB. Furthermore, I demonstrated that the induction of arginase-1 is independent of adaptive immunity. Thus, IL-17A produced by macrophage is responsible for enhanced arginase-1 expression in these cells.

Taken together, my study suggests that HPV16.E7 protein enhances DNCB associated-production of IL-17A which mediates arginase-1 production by inflammatory monocytes (Macrophages) and consequent inflammatory cellular infiltration of the skin. Thus, these findings provide insights into the pro-inflammatory roles of IL-17A and arginase-1 axis in HPV16.E7 expressing skin in response to immunostimulation by DNCB, and imply a potential immune-based therapy strategy to break the tolerance to HPV persistent infection by modulating IL-17A/arginase-1 axis.

Declaration by author

This thesis is composed of my original work, and contains no material previously published or written by another person except where due reference has been made in the text. I have clearly stated the contribution by others to jointly-authored works that I have included in my thesis.

I have clearly stated the contribution of others to my thesis as a whole, including statistical assistance, survey design, data analysis, significant technical procedures, professional editorial advice, and any other original research work used or reported in my thesis. The content of my thesis is the result of work I have carried out since the commencement of my research higher degree candidature and does not include a substantial part of work that has been submitted to qualify for the award of any other degree or diploma in any university or other tertiary institution. I have clearly stated which parts of my thesis, if any, have been submitted to qualify for another award.

I acknowledge that an electronic copy of my thesis must be lodged with the University Library and, subject to the policy and procedures of The University of Queensland, the thesis be made available for research and study in accordance with the Copyright Act 1968 unless a period of embargo has been approved by the Dean of the Graduate School.

I acknowledge that copyright of all material contained in my thesis resides with the copyright holder(s) of that material. Where appropriate I have obtained copyright permission from the copyright holder to reproduce material in this thesis.

Publications during candidature

Peer-reviewed articles

1. Mittal D, Kassianos AJ, **Tran LS**, Bergot AS, Gosmann C, Hofmann J, et al. (2013) Indoleamine 2,3-dioxygenase activity contributes to local immune suppression in the skin expressing human papillomavirus oncoprotein e7. J Invest Dermatol 133:2686-94.

2. Bergot AS, Monnet N, **Tran LS**, Mittal D, Al-Kouba J, Steptoe RJ, Grimbaldeston MA, Frazer IH, Wells JW. HPV16-E7 Expression in Squamous Epithelium induces TSLP-1 secretion, type 2 ILC infiltration, and development of atopic dermatitis-like lesions. Paper accepted for publication by Journal of Immunology and Cell biology.

3. **Tran LS**, Bergot AS, Mattarollo SR, Mittal D, Frazer IH. Human Papillomavirus E7 oncoprotein transgenic skin develops an enhanced inflammatory response to 2,4-Dinitrochlorobenzene by an arginase-1 dependent mechanism (2014). *Journal of Investigative Dermatology* (2014) **134,** 2438–2446; doi:10.1038/jid.2014.186; published online 29 May 2014.

4. **Tran LS**, Mittal D, Mattarollo SR, Frazer IH. Interleukin-17A Promotes Arginase-1 Production And DNCB-Induced Acute Hyperinflammation In Human Papillomavirus E7 Oncoprotein Expressing Skin. Submitted for publication

Oral Presentations

1. **Tran LS**., Bergot AS, Mattarollo S.R, Mittal D, Frazer IH (October 2013). Arginase-1 mediates a hyperinflammatory response to DNCB in the skin expressing HPV E7 oncoprotein. 2013 International Postgraduate Symposium in Biomedical Sciences, University of Queensland.

2. **Tran LS**, Bergot AS, Mattarollo S.R, Mittal D, Frazer IH (August 2013). Human Papillomavirus E7 oncoprotein transgenic skin develops an enhanced inflammatory response to 2,4-Dinitrochlorobenzene by an arginase-1 dependent mechanism. Brisbane Immunology Group Retreat 2013.

Poster Presentations

1. **Tran LS**, Bergot AS, Mattarollo S.R, Mittal D, Frazer IH. IL-17A mediates arginase-1-dependent hyperinflammatory response to DNCB in HPV16 E7 expressing skin (December 2013), 43rd Annual Scientific meeting Australasian Society for Immunology 2013, Wellington, New Zealand.

2. **Tran LS**, Bergot AS, Mittal D, Frazer IH. Arginase-1 mediates DNCB-induced hyperinflammation in HPV16.E7 transgenic skin (November 2013). 16th EMBL International PhD Symposium, Heidelberg, Germany.

3. **Tran LS**, Bergot AS, Mattarollo S.R, Mittal D, Frazer IH (January 2014). HPV E7 oncoprotein induces arginase-1 expression in macrophage resulting in a hyperinflammatory response to DNCB. Keystone symposium: Innate Immunity to Viral Infection, Colorado, USA.

Publications included in this thesis

1. **Tran LS**, Bergot AS, Mattarollo SR, Mittal D, Frazer IH. Human Papillomavirus E7 oncoprotein transgenic skin develops an enhanced inflammatory response to 2,4-Dinitrochlorobenzene by an arginase-1 dependent mechanism (2014). *Journal of Investigative Dermatology* (2014) **134,** 2438–2446; doi:10.1038/jid.2014.186; published online 29 May 2014. Incorporated as **Chapter 2**.

Contributor	Statement of contribution
Le Son Tran (Candidate)	Designed experiments (80%) Performed experiments (95%) Analyzed results (95%) Interpreted results (75%) Wrote and edited the paper (100%)
Anne-Sophie Bergot	Performed experiment (5%) Analyzed results (5%)
Stephen Mattarollo	Interpreted results (5%) Critical review of paper (10%)
Deepak Mittal	Design experiment (10%) Interpreted results (10%) Critical review of paper (40%)
Ian Frazer	Designed experiments (10%) Critical review of paper (50%) Interpreted results (10%)

Contributions by others to the thesis

Prof. Ian Frazer, Dr. Stephen Mattarollo and Dr. Deepak Mittal made significant contributions to: the conception and design of the project; non interpretation of research data and critical revision of the thesis. Prof. Ranjeny Thomas provided anti-IL-17A neutralizing antibody and matched-isotype control antibody.

Statement of parts of the thesis submitted to qualify for the award of another degree

None

Acknowledgements

First and foremost, I would like to express my sincere gratitude to my principal supervisor, Prof. Ian Frazer, for offering me a precious opportunity to undertake my postdoctoral study in an excellent academic environment. It has been a great honor and privilege to be his student. Furthermore, this thesis would not have been possible without his patient guidance, great support and encouragement at all times.

The insights, support, and friendship of my associated supervisors, Dr. Deepak Mittal and Dr. Stephen Mattarollo, have been invaluable on both academic and personal level, for which I am extremely grateful.

I would like to extend my gratitude to my thesis committee members, Prof. Nicholas Saunders, Dr. Kate Stacey and Dr. Germain Fernando, for providing me constructive criticism and advices through my degree milestones. In particular, I am thankful to Dr. Stacey Coles for proofreading my thesis and providing feedback.

I would like to acknowledge the financial support of the University of Queensland Diamantina Institute as well as technical assistance of staffs from TRI Biological Resource Facility and core facility.

My time in Brisbane would not have been enjoyable and memorable without my labmates (Michelle, Alan, Tam Nguyen, Thao); my colleagues (Anne-Sophie, Rohit, Lynn); housemate (Takumi) and best friends (Bao Chi, Tam Duong, Anh).

I am grateful to my teacher in Vietnam, Prof. Duong Ho, for endlessly inspiring my love for biomedical research.

Last, but not least, I wish to thank my family and friends in Vietnam, the United States and Korea for their love and encouragement throughout my life.

Keywords

DNCB, HPV, E7, skin, acute inflammation, immunosuppression, arginase-1, IL-17A, macrophage, immunotherapy.

Australian and New Zealand Standard Research Classifications (ANZSRC)

ANZSRC code: 110707, Innate Immunity, 80%
ANZSRC code: 111204, Cancer Therapy (excl. Chemotherapy and Radiation Therapy), 20%

Fields of Research (FoR) Classification

FoR code: 1107, Immunology, 80%
FoR code: 1112, Oncology and Carcinogenesis, 20%

Table of Contents

List of Figures and Tables

CHAPTER 1: Introduction

CHAPTER 2: HPV E7 Oncoprotein Transgenic Skin Develops An Enhanced Inflammatory Response To DNCB By Arginase-1-Dependent Mechanism

CHAPTER 3: IL-17A Mediates Arginase-1 induction and DNCB-induced inflammation in HPV16.E7 expressing skin

CHAPTER 4: Discussion and Conclusion

List of Abbreviations

ABH	2(S)-amino-6-boronohexonic acid
APC	Antigen presenting cell
Arginase	Arg
BCG-HSP	Bacillus Calmette–Guérin and 71-kDa heat shock proteins
BMDM	Bone marrow-derived macrophage
CIN	Cervical intraepithelial neoplasia
COX-2	Cyclooxygenase-2
CTL	Cytolytic T cell
DCs	Dendritic cells
DMEM	Dulbecco's Modified Eagle Medium
DNCB	2,4-Dinitrochlorobenzene
DNFB	2,4-Dichloronitrobenzene
eIF2α	Eukaryotic initiation factor 2 alpha
eIF2β	Eukaryotic initiation factor 2 beta
FBS	Fetal bovine serum
GCN2	General control nonderepressible 2
GDP	Guanosine diphosphate
GM-CSF	Granulocyte macrophage colony-stimulating factor
GTP	Guanosine triphosphate
HEPES	4-(2-hydroxyethyl)-1-piperazineethanesulfonic acid
HPV	Human Papillomavirus
HSIL	High-grade Squamous Intraepithelial
i.p	Intraperitoneal injection
ICAM-1	Intercellular Adhesion Molecule 1
IFN	Interferon
IL	Interleukin
iNKT	Invariant Natural killer T cell
iNOS	Inducible nitric oxide synthase
IRF1	Interferon regulatory factor-1
K14.E7	Mice which express HPV type 16 E7 oncoprotein under the control of the keratin 14 transcriptional promoter
KC	Keratinocyte
LCs	Langerhand cells

LPS	Lipopolysaccharide
MCP-1	Monocyte chemoattractant protein-1
MDSC	Myeloid-derived suppressive cell
MHC	Major histocompatibility complex
MYD88	Myeloid differentiation primary response gene
NALP3	NACHT, LRR and PYD domains-containing protein 3
NF-κB	Nuclear factor-kappaB
NO	Nitric oxide
Nor-NOHA	Alpha-amino acid N(omega)-hydroxy-nor-l-arginine
OAT	Ornithine aminotransferase
ODC	Ornithine decarboxylase
ORFs	Open reading frames
PAMP	Pathogen-associated molecular patterns
PBS	Phosphate buffered saline
PGE2	Prostaglandin E2
pRB	Retinoblastoma protein
PRR	Pattern recognition receptors
Ptge2s	Prostaglandin E2 synthase
RNS	Reactive nitrogen species
RoRγt	RAR-related orphan receptor gamma
ROS	Reactive oxygen species
SCC	Squamous cell carcinoma
STAT	Signal transducer and activator of transcription
TAP	Transporter associated with antigen processing proteins
TCR	T cell receptor
TGF-β	Transforming growth factor beta
Th cells	T helper cells
TLR	Toll-like receptors
TNF	Tumor necrosis factor
TRAIL	TNF-Related Apoptosis-Inducing Ligand
Treg	Regulatory T cells
VCAM-1	Vascular cell adhesion molecule 1

CHAPTER 1

Introduction

1.1 Human Papillomavirus-an oncogenic virus

1.1.1 HPV-associated cancers

Human Papillomavirus (HPV) infection is an etiological factor for approximately 5.2% of all types of cancer. Based on tissue distribution, HPVs are classified into two major genera: α and β genus (1).

The α-HPV genus, also referred to as mucosal HPV, can be detected mostly in the epithelium of the genital tract. HPVs in this genus are further grouped into low-risk and high-risk types dependent on their potential to cause cancer. Infection with low-risk types (such as HPV6, HPV11) results in genital warts, which are benign and unlikely to develop into cancer. In contrast, high-risk HPV types are responsible for the development of pre-neoplastic and malignant lesions of the uterine cervix, anus, vulva, penis and orophary. Particularly, HPV16 and HPV18 account for 70% of cervical cancer cases worldwide (1). Furthermore, high-risk HPV types are also associated with head and neck squamous cell carcinoma (SCC) (2).

The β-HPV genus (such as HPV5, HPV8), known as cutaneous HPV, causes common warts and might lead to cutaneous SCC (3). It has been well documented that β-HPV types (HPV 5 and 8) are associated with epidermodysplasia verruciformis, a rare autosomal recessive skin disorder (4). Furthermore, cutaneous HPV types might be cofactors in the early onset of cutaneous SCC. A recent study using a meta-analysis approach reported that cutaneous SCC were more likely to carry HPV than normal skin and higher prevalence of HPV was detected in keratinocyte tumors from immunosuppressed patients than those from immunocompetent patients (5). Nonetheless, the association of other HPV types and SCC remained debatable as HPVs are undetectable in SSC in some studies and further studies are required to dissect the role of HPV in skin cancers (6).

1.1.2 Exclusively intra-epithelial infectious cycle of HPV

The genome of HPV is a circular double-stranded DNA molecule consisting of around 8,000 base pairs and up to ten (generally 8) open reading frames (ORFs). These ORFs in HPV16 encode two structural proteins (L1 and L2) and six nonstructural proteins (E1, E2 and E4-E7) (7). HPV particles enter undifferentiated stem cells in the basal layer of the stratified epithelium through microabrasion of the epithelium and establish stable

episomal genome in these cells. Briefly, HPV virions are unable to bind directly to basal cells rather they must first bind via their L1 capsid proteins to heparan sulfate proteoglycans on segments of the basement membrane after epithelial disruption. This process results in a conformation change, leading to exposure of L2 capsid N-treminus to furin cleavage site. Following L2 proteolysis, a previously unexposed surface of L1 binds to an unindentified secondary receptor on keratinocytes, facilitating endocytosis and the invasion of virions (8).

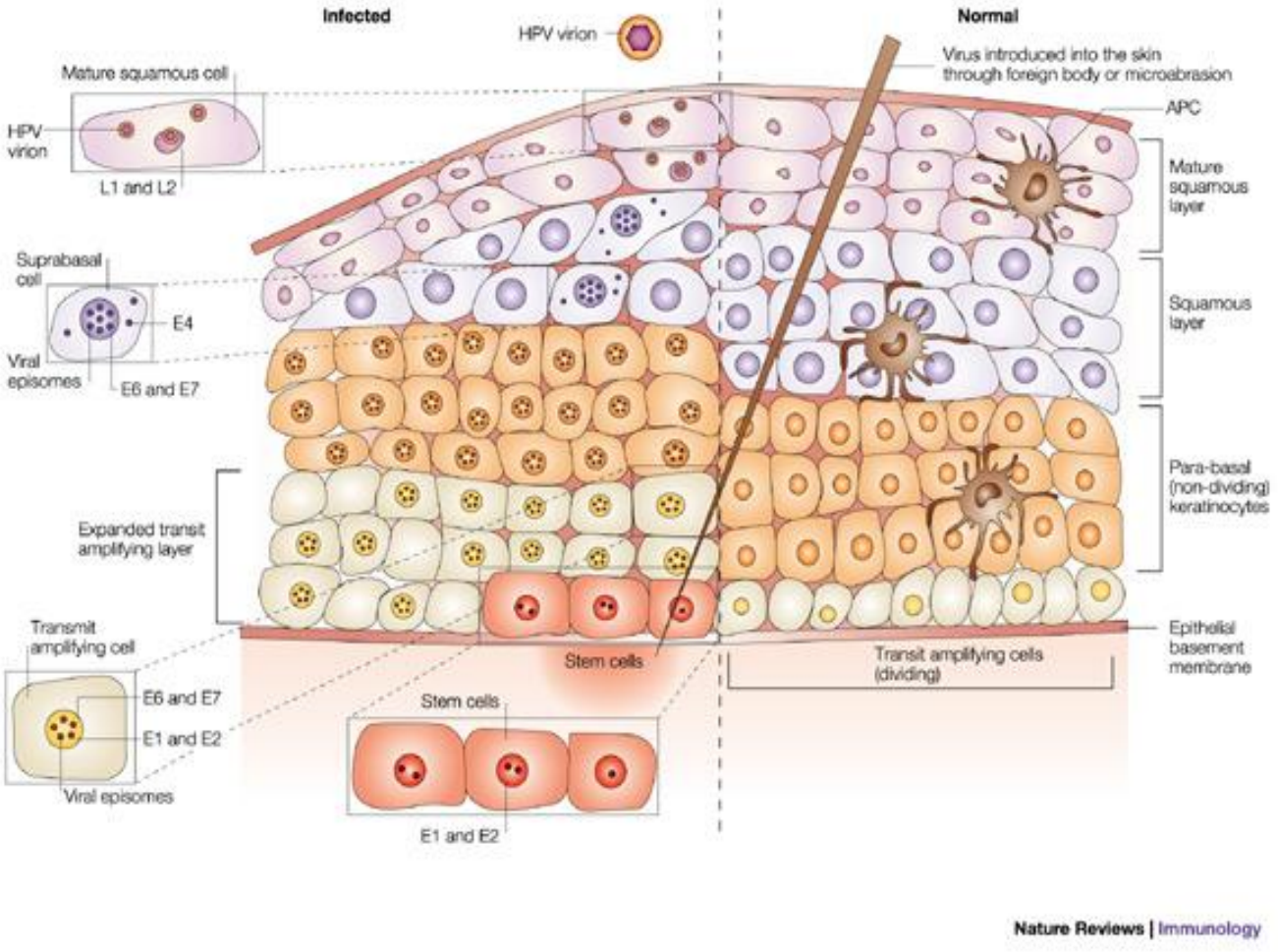

Figure 1.1- HPV exclusively infects the epithelium. HPV life cycle begins with the infection of stem cells in the basal layer. Infected cells migrated vertically to suprabasal layers where virus genome amplification is initiated before the production of complete virions. APC: antigen presenting cells. Adapted from (9).

As the infected cells migrate to the proliferative suprabasal layer, viral early proteins are expressed to initiate viral DNA replication. At this stage, the expression of E6 and E7 oncoproteins is tightly controlled and viral DNA replication is maintained at low level (50-100 copies per cells) (Figure 1.1). When these cells reach the upper differentiated

compartment of the stratum spinosum and granulosum, the oncogenic HPVs have the ability to integrate their own genome into the human chromosome, resulting in a remarkable induction of E6 and E7 genes in carcinomas and many cases of high-grade squamous intraepithelial lesion (HSIL). Additionally, structural proteins (L1 and L2) are also produced to form the viral capsids which are packaged into mature infectious virions along with replicated genomes (1).

1.1.3 HPV carcinogenesis

Two nonstructural proteins (E6 and E7) from HPV types that are strongly associated with risk of cervical cancer ("high risk" HPVs including HPV16 and HPV18) are capable of interacting with a number of cellular proteins, particularly tumor suppressors including p53 and retinoblastoma protein (pRB) respectively, thereby inducing genomic instability, accumulation of oncogene mutations and loss of cell-growth control (10, 11). In addition, these nonstructural proteins are consistently expressed in premalignant cancer and strongly expressed in invasive cancer associated with high risk HPVs (12). Indeed, E6 and E7 proteins have been shown to be involved not only in the regulation of viral replication and transcription, but also in the modulation of the host immune response to HPV infection (13).

In summary, infection with high risk HPVs displays tropism towards squamous epithelium and results in overexpression of E6 and E7 oncoproteins that cause epidermal hyperplasia and carcinoma.

1.2 Natural immune response to HPV infection and HPV-mediated immunosuppression

1.2.1. Natural immune response to HPV infection

The majority of HPV infections (80%) regress spontaneously, which is likely to be as a consequence of an effective immune response (Figure 1.2) (2). Regression of HPV-induced lesions is strongly associated with the infiltration of virus specific T cells including $CD4^+$ and $CD8^+$ T cells, supporting a role for a cell-mediated immune response in lesion regression (15). $CD8^+$ T cells are thought to produce Th1 cytokines, particularly IFNγ and exert cytolytic effects on target cells through MHC class I (MHCI) (16). Likewise, $CD4^+$ T cells also secrete IFNγ but these cells can induce apoptosis via ligation of death receptors

with Fas or TRAIL (17). It has been reported that the cell-mediated immune response against HPV-derived proteins such as E2, E6 and E7 is of critical importance in the eradication of virus infection and lesion regression (18). The cell-mediated immunity is closely followed by humoral response in which B cells are stimulated by antigen presenting cells (APC) and $CD4^+$ helper T cells to produce antibodies against major coat L1 protein (19). However, infected patients develop weak or no antibody responses to viral L2 protein and oncoproteins including E2, E6, E7 (20).

In approximately 10% to 20% of infections, HPVs have skewed the host innate immune response towards chronic inflammation that facilitates their persistent infection and eventually invasive cancer (2). Accumulating evidence suggests that the establishment of HPV persistent infection and eventually invasive cancer is associated with virus-induced immunosuppressive mechanisms. The immunosuppressive mechanisms of HPV impact on different stages of innate and adaptive immunity including cytokine production, cross-presentation of antigens and antibody response (21).

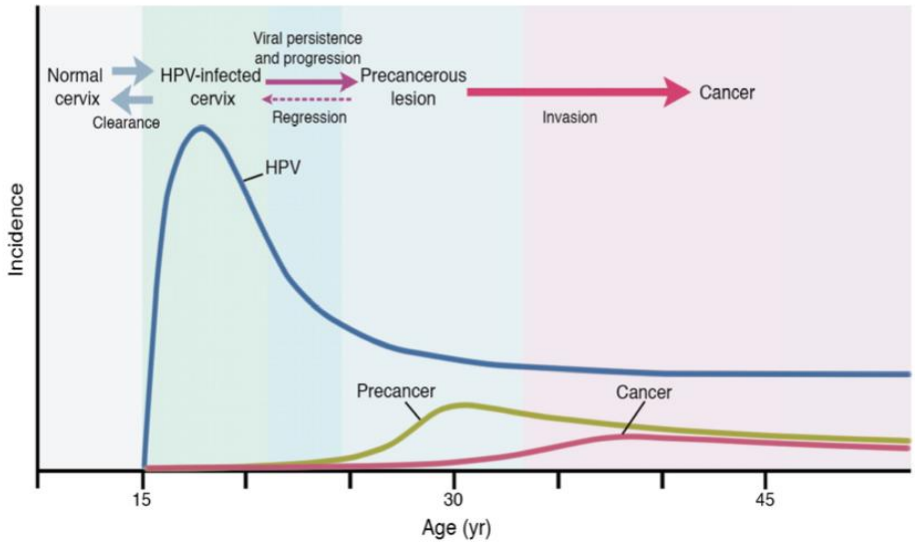

Figure 1.2- The progression of HPV associated cervical cancer. Approximately 80% of HPV infections regress spontaneously by effective immune responses. 10%-20% of HPV infections progress to persistent infection and ultimately become invasive cancers. Adapted from (14).

1.2.2 Modulation of epithelial innate immunity by HPV

HPV infection and replication is restricted to the squamous epithelial tissues which cover the cavities and surfaces of the body including skin, gut, lung and genital tracts, and

which function as immune barriers against pathogens (1). The skin is subdivided into two distinct compartments, the epidermis and dermis. The epidermis is comprised of 95% keratinocytes (KCs) which act as sentinels of innate immunity through their ability to detect pathogens, secrete cytokines or become non-professional antigen presenting cells (9, 18).

HPV has developed several strategies to evade the immune defenses. Firstly, as the virus life circle is strictly dependent on the differentiation program of epithelial cells, it is rare to detect HPV in other tissues other than squamous epithelial cells (1). This helps minimise the exposure of HPV antigens to the host immune system. Further, the virus does not cause cell death or inflammation during DNA replication, virion assembly and release process. Moreover, the expression of HPV E7 oncoprotein is restricted to the nucleus of keratinocytes where it is inaccessible for APC. In addition, the expression of viral late proteins (L1 and L2) is maintained at moderate levels and restricted to the differentiated superficial cell layers which are programmed to undergo apoptosis, thereby evading immune surveillance (2, 21).

Furthermore, HPVs can dampen the generation of anti-viral cytokines by KCs. KCs express Toll-like receptors (TLRs) which can detect the presence of pathogens via the recognition of pathogen-associated molecular patterns (PAMPs). The recognition of viral infection is followed by the release of numerous proinflammatory cytokines that are required for the elimination of pathogens. HPV-16 E6 and E7 oncoproteins have been shown to inhibit the expression of TLR9 which is an important TLR sensing dsDNA virus infection (22). As a result, the majority of HPV infection is silent and inaccessible for immune recognition.

Activation of TLR signaling in KCs results in type I IFN induction which is crucial for antiviral responses. The E6 and E7 oncoproteins of high risk HPV types have delayed the initiation of immune response in KCs by directly blunting the transcription of IFNα and IFNβ (23). Additionally, HPV16 and HPV18 E7 proteins have been shown to interfere with IFN-mediated signaling pathways through its ability to bind to interferon regulatory factor-1 (IRF1), thereby reducing the transcription of IRF1 target genes such as monocyte chemoattractant protein-1 (MCP-1) and transporter associated with antigen processing protein-1 (TAP1) (24, 25).

Tumor necrosis factor (TNF) is an activator of nuclear factor kappaB (NFκB) which is involved in the prohibition of cell proliferation, differentiation and induction of apoptosis. It has been shown that TNF exerts its anti-proliferative effect on HPV-16-immortalized keratinocytes through induction of NF-κB. However, several studies have reported that E6

and E7 proteins down-regulate the expression of TNF and NFκB, thereby protecting HPV from the pro-inflammatory effect of these molecules (21).

1.2.3 Modulation of antigen presentation in APC

In immune-competent individuals, viral antigens are processed and cross-presented to T cells by innate immune cells including macrophages, dendritic cells (DCs), and Langerhand cells (LCs) (18).

DCs have the ability to link the innate and adaptive immune responses by presenting viral antigen to T cells in the lymphoid peripheral organs. It has been shown that the activation of the cell-mediated immune response is essential for the eradication of HPV infection (18). However, by unknown mechanisms HPV can induce the loss of LCs which are the principal DC population residing in the skin (26). Furthermore, data from patients and HPV transgenic mice have revealed that E7 loaded DCs fail to undergo maturation and immature DCs are tolerogenic rather than immunogenic to E7 specific T cells in draining lymph nodes (27). Additionally, E5 protein is responsible for the loss of MHC class I and transporter associated with antigen processing proteins (TAP) in HPV-related cancers (28)**.** Thus, these mechanisms enable HPVs to evade the surveillance of the innate immune system and establish a persistent infection.

1.2.4 Modulation of T helper cell- derived cytokine production by HPV

$CD4^+$ T-helper cells set the cytokine milieu, determining the direction of the immune response to pathogens. Data from patients with intraepithelial and invasive cancer showed that T-helper cytokine network is deregulated during the carcinogenesis of cervical cancer (29). Infection with papillomavirus can shift the differentiation of T-helper cell towards Th2 and T-regulatory cell phenotypes and reduce Th1 phenotype, leading to suppression of cellular immunity and progression to cancer (29). Th1 cytokines including IL-2, TNFα and IFNγ were reduced in HPV-associated lesions as compared to healthy women. Conversely, these patients displayed increased level of IL-4 which is a signature of Th2 cells (30, 31).

Regulatory T cells (Treg) are a $CD4^+$ T cell subset that express CD4, CD25 and transcription factor FOXP3 and mediate peripheral tolerance. Treg cells produce IL-10 which can hinder cross-presentation by DCs, thereby preventing from an effective immune response to malignant cells. This cytokine has been shown to be associated with cervical

cancer progression. HPV E2, E6 and E7 proteins were shown to bind directly to the IL-10 regulatory region to active gene transcription (36).

Th17 cells are a distinct subset of T cells which are manifested by the production IL-17A. It has been reported that IL-17A induced by Listeria-based immune therapy promotes the regression of tumor in HPV transplantatable mouse model (32). In addition, the low concentration of transforming growth factor beta (TGF-β) and high level of IL-6 in the local inflammatory milieu are capable of activating Th17 cells to eliminate viral infection at mucosal surfaces (33). Nonetheless, in the context of cervical cancer, HPV E6 and E7 proteins induce a high level of TGF-β, which might shift differentiation of naïve T cells into regulatory T cells (Tregs) instead of Th17 cells, which generate the local immuno-suppression resulting in persistent infection (2, 34). In contrast, a recent study using HPV16 E7 trangenic skin transplantation has shown that IL-17A produced by $CD4^+$ T cells is responsible for the suppression of immune effector functions (35).

In conclusion, the innate immune response to HPV infection plays a crucial role in limiting viral infection during the early phase of infection and in shaping adaptive immunity. Nonetheless, high risk HPVs are able to subvert the recognition of innate immune cells as well as modulate the expression of T cell-derived cytokines through the action of their oncoproteins, thereby leading to their persistent infection and tumorigenesis.

1.3 Models of HPV pathogenesis

HPV E6 and E7 oncoproteins play crucial roles in cell transformation as well as immune-suppression. Therefore, development of a model that can simulate the complex viral oncoprotein-host immunity interactions might be useful for study of the immunosuppressive mechanisms driven by HPV and antiviral interventions.

1.3.1 In-vitro model

It had been impossible to reproduce the HPV life cycle *in-vitro* since the virus is tissue tropic and its life cycle is tightly associated with the differentiation program of host keratinocytes. Recent studies have revealed that HPV-infected keratinocytes represent suitable and reliable tools to understand the interactions between viral proteins and cellular proteins as well as the epithelial immune response to the virus. There are two different approaches to generate HPV-infected keratinocytes: 1) immortalized cell lines derived from *in-vivo* lesions infected with HPV; 2) transfection of low-passage human keratinocytes

with full or partial HPV genomes. Subsequently, these immotalized cells will produce viral particles under differentiating conditions (37).

Although HPV infected epithelial cells have been used as a tool to understand viral life cycle and the consequence of viral oncoproteins on cytokine production by keratinocytes, this model is labour intensive and time-consuming. Furthermore, the yield of immortalised clones after viral genome transfection is vey low even under optimal conditions (37).

1.3.2 In-vivo models

- *PV mouse model*

Naturally Papillomavirus (PV) infected animals including rabbits, cattle and rats have been employed as models to study HPV pathogenesis. However, these models are not favourably used in laboratory studies due to the size of animals as well as the lack of available reagents for validation. Thus, a recent mouse model (musPV) based on mice naturally infected with PVs has been developed. These mice develop papillomas and are able to transmit PV to others immune-compentent mice. This model has been used to elucidate the mechanism of PV latency and role of the immune system. However, findings from this model might not be relevant to human diseases caused by HPV due to the marked differences between musPV and HPV (38), and the need for immune suppression to allow infection with musPV.

- *Xenograft models*

Buitrago-Perez et al. developed a humanized model in which human skin transfected with plasmids carrying the HPV5 or HPV16 E7 gene was subsequently transplanted onto *nu/nu* immunodeficient mice. These mice displayed similar histopathological and molecular features as observed in HPV-associated lesions. Therefore, this model is proposed for studies of molecular mechanisms underlying HPV pathogenesis as well as pre-clinal validation of therapies for HPV-associated cancer (39). Although this model is able to recapitulate physiological conditions in a human context, it lacks a proper immunity and might not be useful to address anti-tumor therapies based on immune system interactions.

❖ *Tumor transplantable model*

The tumor transplantable model is generated by subcutaneously injecting immune-competent mice with TC-1 cells, which are primary mouse lung epithelial cells co-transfected with HPV16 E6 and E7 and an activated ras oncogene (40). This model does not consider the properties of a naturally slow-growing tumor in which the antigen expression is maintained at a low level to evade the immune surveillance. Studies using this model to test the pre-clincal benefit of therapies have revealed that regression of a tumor is mediated by E7 specific $CD8^+$ T cells (16). Nonetheless, therapeutic approaches proposed by these studies that have showed promising results in this model, have mostly failed at clinical phase (13). This could be explained by the fact that fast growing tumor cells in this model might have different biological features from the slow-growing *in-situ* tumors.

❖ *HPV transgenic mouse*

K14.HPV16.E6/E7 mice which express HPV type 16 E6 or E7 oncoproteins within basal keratinocytes under the control of the keratin 14 transcriptional promoter, show epithelial hyperplasia (41-43). The Frazer group has previously shown that skin grafts expressing HPV16.E6/E7 oncoprotein are not spontaneously rejected when transplanted onto syngeneic animals, but are rejected when certain components of the innate immune system are unavailable, confirming that expression of E6 or E7 oncoprotein in the epithelium results in the establishment of a local suppressive environment and the subversion of antigen specific $CD8^+$ T cells. By using this model, Mattarollo et al. revealed that invariant natural killer T cells (iNKTs) cell depletion causes K14.E7 skin graft rejection, suggesting that NKT cells infiltrating the skin are involved in the establishment of a local immune suppression environment in hyperplastic skin (44).

When compared with the tumor transplantation model, the K14.E7 transgenic model better mimics the immunobiology of the chronic infection with HPV and of precancerous lesions caused by HPV (45). Although HPV specific antigen immunisation is sufficient to eradicate tumors in murine transplantable models, this immunotherapy strategy is ineffective in patients with HPV-associated cancer (46) and in the skin graft model. Thus, the K14.E7 model has been extensively used as model of HPV-associated squamous cancer to investigate the immunosuppressive mechanisms mediated by HPV (47).

K14.E6/E7 transgenic mice might serve as an *in-vivo* model to study the interaction between the immune response and high-risk HPV oncoproteins. The in-depth

understanding of immunosuppressive mechanisms driven by HPV oncoproteins might lead to the development of effective immunotherapies to reverse these mechanisms.

1.4 Immune-based vaccines for established HPV-associated diseases

Although efficient prophylatic vaccines (Gardasil and Cervarix) that trigger protective immune responses against HPV infections have been designed and approved by the Health Authorities from different countries, the lack of knowledge on cervical cancer and HPV among the communities in developing countries restricts participation in a vaccination program. Furthermore, the cost of the vaccines is high which will hinder those with a low income from being able to afford the vaccination. As the female population in the developing countries continues to rise with an increase in life expectancy, it is expected that the number of cases of HPV-associated cancers will rise further in the years to come (48). Thus, development of new therapies for HPV persistently infected patients remains an important health and economic task.

1.4.1 HPV E6 and E7 specific immune therapies

It has been shown that the expression level of HPV L1 and L2 in cervical cancer or infected basal cells is undetectable. In contrast, the E6 and E7 proteins that are required for oncogenic processes increased with the severity of HPV-mediated neoplasia. Therefore, these oncoproteins have become potent targets for specific immune therapies which can activate cell-mediated immune response to eradiate HPV-associated lesions (49).

- *Peptide/protein vaccination targeting HPV oncoproteins*

Peptide/protein vaccination aims to boost tumor antigen specific $CD4^+$ T cells and primed $CD8^+$ effector T cells. Vaccination with overlapping synthetic E6 and E7 long peptide in patients with $HPV16^+$ high-grade cervical squamous intraepithelial lesions resulted in enhanced infiltration of virus specific $CD8^+$ T cells (50). Protein vaccines including HPV16.E7 protein covalently linked with a *Mycobacterium bovis* BCG-Heat shock protein (HSP) induced complete regression in 35% of patients with high-grade squamous intraepithelial (HSIL) (51). However, most of peptide/protein-based strategies are unlikely to induce sufficient T cell responses against established and advanced disease stages (52). Indeed, a study using HPV16 E7 transgenic skin grafting model

reported that immunisation with E7 peptide was unable to induce graft rejection despite the induction of specific $CD4^+$ and $CD8^+$ T cells (53). One possible explanation for the failure of specific vaccine is that E7 expressing epithelial cells produce immunosuppresive molecules which can inhibit CTL-mediated graft rejection (42, 44, 54). Alternatively, trafficking of E7-specific CD8+ T-cell to skin might be impaired by this local suppressive environment. Furthermore, these effector cells may not respond optimally to immunization in an E7 graft recipient due to the ineffective antigen presentation (42).

❖ *DNA vaccine*

A DNA vaccine is constructed by introducing gene encoding HPV oncoproteins into a recombinant plasmid that enables the expression of these oncoproteins within mammalian cells. Consequently, these proteins can be delivered and packaged into MHC class I molecules in dendritic cells, thereby stimulating anti-tumor immune response by inducing cytolytic T cell (CTL) activity in $CD8^+$ T cells (55).

Although DNA vaccines are regarded as a safe, simple and stable antigen-specific therapy, there are still some concerns that HPV oncogenes might be integrated into the host genome and potentially induce oncogenic transformation by inhibiting tumor suppressor genes. DNA vaccines encoding a mutant HPV16.E7 protein in which three point mutant sites were introduced to the pRb binding motif of the E7 protein is designed to reduce the transforming activity. This strategy has been shown to provide an antitumor effect in the HPV16.E7 transplantable mouse model (55).

❖ *Dendritic cell- based vaccine*

To enhance cell-mediated immunity against HPV, dendritic cell-based vaccines have been developed by loading viral oncoprotein/peptide to autologous DCs. These cells are capable of taking up antigens, migrating to lymph nodes and priming specific $CD4^+$ and $CD8^+$ T cell responses (56). Human DCs which were isolated from HPV infected patients, and subsequently pulsed with tumor lysate and matured with dsRNA Poly [I]:poly [C] analogue, showed enhanced HPV specific CTL and T helper responses both *in-vivo* and in clinical trials. However, the DC-based vaccine is an expensive approach and cannot be produced in a large scale, thereby imposing limitations on its clinical applications (57).

1.4.2 Immunostimulatory adjuvant as a non-specific immunotherapy

The efficacy of therapeutic strategies is dependent not only on the specific immune response to viral antigens but also on the inflammatory environment. Immunostimulants are thought to activate the innate immunity and are essential for a sufficient and durable adaptive immune response. In this perspective, increasing evidence has demonstrated clinical benefits of immune adjuvants in HPV-associated lesions.

❖ *Listeria monocytogenes-based vaccine*

The administration of Listeria bacteria around the time of grafting (4 days before or 8 days after grafting) is capable of breaking tolerance and triggering the rejection of the K14.E7 graft. This immunotherapy strategy is involved in complex action mechanisms that stimulate innate and cell-mediated immunity while reducing immunosuppressive (58). In fact, the rejection of the HPV16.E7 skin graft is promoted by the release of proinflammatory cytokines, thereby activating the maturation of DCs and cross presentation of keratinocyte-derived E7 protein (27). Furthermore, vaccination with immunotherapeutic Listeria induces IFNγ and IFNγ-dependent chemokines production, resulting in the enhanced migration of tumor-infiltrating T cells in the TC1 transplantable tumor model (59). Thus, an efficient innate response stimulated by Listeria may assist the regression of HPV-associated lesions. Several clinical trials are conducted to examine the efficacy of Listeria-based vaccine for the treatment of HPV-related human cancers (60). However, cytokine-mediated toxicity and a course of antibiotic treatment to assure complete clearance of bacteria should be taken into account (61).

❖ *Imiquimod*

Imiquimod which is a TLR7 agonist, is capable of activating macrophages and mucosal DC to secrete pro-inflammatory cytokines including IFNα, TNFα and IL-12 (62). These cytokines have been shown to promote antigen presentation and maturation of LCs. In phase III trial, application of imiquimod induced complete regression of genital warts without recurrence following treatment (63).

❖ *2,4-Dinitrochlorobenzene (DNCB)*

Contact hypersensitivity induced by topical application with DNCB, an allergen, was first described as an effective therapy for malignant melanoma in the early 1970s (64). In addition, it was also used to treat condylomata acuminata caused by HPV infection. A

clinical study reported that 13 of 15 patients exhibited complete clearance of lesion following DNCB treatment (65). Additionally, DNCB was recognised as a potent therapy for resistant warts caused by HPV. However, the use of DNCB for treatment has been discouraged because of its mutagenic and carcinogenic potential (66). Furthermore, the mechanisms of action for DNCB as an immunotherapeutic modality are poorly understood. It is speculated that understanding how induction of a vigorous acute inflammatory response can break the locally immunosuppressive environment caused by HPV and restore the effector function of adaptive immunity, might lead to more acceptable treatments for persistent HPV infection.

1.5 Mechanisms of DNCB-induced cutaneous inflammation

1.5.1 Activation of T-cell mediated immune response

DNCB-induced contact hypersensitivity is thought to be a T cell mediated-process. There are two distinct phases to achieve effective T cell-mediated immunity. In the sensitization phase, the skin is exposed to low-molecular weight allergens such as DNCB that undergo the haptenation process by forming covalent bonds with lysine, tyrosine, histidine and cysteine groups of epidermal cell proteins. Haptenated proteins are highly immunogenic and taken up by LCs, antigen presenting cells in the skin. These cells subsequently migrate to skin draining lymph nodes where they cross-present haptenated peptides to $CD4^+$ and $CD8^+$ T cells (Figure 1.3) (67).

When the skin is re-exposed to an allergen, the elicitation phase is initiated, in which primed $CD4^+$ and $CD8^+$ T cells are expanded, enter the circulation and home to the site of inflammation. Once entering the skin, $CD4^+$ and $CD8^+$ T cells show different effector functions. Activated $CD8^+$ T cells produce IFN-γ which has been shown to promote other cytokines and chemokines production and exert cytotoxic activity in contact hypersensitivity, while $CD4^+$ helper T cells including Th1/Th2/Th17 and regulatory T cells are both important mediators and regulators of contact hypersensitivity (68, 69).

Not only $CD8^+$ T cells, $CD4^+$ Th1 cells were also shown to produce IFNγ in contact hypersensity. In vivo depletion of IFNγ production by $CD4^+$ Th1 cells in C57BL/6 mice caused impaired CHS responses to DNFB and oxazolone compared with wild-type animals (70).

Th2 cytokine IL-4 is predominantly regarded as negative regulators of the DNCB-induced inflammatory response (71, 72). However, these cytokines have been shown to

be responsible for the amplification and chronicity of allergic skin inflammation in a mouse model of allergic skin inflammation. Deficiency in these cytokines in these mice displayed an impaired ear swelling response to DNCB application (73, 74).

Regulatory $CD4^+$ T cells have been shown to promote resolution of contact hypersensitivity. In deed, depletion of regulatory T cells increases the level and duration of the contact hypersensitivity response. Furthermore, this cell subset has been shown to reduce the number of IFNγ-producing CD8 T cells (75). IL-10 produced by Treg is also responsible for alleviated inflammatory response to contact allergen (76).

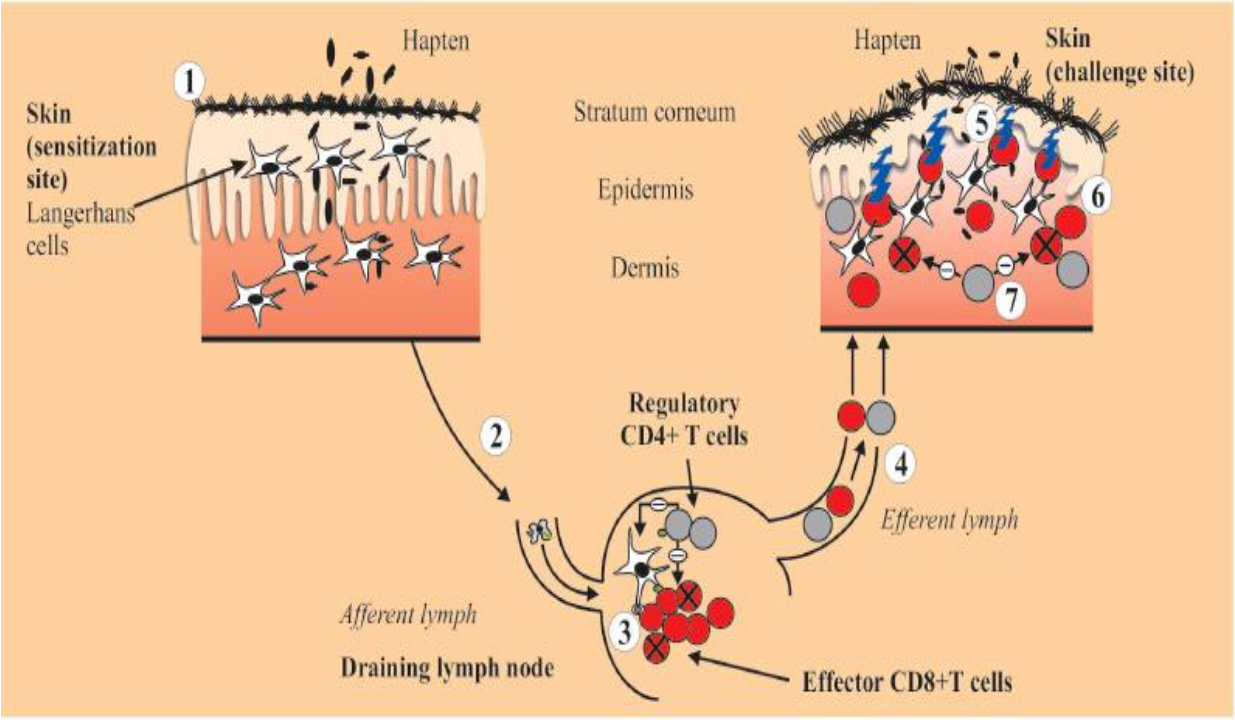

Figure 1.3- The mechanism of action of allergic contact hypersensitivity. The sensitization and elicitation phase of contact hypersensitivity are outlined. **Sensitization phase (step 1-4). (1)** Hapten applied to the skin is haptenated with self-proteins and haptenated proteins are taken up by LCs. **(2)** These LCs migrate to the skin draining lymph node and **(3)** present antigen to both $CD4^+$ and $CD8^+$ T cells. **(4)** Hapten-specific T cells are expaned in the lymph node and circulate via efferent lymph and home to the site of inflammation. **Elecitation phase (step 5-7). (5)** When the skin is re-exposed to the same hapten, DC and keratinocytes present haptenated peptides to specific T cells. **(6)** Activated $CD8^+$ T cells exert CTL activity, induce apoptosis of KCs and promote proinflammatory cytokines and chemokines. **(7)** $CD4^+$ T cells are differentiated into Th1/Th2/Th17 or Treg which produce both pro-inflammatory and anti-inflammatory cytokines. Adapted from (77).

The cytokine milieu produced during inflammation to hapten is far more complex than a simple Th1/Th2 paradim would explain (78). Th17 T cells, a distinct subset of $CD4^+$ helper T cells which secrete IL-17A, IL-17F, IL-21 and IL-22, have been recently emerged as important effector cells of contact hypersensitivity (79, 80). The differentiation and maturation of this subset are orchestrated by transcriptional factors including RORγt and STAT3, respectively (81). Th17 cells differentiation are regulated by a complex signaling network. In studies using murine models, inflammasome activated IL-1β and IL-18 were shown to induce the differentiation of Th17 cell (82). Furthermore, IL-6 when combined with TGFβ was described as the strongest inducer of Th17 cell differentiation while IL-23 is thought to act on the expansion, maintenance of Th17 cells (83).

IL-17A signals through a receptor complex composed of IL-17RA/IL-17RC and plays a pivotal role in inflammatory response to 2,4-dichloronitrobenzene (DNFB), an analog of DNCB. Studies using experimental models of contact hypersensitivity demonstrated that IL-$17A^{-/-}$ mice developed alleviated ear swelling response to allergen compared with wild-type mice (84, 85). In these studies, IL-17A was reported to induce hyperinflammation and recruitment of macrophages and neutrophils to the skin (84, 85). Furthermore, in adoptive transfer experiments, $CD4^+$ T cells isolating from IL-17A sufficient mice animals can recover the inflammatory response in IL-17A deficient animals (86). Thus, IL-17A-derived $CD4^+$ T cells is an important mediator in allergen induced inflammation. Furthermore, T cell-derived IL-17A was shown to stimulate cytokine production including granulocyte macrophage colony-stimulating factor (GM-CSF), IL-6 and intercellular adhesion molecule (ICAM-1) expression by human keratinocytes, thereby amplifying the nickel-induced skin inflammatory response (87). A recent study has reported that exposure to DNFB results in IL-1β release by keratinocyte which in turn activates γδT, particularly dendritic epidermal T cells, to produce IL-17A and subsequently drive inflammatory response (86). Interestingly, IL-17A has been recently shown to mediate the Th2 inflammation in a murine model of atopic dermatitis, a chronic skin inflammatory disease (88).

In summary, topical application of DNCB leads to the activation of T cell-mediated immune response that is manifested by the production of T cell-derived cytokines. It has been shown that different types of allergens results in different cytokine profile responses. Contact allergens such as DNFB, oxazolone and DNCB preferentially induce Th1-predominant responses, whereas allergens such as trimellitic anhydride and FITC might induce Th2-predominant responses (70). Additionally, IL-17A produced by Th17 cells has

been recently described as an important mediator of inflammatory response to various contact allergens (78, 80).

1.5.2 Stimulation of innate immunity

Although activation of T-cell mediated immune responses is the proposed mechanism of the clinical effect of DNCB, there is limited data concerning innate immunity mechanisms. Acute cutaneous inflammatory response to DNCB is initiated by the secretion of IL-1β and IL-18 by KCs and DCs. These cytokines are first produced as inactive precursors in the cytoplasm and then cleaved into active forms by caspase-1 activity which is driven by a multiprotein complex, known as inflammasome. Allergen application triggers epidermal cells to release extracellular danger signals (ATP, ROS and low-molecular weigh hyaluronic acid) which are implicated in the activation of NALP3 inflammasome (89, 90). Activation of NALP3 inflammasome causes secretion of active proinflammatory cytokines including IL-1β and IL-18 which are crucial for DC maturation and migration (91). Additionally, production of these cytokines during sensitization phase is critically required for hapten-specific and non-specific proliferation of draining lymph node cells (92). Indeed, the role of the inflammasome was confirmed in NALP3 deficient mice which developed impaired contact hypersensitivity response to allergens (91). The regulation of NALP3 activation by danger signals is largely unknown. A recent study by Guadar et al. suggested that type I IFN (IFNα and IFNβ) inhibit the activation of the NLRP3 inflammasomes in a STAT1 transcription factor dependent manner, thereby suppressing caspase-1-dependent IL-1β maturation (93)

Furthermore, application of DNCB to rat skin caused migration and activation of peripheral blood granulocytes which produced nitric oxide (NO) and TNFα (69). Dendritic cells, particularly LC cells in the skin, are crucial arms of innate immunity. DNCB application leads to the induction of costimulatory molecule CD86, class II MHC molecules and secreted cytokines including IL-12, IL-6 and IL-23 in these cells which subsequently could drive T cell polarization (94).

Topical immunotherapy with DNCB might thus be an additional treatment approach that works by inducing a vigorous acute inflammation and stimulating T cell-mediated immune response which in turn can break the tolerance induced by HPV persistent infection.

1.6 Dual regulatory roles of arginase in innate immunity

1.6.1 Introduction to arginase

❖ *Arginase and L-arginine metabolism*

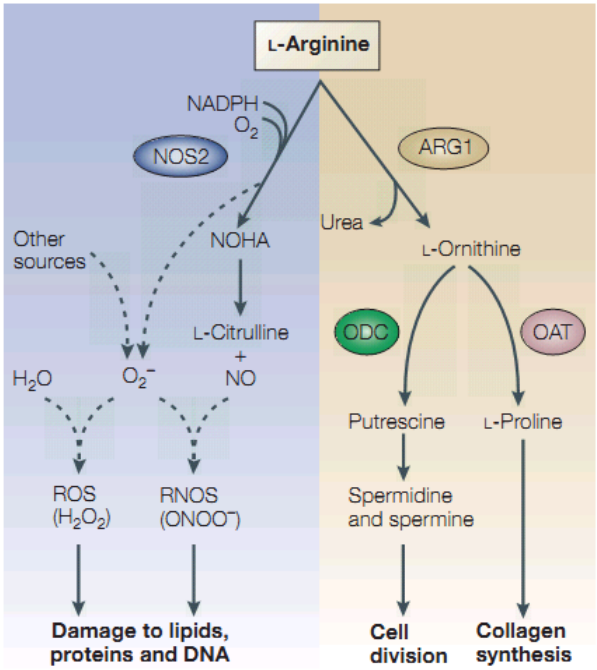

Figure 1.4- L-arginine metabolism by iNOS and Arginase-1. Arginase-1 and iNOS (NOS2) are the key mediators of L-arginine metabolism. Arginase-1 converts L-arginine into urea and L- Ornithine which is further required for the synthesis of important intermediate products (Putrescine and L-proline) for cell division and collagen synthesis. NOS2 (iNOS) metablizes L-arginase into Nω-OH-L-arginine, and then Nω-OH-L-arginine is transduced to form NO and L-citruline which are further converted to reactive nitrogen oxides. ARG1: Arginase-1; ODC: Ornithine decarboxylase; OAT: Ornithine aminotransferase; NO: Nitric oxide; NOHA: Nω-OH-L-arginine. Adapted from (95)**.**

L-arginine is regarded as a non-essential amino acid because it can be synthesized by epithelial cells of the small intestine and the proximal tubules of the kidney from citrulline. However, in certain physiological conditions such as trauma and infection, this amino acid becomes conditionally essential. L-arginine is transferred to the inner cell compartment via the y+ system of cationic amino acid transporters. Once in the cells, L-arginine is metabolized by either arginase or nitric oxide synthases (NOS) (95). While NOS

converts L-arginine into citrulline and NO, arginase catalyzes the hydrolysis of L-arginine into urea and L-ornithine. L-ornithine is further metabolized into either polyamines (putrescine, spermidine) or L-proline by ornithine decarboxylase and ornithine aminotransferase, respectively. Polyamines are implicated in cell proliferation and differentiation while L-proline is essential for the synthesis of collagen. L-argnine can be recycled from L-citrulline via argininosuccinate synthase and argininosuccinate lyase (96) (Figure 1.4).

❖ *The distribution of arginase*

Mammalian arginase consists of two isoforms: arginase-1 and arginase-2 which are encoded by two distinct genes and are different in their tissue distribution and subcellular localization. Arginase-1 is a cytoplasmic and inducible isoform which is strongly expressed in liver and constitutes the majority of total body arginase activity. In contrast, arginase-2 is a mitochrondrial isoform which is constitutively expressed in various mammalian tissues including kidney, prostate, small intestine and the lactating mammary gland. Both isoforms are induced in murine macrophages, and myeloid derived suppressive cells (MDSCs) in response to different stimuli. In skin, both isoforms are expressed in keratinocytes, fibroblasts. Arginase activity in skin is located predominantly in the epidermis (97). In humans, arginase activity can be detected in serum of patients with colorectal, breast, prostate and skin cancer. Additionally, arginase can also be expressed either by tumor cells or tumor associated myeloid cells (98).

❖ *The regulation of arginase expression*

Arginase-1 expression in myeloid cells can be induced by a variety of factors. ProstanglandingE2, GM-CSF, lipopolysaccharide (LPS) (99) and Th2 cytokines including IL-4, IL-10 and IL-13 are key inducers of arginase-1. These molecules bind to their cognate receptors that in turn activate STAT6. This transcriptional activator binds to the 5’ flanking region and induces the expression of the arginase-1 gene (Figure 1.5). In addition, arginase-1 is also induced by mycobacteria through a STAT6 independent mechanism. In this mechanism, the presence of mycobacteria is detected by TLR which in turn activates MyD88 signaling pathway. This signal transduction pathway recruits the transcriptional factor CEBP-β instead of STAT6 to up-regulate expression of arginase-1 in macrophages (100).

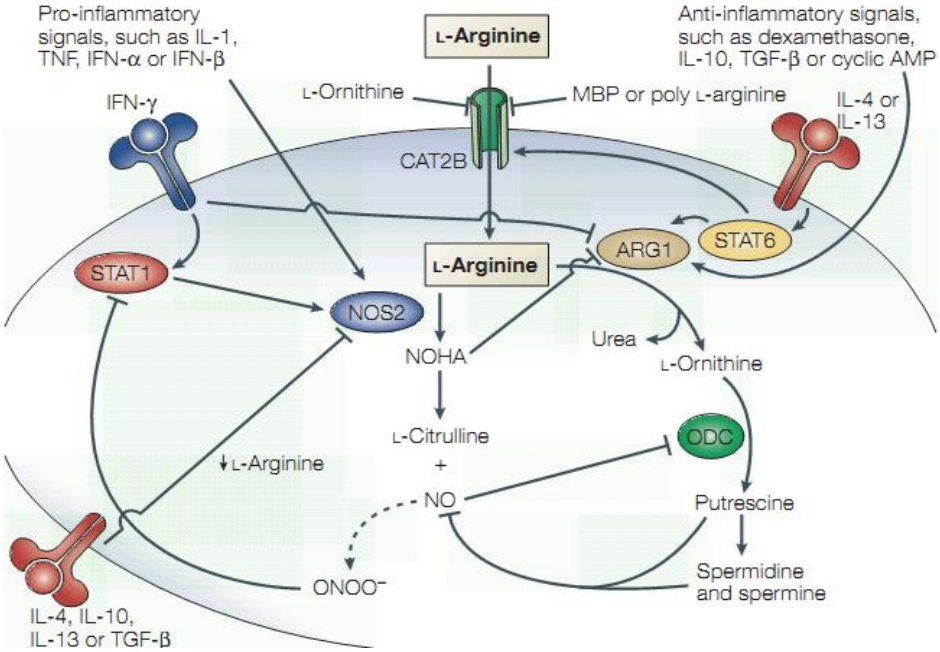

Figure 1.5- Arginase expression is reciprocally regulated by Th1 and Th2 cytokines. While Th2 cytokines (IL-4; IL-13), IL-10, TGFβ and cyclic AMP induce the expression of arginase via STAT6 transcription factor, Th1 cytokines (IFNγ, TNFα), IL-1; IFNα and IFNβ induce iNOS (NOS2) via STAT1 transcription factor and downregulate arginase-1 expression. Adapted from (95).

Arginase-1 expression in myeloid cells is negatively regulated by the Th1 cytokine IFNγ which induces iNOS expression. The induction of iNOS in macrophages results in the inhibition of arginase expression due to the competition for the common substrate L-arginine. Moreover, the production of NO by iNOS might abrogate the induction of arginase-1 mediated by IL-4 and IL-10. However, LPS which is known as an inducer of Th-1 cytokines has been shown to induce arginase-1 expression in macrophages (101). In addition, Liscovsky *et al* (2009) showed that the induction of arginase in murine macrophage by oligodeoxinucleotides containing CpG motifs is dependent on the production of IFNγ (102).

1.6.2 Myeloid derived suppressor cell (MDSC) derived-Arginase- an immune suppressive factor

- *Arginase and T cell function*

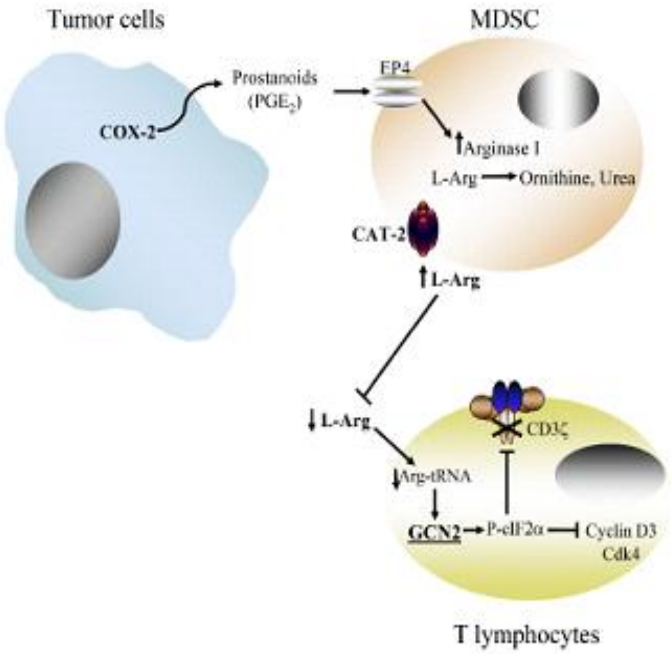

Figure 1.6- Arginase induces T cell dysfunction. COX-2/PGE2 produced by tumor cells activates MDSCs to express arginase-1, thereby depleting L-arginine in the milieu. Depletion of L-arginase by arginase-1 leads to the suppression of T cell function by dampening the synthesis of CD3ζ and cdk4 in T cells. Adapted from (103).

MDSCs are heterogenous populations of immature myeloid cells comprising macrophages, granulocytes and dendritic cells. They accumulate in the blood, lymph nodes, bone marrow and tumor environment in most patietnts and experimental animals with cancer. MDSCs are capable of inducing T cell dysfunction by suppressing the activation and proliferation of $CD4^+$ and $CD8^+$ T cells (104) or indirectly by promoting the differentiation of Treg (105).

MDSC infiltration has been shown to be associated with the progressive course of HPV-induced cancer (106, 107). A recent study has reported that MDSCs are increased in number in blood from patients with HPV-associated oropharyngeal cancer. After chemoradiotherapy, these patients showed a remarkable increase in the number of circulating MDSC and loss of HPV specific T cell responses (106). Interestingly, HPV16 E2 protein expresssed in squamous cell carcinoma cell line reduces the proportion of MDSCs and the production of MDSC-related mediators including iNOS and IDO, leading to enhanced anti-tumor responses (108). However, the precise role of MDSCs in HPV-associated cancer has not been addressed in these studies and requires further studies.

Since the first study conducted in 1970, accumulating evidence has suggested that arginase is one of the most important mediators employed by MDSCs to dampen T cell

functions (95). Arginase expressed by MDSCs has been shown to modulate the function of T cells through the depletion of L-arginine in the surrounding milieu. The starvation of L-arginine results in the activation of GCN2 kinase, which in turn induces the phosphorylation of translational factor eIF2α. Phosphorylated eIF2α subsequently binds to eIF2β with a strong affinity. In this case, eIF2α loses its ability to exchange GDP for GTP. Consequently, this eI2F complex is unlikely to activate methionine aminoacyl tRNA thereby blocking the initial step of the translational process in T cells (Figure 1.6). Indeed, the deprivation of L-arginine has been shown to induce the diminished synthesis of cyclin D3 and cyclin dependent kinase 4 leading to the loss of proliferation and ability to produce IFNγ in T cells (95). In addition, L-arginine is required for the synthesis of CD8 and CD3 receptors. Depletion of L-arginine might result in impaired T cell receptor (TCR) signaling (109).

Additionally, in the presence of low concentrations of L-arginine, arginase-1 and iNOS can synergistically induce T cell dysfunction. Arginase and iNOS expressed by MDSCs might accelerate the production of reactive nitrogen and oxygen species (RNS and ROS), respectively, which are toxic for T cells (95). Furthermore, co-expression of arginase and iNOS might lead to the production of peroxinitrites ($ONOO_2$). This strongly reactive agent induces the nitration of TCR, thereby affecting its conformation flexibility and interaction with MHC molecules. As a result, the binding of peptide on MHC to $CD8^+$ T cell is abrogated (103).

- *The regulatory effect of arginase on NOS function*

Three different isoforms of NOS (NOS1, NOS2 and NOS3) have been identified. NOS1 (neuronal NOS or nNOS) and NOS3 (endothelial NOS or eNOS) are constitutively expressed in neuronal tissues and endothelium, respectively, while NOS2 (cytokine-inducible NOS or iNOS) is induced in several tissues and cell types, including macrophages, DCs and the vascular endothelium. NOS enzymes are known to convert L-arginine to citrulline and nitric oxide (NO), which are essential for cytotoxic mechanisms to protect against infection (103). NO generated by iNOS induction has been shown to block T cell function by interfering with the IL-2 signaling pathway (109). In addition, iNOS expression is an important marker of classically activated macrophages (M1 macrophage) which are implicated in anti-tumor mechanisms. On the other hand, it has also been reported that NO promotes the tumor growth by stimulating neo-angiogenesis and metastasis.

Although the co-expression of arginase and iNOS has been reported in MDSCs, arginase is more likely to function as a controller of iNOS activity in inflammatory monocytes (110). Firstly, endowed with higher capacity to catalyse the hydrosis of L-arginine, arginase efficiently competes with iNOS for the common substrate. Therefore, in the limited availability of L-arginine, arginase is able to deplete the substrate in the extracellular environment, resulting in the inhibition of iNOS activity. Additionally, the deprivation of L-arginine has been shown to be responsible for the blockage of the translational process and decreased stability of iNOS mRNA (95).

A number of recent studies showed that arginase and iNOS participate in the maintenance of nonresolving or chronic inflammation in several disease models. “Danger signal” generated by trauma triggers the recruitment of iNOS expressing cells which are required for the clearance of dead cells and the re-epithelialization (111). Subsequently, MDSCs expressing arginase are recruited to the wound site and induce the synthesis of collagen mediated by fibroblasts which is crucial for tissue remodeling. Ariel *et al.* (2012) reported that arginase expressed by alternatively activated macrophages (M2 macrophage) is implicated in the resolution of inflammation which protects wounded mice from excessive tissue repair (112). However, a malignant tumor tends to constantly cause tissue damage, which may result in depletion of L-arginine in the tumor environment and nonresolving inflammation (103). In addition, Kavalukas *e. al.* (2012) showed that inhibition of arginase promotes the production of NO and ultimately leads to the resolution of inflammation in wounded mice (96). Furthermore, L-arginine metabolism has been shown to play an important role in psoriasis, which is also known as a chronic inflammatory disease of the skin driven by IL-17A (113). This disease is manifested by the hyperproliferation and reduced differentiation of keratinocytes, which is mediated by the interplay between arginase-1 and iNOS. This study revealed that overexpression of arginase-1 contributes to the development of psoriasis by confining NO production (114). Thus, these studies have highlighted the immunosuppressive functions of arginase in chronic inflammation.

❖ *The potential implication of arginase for the establishment of persistent infection and tumorigenesis mediated by HPV infection*

Arginase might be implicated in the establishment of immunosuppressive environment or chronic inflammation that favors the persistent infection of HPV and cancer progression. This notion is supported by a recent study that demonstrates enhanced production of Th2 cytokine IL-13 and IL-10 in the serum of cervical cancer patients,

coincided with an increase of arginase activity and depletion of L-arginine (115). Furthermore, Lepique *et al* (2009) showed that in a HPV-16 induced tumor mouse model (TC-1 model), macrophages expressing high level of arginase-1 facilitate tumor growth by dampening antitumor T cell function. In this study, the absence of tumor infiltrated macrophages accelerates the recruitment of T lymphocytes to tumor environment and delays tumor growth (116). In this regard, Coussens *et al* (2000) found that M2 macrophages infiltrate the skin and mount chronic inflammation which promotes the progression from dysplasia to invasive cancer (117). Although arginase has been described as one of the most specific markers of the M2 macrophage (95), whether arginase is implicated in the progression of HPV associated cancer has not been demonstrated in this study. Thus, whether arginase is responsible for facilitating tumor growth has not been justified by these studies, despite its association with HPV-related tumors.

It has been suggested that HPV-specific CD4 + and CD8 + T cells within a cervical cancer environment are functionally inactive. Mattarollo *et al* (2010) showed that skin infiltrated invariant natural killer T cells (iNKTs) are involved in the establishment of a local immune suppression environment that subvert $CD8^+$ specific T cells in HPV16.E7 expressing skin (44). However, the mechanism by which NKT cells are activated to exert their function is still a matter of ongoing research. A recent study by Terabe *et al.* (2000) has identified the cross-talk between NKT cells and MDSCs in the regulation of the immune response. In this study, they reported that IL-13 expressed by NKT cells can activate MDSCs to suppress T cell function. In addition, IL-13 is widely known as an inducer of arginase (118). Thus, arginase might be involved in the subvertion of the effector T cells in HPV persistent infection.

In addition, arginase and iNOS coordinately contribute to the production of ROS (95). A recent study by Marco *et al* (2012) has shed the new light on the association of the production of ROS with HPV-16 neoplastic progression. This study indicated that the increased production of ROS results in the oxidative modification of cellular proteins and DNA damage. Consequently, these detrimental effects trigger the progression of a dysplasia lesion to cervical cancer (119).

In summary, these findings lend support to the idea that arginase might be exploited by HPV to establish an immunosuppressive environment that facilitates the persistent infection and tumor development.

1.6.3 Arginase derived-monocytes/macrophages-an inducer of acute inflammation

Arginase is not solely an immune-suppressive mediator. Recent studies have reported that arginase is an important stimulator in several inflammation episodes.

Arginase-1 produced by macrophages has been shown to play critical role in the pathophysiology of asthma which is a complex disease manifested by allergic airway inflammation and airway hyperreactivity. In mouse models of asthma, arginase-1 mediated allergic inflammatory response in lung epithelial cells through the modulation of NFκB signaling pathway (120, 121). Furthermore, treatment with arginase specific inhibitor, 2(S)-amino-6-boronohexonic acid (ABH), significantly ameliorated pulmonary inflammation and airway fibrosis in guinea pigs repeatedly exposed to LPS. The alleviated inflammation in these animals was concomitant with decreased IL-8 production and neutrophil infiltration (122).

In vascular inflammation, arginase-1 efficiently competes with iNOS for the common substrate L-arginine, leading to inhibition of iNOS expression and NO production. Since endothelium-derived NO is reported to suppress expression of adhesion molecules such as VCAM-1, ICAM-1 (123), limiting NO bioavailability through arginase results in enhanced inflammation (124). Likewise, this mechanism action of arginase was further supported by a recent study that the blockade of arginase activity by another arginase inhibitor, alpha-amino acid N(omega)-hydroxy-nor-l-arginine (nor-NOHA), resulted in alleviated inflammation, crypt damage via enhanced NO production in the colon tissue of dextran sodium sulfate-induced colitis mouse model (125).

In a mouse model of atherogenesis, arginase-2 but not arginase-1 enhances monocyte adhesion to endothelial cells and triggers the production of proinflammatory cytokines through mitochondrial reactive oxygen species (126). Liu *et al.* show that infiltrating myeloid cells produce arginase-1 which promotes angiogenesis and further recruitment of monocytes in laser-induced injury murine model (127).

Taken together, arginase can enact either inhibitory or stimulatory effect on the immune system dependent on the inflammation context. In tumor environment, it has been well established that arginase-1 produced by MDSCs is an important immunesuppressive mediator which inhibit cell-mediated immunity. On the other hand, cells of myeloid cell origin are among the first components of the immune system that are recruited to the site of inflammation and arginase-1 produced by macrophages is responsible for the exacerbation of inflammatory response in epithelial and vascular inflammation. Although

arginase-1 has recently emerged as an important regulator of the inflammatory response in numerous disease models, the association between arginase and the clearance of HPV infection remains poorly understood.

1.7 Purpose of the study

Although the majority of HPV infections regress pontaneously, 10% of infections are persistent and eventually progress to invasive cancer. In addition, although recent vaccines (Gardasil and Cervarix) have been shown to efficiently protect against HPV infection, HPV vaccination is only targeted at adolescents who have not previously been exposed to HPV (128). Furthermore, the high cost of the vaccine hinders accessibility for those with a low income. Therefore, the development of effective immunological therapies which are able to prevent infected patients from developing a persistent infection and invasive cancer remains an important health and economic concern.

DNCB-induced acute inflammation is speculated to alter the local immune-suppressive environment induced by HPV oncoproteins. However, the mechanism action of DNCB in association with HPV infection is largely unknown. Furthermore, clinical application of DNCB therapy has been hampered due to its mutagenic and carcinogenic potentials. Therefore, the objective of this study is to understand the innate immune response to DNCB in model of HPV-associated squamous cancer, K14.E7 mice. Our findings might contribute to the development of better immune-based therapies for HPV persistently infected patients.

1.8 Hypotheses and aims

❖ *This study investigated the following hypotheses:*

1. The expression of HPV16.E7 protein in the epithelium alters the levels and features of cutaneous inflammatory response to DNCB in K14.E7 mice as compared to wild-type mice.
2. Arginase-1 and arginase-2, important regulators of innate immunity, are responsible for regulating the DNCB-induced inflammation in HPV16.E7 expressing skin.
3. Inflammatory cytokines including Th2 cytokines/IL-6/IL-17A contribute to the induction of arginase and mediate DNCB-induced inflammation in HPV16.E7 expressing skin.

❖ *The aims of this study are to*

1. Examine the ear swelling response, the inflammatory cell infiltrate and cytokine producing profile of wild-type C57BL/6 and K14.E7 skin exposed to DNCB and investigate the role of lymphocytes in DNCB–induced inflammation in K14.E7 mice.

2. Analyse the production and the source of arginase-1/2, and their involvement in regulating DNCB -induced inflammation in K14.E7 mice.

3. Investigate the production and involvement of Th1, Th2 and Th17 cytokines in the regulation of arginase-1/2 and DNCB-induced inflammation in K14.E7 mice.

4. Examine the survival of K14.E7 skin grafts following DNCB treatment and E7 peptide vaccination.

CHAPTER 2

HPV E7 Oncoprotein Transgenic Skin Develops An Enhanced Inflammatory Response To DNCB By Arginase-1-Dependent Mechanism

2.1 Foreword

Stimulation of the innate immune system with DNCB is speculated to alter the local immunosuppressive environment induced by HPV. However, the immunostimulatory mechanism of DNCB in association with HPV-induced carcinogenesis has not been elucidated yet. The first aim of this chapter is to characterize the DNCB-induced inflammation in K14.E7 skin. As arginase has been shown to functions as an important regulator of inflammation and innate immunity, this chapter also aims to analyse the production, the source of arginase and its involvement in the regulation of DNCB-induced inflammation in K14.E7 skin. The work addressing these two aims has been published on Journal of Investigative Dermatology (2014) 134**,** 2438–2446.

2.2 Article 1

Original Article

Subject Category: Tumor Biology

Journal of Investigative Dermatology (2014) 134, 2438–2446; doi:10.1038/jid.2014.186; published online 29 May 2014

Human Papillomavirus E7 Oncoprotein Transgenic Skin Develops an Enhanced Inflammatory Response to 2,4-Dinitrochlorobenzene by an Arginase-1-Dependent Mechanism

Le Son Tran[1], Anne-Sophie Bergot[1], Stephen R Mattarollo[1], Deepak Mittal[1,2,3] and Ian H Frazer[1,2]

[1]The University of Queensland Diamantina Institute, Translational Research Institute, Brisbane, Queensland, Australia

Correspondence: Ian H. Frazer, The University of Queensland Diamantina Institute, Translational Research Institute, 37 Kent Street, Woolloongabba, Brisbane, Queensland 4102, Australia. E-mail: i.frazer@uq.edu.au

[2]These authors contributed equally to this work.

[3]Current address: QIMR Berghofer Medical Research Institute, Herston 4006, Queensland, Australia.

Received 23 November 2013; Revised 5th March 2014; Accepted 21st March 2014 Accepted article preview online 14th April 2014; Advance online publication 29th May 2014

Abstract

We have shown that the expression of human papillomavirus type 16 E7 (HPV16.E7) protein within epithelial cells results in local immune suppression and a weak and ineffective immune response to E7 similar to that occuring in HPV-associated premalignancy and cancers. However, a robust acute inflammatory stimulus can overcome this to enable immune elimination of HPV16.E7-transformed epithelial cells. 2,4-Dinitrochlorobenzene (DNCB) can elicit acute inflammation and it has been shown to initiate the regression of HPV-associated genital warts. Although the clinical use of DNCB is discouraged owing to its mutagenic potential, understanding how DNCB-induced acute inflammation alters local HPV16.E7-mediated immune suppression might lead to better treatments. Here, we show that topical DNCB application to skin expressing HPV16.E7 as a transgene induces a hyperinflammatory response, which is not seen in nontransgenic control animals. The E7-associated inflammatory response is characterized by enhanced expression of Th2 cytokines and increased infiltration of $CD11b^{+}Gr1^{int}F4/80^{+}Ly6C^{hi}Ly6G^{low}$ myeloid cells, producing arginase-1. Inhibition of arginase with an arginase-specific inhibitor, N^{ω}-hydroxy-nor-l-arginine, ameliorates the DNCB-induced inflammatory response. Our results demonstrate that HPV16.E7 protein enhances DNCB-associated production of arginase-1 by myeloid cells and consequent inflammatory cellular infiltration of skin**.**

Abbreviations:

CIN, cervical intraepithelial neoplasia; DNCB, 2,4-dinitrochlorobenzene; HPV, human papillomavirus; Nor-NOHA, N^{ω}-hydroxy-nor-l-arginine; mRNA, messenger RNA

Introduction

Persistent infection with oncogenic human papillomaviruses (HPV), particularly HPV16, is associated with selective expression of two virally encoded proteins (E6 and E7) (129). One action of HPV16.E7 protein is to subvert the innate immune system through the downregulation of IFNγ pathways, modulation of antigen presentation, and suppression of Toll-like receptor 9 protein (21).

K14.E7 transgenic mice, which express HPV16.E7 oncoprotein within basal keratinocytes under the control of the keratin 14 transcriptional promoter, have been extensively used as a model of HPV oncoprotein–induced immune suppression associated with human squamous cancers, in which only the *E6* and *E7* genes of the papillomavirus are expressed (45). We have previously shown that skin grafts expressing HPV16.E7 oncoprotein are not spontaneously rejected when transplanted onto syngeneic animals, but they are rejected when certain components of the innate immune system are unavailable, confirming that the expression of HPV16.E7 in the epithelium results in the establishment of a local suppressive environment and the subversion of antigen-specific T cells (44, 54). Therefore, successful strategies targeting HPV-associated cancer need to circumvent or disrupt the local suppressive environment.

Topical immunotherapies with immunostimulatory agents have been used clinically to treat cancerous lesions including squamous cell and basal cell carcinoma in immunocompetent and immunosuppressed patients (130). Topical application of 2,4-dinitrochlorobenzene (DNCB) is an effective therapy for condylomata acuminata caused by HPV infection. DNCB induced the complete clearance of HPV-associated warts in 13/15 patients (65). The efficacy of this treatment is attributed to the immunostimulatory role of DNCB that might activate cell-mediated immunity (69). However, the use of DNCB for treatment has been discouraged because of its mutagenic potential (66). We speculated that understanding how induction of a vigorous acute inflammatory response by DNCB can break the locally immune-suppressive environment and restore the effector function of adaptive immunity might lead to more acceptable treatments for persisting HPV infection.

Arginase, which metabolizes l-arginine to *N*-ornithine and urea, has been identified as a crucial regulator of inflammation. Mammalian cells express two different isoforms, arginase-1 and arginase-2, which are encoded by two distinct genes and are different in their tissue

distribution and subcellular localization (95). Arginase can function as an immunosuppressive factor in the tumor environment (131), in viral (132), or in parasitic infection (133). However, this enzyme has also been identified as an important proinflammatory factor in numerous disease models (134-136). As inflammation decides the fate of HPV infection and arginase is an important regulator of inflammation and immunity, we investigated the interaction between DNCB-induced inflammation and HPV16.E7 protein in induction of arginase in K14.E7 transgenic mice. We show here that K14.E7 transgenic mice exhibit an enhanced local inflammatory response to DNCB treatment, compared with nontransgenic mice, and that myeloid cells express increased arginase-1, which specifically promotes DNCB-induced inflammation.

Results

K14.E7 mice develop a robust inflammation response to DNCB

An inflammatory response was induced in wild-type nontransgenic C57BL/6 and in E7 transgenic K14.E7 mice by applying DNCB topically to the ear skin. The mean increase in ear thickness was monitored as an indicator of inflammatory reaction (137). K14.E7 mice displayed a significantly higher degree of ear swelling than C57BL/6 mice, which peaked at day 3 in response to a single application of DNCB (Figure 2.1a).

T lymphocytes have been found in several skin inflammation diseases and have an important role in the production of inflammatory cytokines and in the recruitment of innate immune cells (138). They also drive the enhanced inflammatory response seen on repeated exposure to DNCB (70). In addition, our previous study showed that lymphocytes are increased in number in K14.E7 skin (139). Therefore, we investigated whether the enhanced inflammatory response to first exposure to DNCB in K14.E7 skin was dependent on local lymphocyte function. K14.E7 mice deficient in lymphocytes ($Rag^{-/-}$ ×E7), when exposed to DNCB, exhibited a similar level of ear swelling as K14.E7 mice, and stronger than control $Rag^{-/-}$ mice over 5 days after DNCB treatment (Figure 2.1a). Thus, DNCB-treated K14.E7 mice exhibit a hyperinflammatory response on first exposure to DNCB, which is independent of an adaptive immune response.

DNCB-treated K14.E7 skin displays an enhanced infiltration of myeloid cells and Th2 cytokine expression

To characterize further the inflammation in DNCB-treated K14.E7 skin, we examined the infiltration of immune cells. Histological examination suggested that the greater ear swelling in K14.E7 mice corresponded to a significant increase in the number of immune cells infiltrating the dermis (Figure 2.1b). As expected, the thickness of the K14.E7 epidermal layer remained unchanged following DNCB treatment (control: 42.4±3.7 μm, DNCB: 40±3.5 μm, Supplementary figure 2.1). $Rag^{-/-}$ × E7 mice develop similar ear swelling and inflammatory cell infiltration in the dermis as K14.E7 mice, whereas control $Rag^{-/-}$ mice do not (Figure 2.1a and b). Thus, the increased ear swelling in K14.E7 in response to DNCB mice was mainly

contributed by infiltration of cells of the innate immune system in the dermis, and it was independent of lymphocytes.

Flow cytometry analysis revealed that DNCB-treated K14.E7 ears recruited significantly higher numbers of myeloid cells ($CD45.2^+CD11b^+$) than similarly treated C57BL/6 ears. We observed the same trend when we compared $Rag^{-/-}$xE7 mice with $Rag^{-/-}$ mice (Figure 2.2a). In contrast, the number of non-myeloid bone marrow–derived cells ($CD45.2^+CD11b^-$) remained unchanged and was comparable in all four groups following DNCB treatment (Figure 2.2b). Thus, the expression of HPV16.E7 in the skin mediates the enhanced recruitment of myeloid cells, and this effect is independent of adaptive immunity.

IL-1β and IL-6 are major cytokines secreted from the local inflammation site and promote the recruitment of innate immune cells (140, 141). DNCB treatment resulted in a significant increase in IL-1β messenger RNA (mRNA) expression in both C57BL/6 and K14.E7 skin (Table 1). In addition, IL-6 mRNA expression was significantly increased in DNCB-treated K14.E7 skin but not in nontransgenic skin, suggesting that IL-6 might be responsible for the enhanced recruitment of myeloid cells in K14.E7 skin.

Further, DNCB treatment of K14.E7 mice significantly induced mRNA expression of prostaglandin E2 synthase and Th2 cytokine IL-4 and IL-10. In contrast, there was no significant change in the expression of these factors in DNCB-treated C57BL/6 mice. Th1 cytokines displayed decreased (tumor necrosis factor-α) or unaltered (interferon gamma) expression after DNCB treatment (Table 1).

Together, these results suggest that after a single DNCB treatment to previously unexposed animals, K14.E7 mice mounted an enhanced inflammatory response, which is accompanied by $CD45.2^+CD11b^+$ myeloid cell infiltration and amplified Th2 cytokine expression.

Arginase-1 is specifically induced in DNCB-treated K14.E7 mice

Inflammation and myeloid cell activation can be associated with the induction of arginase (109). We speculated that arginase activity might contribute to enhanced inflammation of K14.E7 skin in response to DNCB. To test this hypothesis, we first investigated arginase activity in the skin of C57BL/6 and K14.E7 mice following DNCB treatment. Arginase activity was comparable in control K14E7 and C57BL/6 ear skin (Figure

2.3a), as was arginase mRNA expression (Figure 2.3b and RNAseq data not shown). DNCB-treated K14.E7 skin, however, demonstrated a substantially higher amount of arginase activity than DNCB-treated C57BL/6 skin (Figure 2.3a). Arginase activity is contributed by two arginase isoforms. Increased arginase activity in K14.E7 mice corresponded to markedly increased (fourfold) arginase-1 mRNA expression. Conversely, the expression of arginase-1 mRNA remained unchanged in DNCB-treated C57BL/6 mice (Figure 2.3b). In contrast to arginase-1, there was no significant induction of arginase-2 mRNA in either C57BL/6 or K14.E7 skin (Figure 2.3c).

Arginase-1, but not arginase-2, is induced in K14.E7 mice following 2,4-dinitrochlorobenzene (DNCB) treatment, and this regulation is lymphocyte independent.

K14.E7 mice lacking lymphocytes ($Rag^{-/-}$ ×E7) not only exhibited a similar level of ear swelling as K14.E7 mice but also of arginase-1 mRNA and arginase activity following DNCB treatment. Notably, Arginase-1 and arginase-2 mRNA expression are not increased in control $Rag^{-/-}$ mice following DNCB treatment (Figure 2.3b and c). Thus, the induction of arginase in K14.E7 skin is independent of adaptive immunity.

To examine whether the induction of arginase was unique to skin expressing HPV16.E7 oncoprotein as a transgene, K14.hGh and K5.OVA mice expressing human growth hormone or ovalbumin, respectively, under the control of keratin promoters were treated with DNCB. In contrast to K14.E7 mice, there was no change in the level of arginase activity of K14.hGh or K5.OVA mice following DNCB treatment (Figure 2.3d). Furthermore, the ear swelling of these transgenic mice (K5.OVA: 22.5±5 µm; K14.hGh: 17.5±5 µm, day 5) was similar to that of C57BL/6 mice (17.5±5 µm, day 5) and markedly lower than in K14.E7 mice (198±99 µm, day 5) (Supplementary figure 2.2). Thus, these results suggest that increased arginase activity, likely derived from activated myeloid cells, might be a consequence of exposure of K14.E7-expressing epithelial cells to DNCB.

$CD11b^{+}Gr1^{int}F4/80^{+}Ly6C^{hi}Ly6G^{low}$ cells are the major source of arginase-1 in DNCB-treated K14.E7 mice

Arginase-1 can be induced in myeloid cells including macrophages, dendritic cells, and myeloid-derived suppressive cells in response to a wide range of stimuli (142, 143). These myeloid cells express surface CD11b(144). To confirm whether myeloid cells were the source of DNCB-induced arginase-1 in K14.E7 skin, $CD45.2^{+}CD11b^{-}$ and $CD45.2^{+}CD11b^{+}$ cells (Supplementary Figure S2.4) were isolated from DNCB-treated C57BL/6 and K14.E7 mice and analyzed for arginase activity and arginase-1 mRNA expression. $CD11b^{+}$ myeloid cells from DNCB-treated K14.E7 mice produced significantly higher levels of arginase activity per cell compared with $CD11b^{-}$ cells, and compared with $CD11b^{+}$ myeloid cells from DNCB-treated C57BL/6 mice (Figure 2.4a). In addition, arginase-1 mRNA expression was substantially detected in $CD45.2^{+}CD11b^{+}$ cells in DNCB-treated K14.E7 mice, but not in $CD11b^{-}$or $CD11b^{+}$ cells from C57BL/6 mice (Figure 2.4b). Although arginase-2 mRNA was also detected in $CD45.2^{+}CD11b^{+}$ cells in K14.E7 skin, arginase-2 mRNA expression was 10 times lower than arginase-1 (Figure 2.4b). Thus, DNCB-activated myeloid cells ($CD45.2^{+}CD11b^{+}$) produce the increased arginase-1 observed in DNCB-treated K14.E7 skin.

CD11b is expressed on different myeloid subsets including macrophages/monocytes and granulocytes. To further define which cell subset expresses arginase-1 in DNCB-treated K14.E7 mice, we examined the expression level of arginase-1 in different populations of $CD11b^{+}$ cells based on the expression of macrophage marker F4/80 and granulocyte marker Gr1. We found that $F4/80^{+}Gr1^{int}$ cells expressed significantly higher levels of arginase-1 than other cell populations (Figure 2.4c). Furthermore, arginase-1 was abundantly expressed in inflammatory monocytes that express $Ly6C^{hi}Ly6G^{low}$ but not in $Ly6C^{low}Ly6G^{hi}$ granulocytes (Figure 2.4d).

Suppression of arginase ameliorates the ear swelling of inflamed K14.E7 skins

Arginase can be paradoxically involved in the upregulation or downregulation of inflammatory responses. N(omega)-hydroxy-nor-l-arginine (nor-NOHA), which is an intermediate in the l-arginine/NO pathway, is widely used as a specific, reversible inhibitor of arginase both *in vitro* and *in vivo* (145, 146). To understand whether arginase promoted or suppressed the inflammatory response of K14.E7 mice to DNCB, we administered nor-NOHA or saline buffer to K14.E7 mice 1 day before DNCB treatment and daily for 4 days.

Ear tissue was harvested after 24 hours of DNCB treatment with or without arginase inhibitor, and the expression and activity of arginase were determined. Nor-NOHA, as expected, did not suppress the transcription of arginase-1 gene (Figure 2.5a), but caused a concentration dependent inhibition of arginase activity in DNCB-treated K14.E7 ear skin (Supplementary figure 2.5). Increasing dose of nor-NOHA from 100 µg/mouse (used by Bratt et al. 2009) to 500 µg/mouse (used in this study) improved the inhibitory efficacy in DNCB treated K14.E7 ear skin (Figure 2.5b).

Furthermore, swelling of DNCB-treated K14.E7 skin was reduced in animals treated with arginase inhibitor (Figure 2.5c). Consistent with the ear swelling data, arginase inhibition decreased the number of infiltrating cells in the dermis of DNCB-treated K14.E7 mice (Figure 2.5d and e). These results demonstrate that arginase-1 induced by DNCB in K14.E7 transgenic ear skin, but not in C57BL/6 ear skin, itself contributes to exacerbated inflammatory response to DNCB in K14.E7 skin by recruitment of further inflammatory cells.

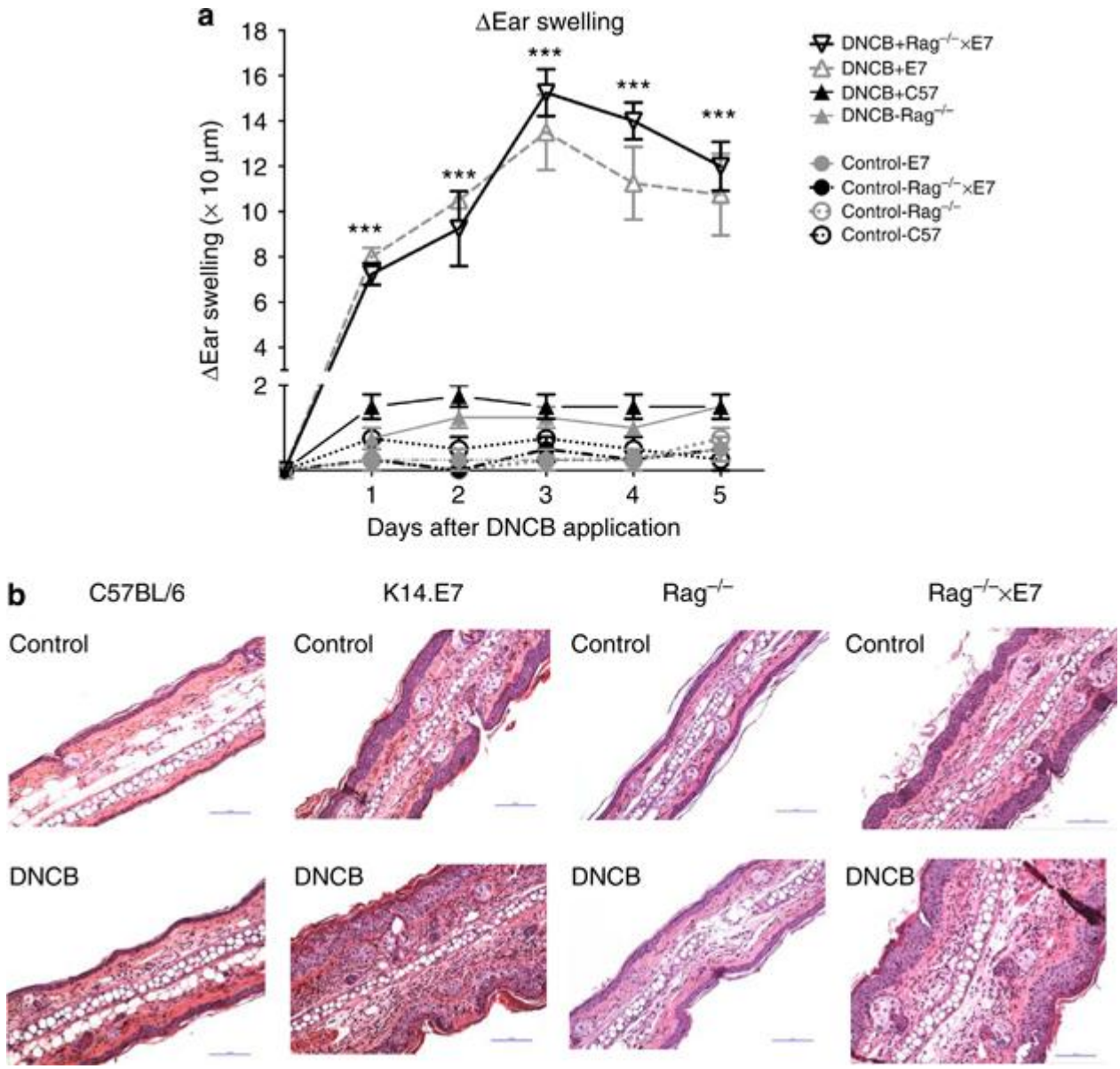

Figure 2.1- K14.E7 mice exhibit an enhanced inflammatory response to 2,4-dinitrochlorobenzene (DNCB). Ear swelling of C57BL/6, K14.E7, $Rag^{-/-}$, and $Rag^{-/-}$ × E7 mice in response to DNCB or vehicle over 5 consecutive days (**a**) measured by caliper. Data are means±SEM, and are representative of two independent experiments with four mice per group. ***P<0.001. Histology of representative sections from C57BL/6, K14.E7, $Rag^{-/-}$ × E7, and $Rag^{-/-}$mice (**b**) at 1 day post DNCB or vehicle application. Hematoxylin and eosin stain, original magnification × 200, scale bar=100 μm (representative of four mice per group).

Table 1- Expression of cytokine mRNA in response to DNCB or vehicle in K14E7 and C57 mice

Cytokine	Expression relative to housekeeping gene *RPL32*				*P*
	C57BL/6		K14.E7		
	Vehicle	DNCB	Vehicle	DNCB	
IL-1β (× 10^4)	6.8±0.8	51±4	221±132	1490±900	#, +, *, @
IL-6 (× 10^4)	50±8	55±29	142±103	5310±2870	+, @
IL-4 (× 10^{11})	1.3±2.2	3.0±3.1	15.1±14.2	74.5±53.3	+, @, *
Ptge2s (× 10^4)	75±74	91±127	158±34	480±124	+, @
IL-10 (× 10^4)	0.4±0.3	0.8±0.8	4.0±1.1	7.0±1.6	+, *
IFNγ (× 10^4)	0.2±0.2	0.11±0.12	1.9±1.1	1.1±0.9	*
TNFα (× 10^4)	3.2±2.9	2.7±1.6	41.3±15.2	3.4±2.2	*, @

Abbreviations: DNCB, 2,4-Dinitrochlorobenzene; mRNA, messenger RNA; Ptge2s, prostaglandin E2 synthase; TNFα, tumor necrosis factor-α.

#*P*<0.05 C57 DNCB versus vehicle.

+*P*<0.05 K14E7 DNCB versus vehicle.

**P*<0.05 K14E7 vehicle versus C57 vehicle.

@*P*<0.05 change in expression for DNCB-treated K14E7 versus DNCB-treated C57.

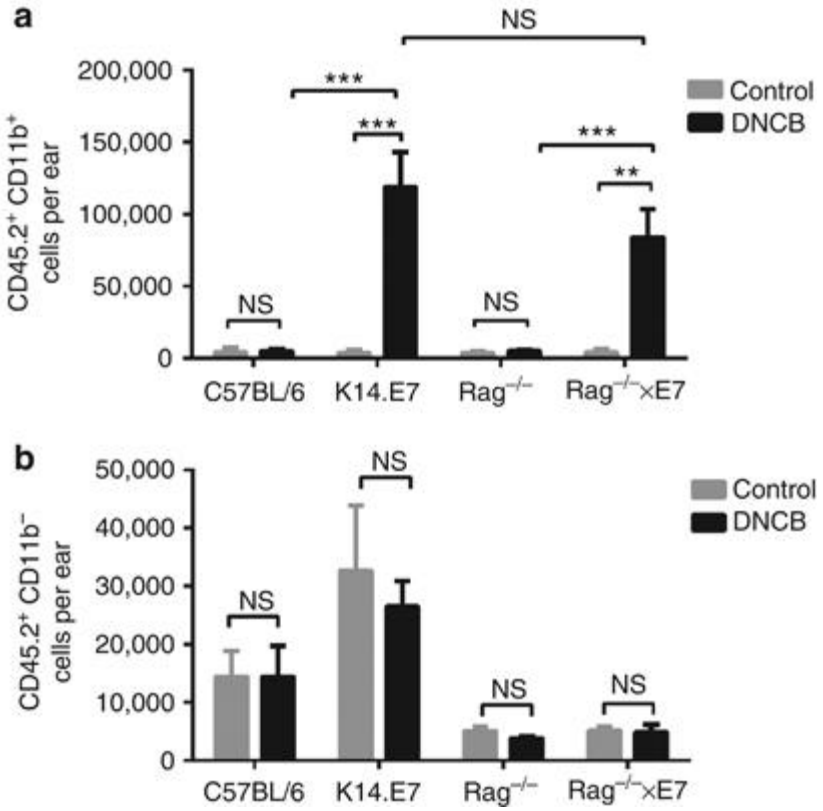

Figure 2.2- K14.E7 mouse skin has an enhanced myeloid cell infiltration in response to 2,4-dinitrochlorobenzene (DNCB). Absolute counts of leukocyte cells in the skin of C57BL/6 (*n*=4), K14.E7 (*n*=6), $Rag^{-/-}$ (*n*=5), and $Rag^{-/-}$ × E7 (*n*=5) mice following DNCB treatment. Absolute numbers of $CD45.2^{+}CD11b^{+}$ myeloid cells (**a**) and $CD45.2^{+}CD11b^{-}$ cells (**b**) were determined by flow cytometry. Data are presented as means±SEM and are representative of two independent experiments. NS, not significant. ***P*<0.01, ****P*<0.001.

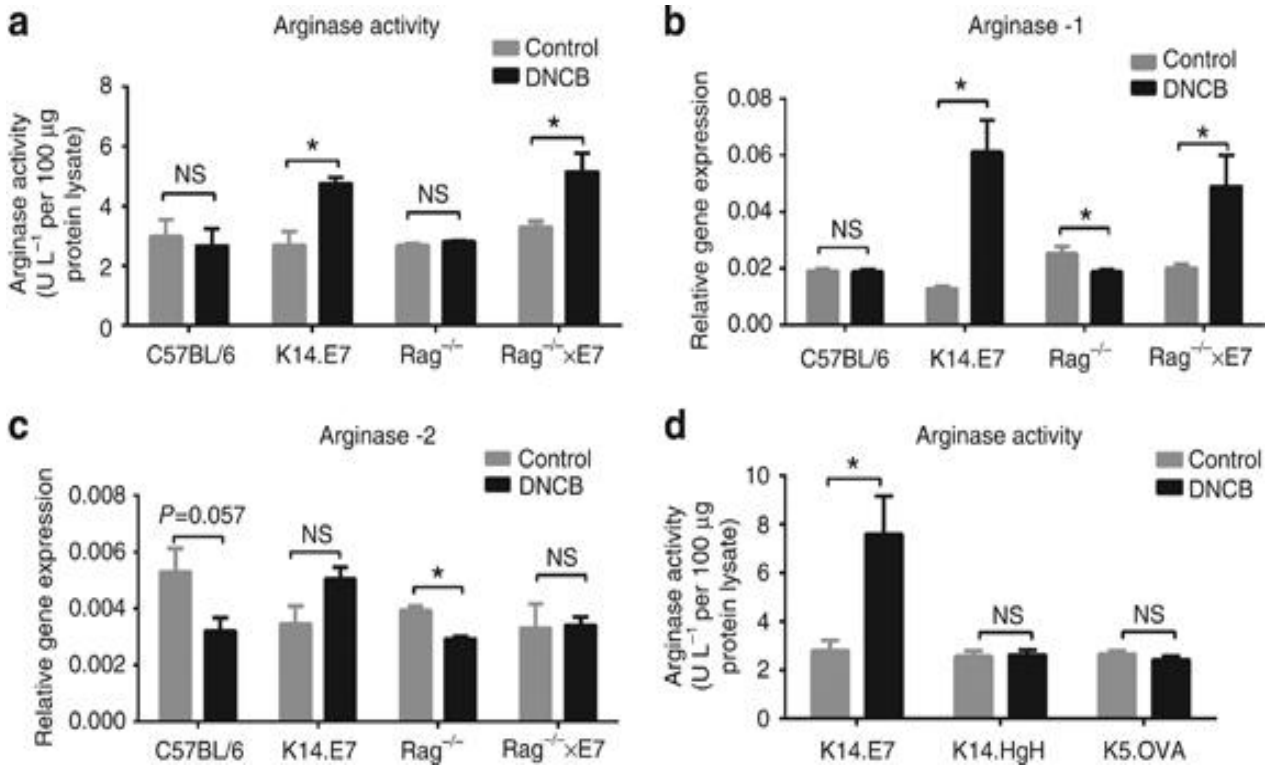

Figure 2.3- Arginase-1, but not arginase-2, is induced in K14.E7 mice following 2,4-dinitrochlorobenzene (DNCB) treatment, and this regulation is lymphocyte independent. Arginase activity was measured by determining the release of urea product from 100 µg of protein lysate per sample. Protein lysates were prepared from ear tissues of DNCB or vehicle-treated C57BL/6, K14.E7, $Rag^{-/-}$, $Rag^{-/-}$ × E7, K14.HgH, and K5.OVA ear tissues. Relative gene expression levels of (**b**) arginase-1 and (**c**) arginase-2 messenger RNAs were determined by real-time PCR in the skin of C57BL/6, K14.E7, $Rag^{-/-}$, and $Rag^{-/-}$ × E7 mice 1 day following DNCB treatment, normalized against the housekeeping gene *RPL32*. Data are presented as means±SEM and are representative of two independent experiments (*n*=4 mice per group). NS, not significant. **P*<0.05.

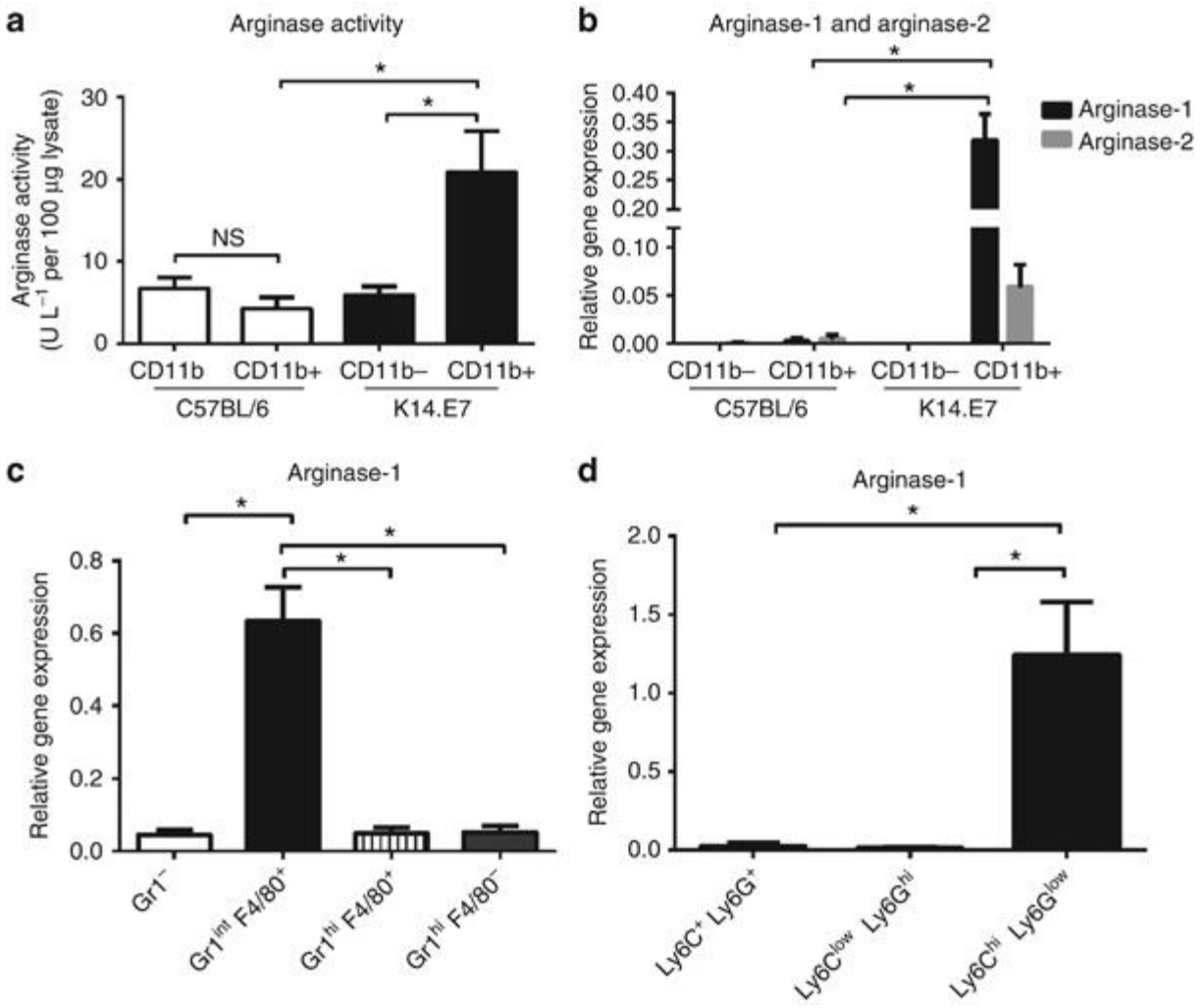

Figure 2.4- CD11b^{+}Gr1^{int}F4/80^{+}Ly6G^{low}Ly6C^{hi}cells produce arginase in 2,4-dinitrochlorobenzene (DNCB)-treated K14.E7 skin. Arginase activity produced by CD45.2^{+}CD11b^{+} and CD45.2^{+}CD11b^{-} populations from DNCB-treated C57BL/6 and K14.E7 mice (**a**) was determined as described in Materials and Methods. Arginase-1 and arginase-2 mRNA expression (**b**) levels were determined by real-time PCR. Arginase-1 messenger RNA (mRNA) expression levels in Gr1^{-}F4/80^{+}; Gr1^{int}F4/80^{+}; Gr1^{hi}F4/80^{+}; and Gr1^{-}F4/80^{-} subsets from DNCB-treated K14.E7 mice were determined (**c**) by real-time PCR. Real-time PCR analysis of arginase-1 mRNA expression in different cell subsets (**d**) was based on the expression of Ly6C and Ly6G antigens. Data were pooled from four independent experiments. In each experiment, six C57BL/6 and two K14.E7 mice were treated with DNCB or vehicle. Means±SEM. NS, not significant. *P<0.05.

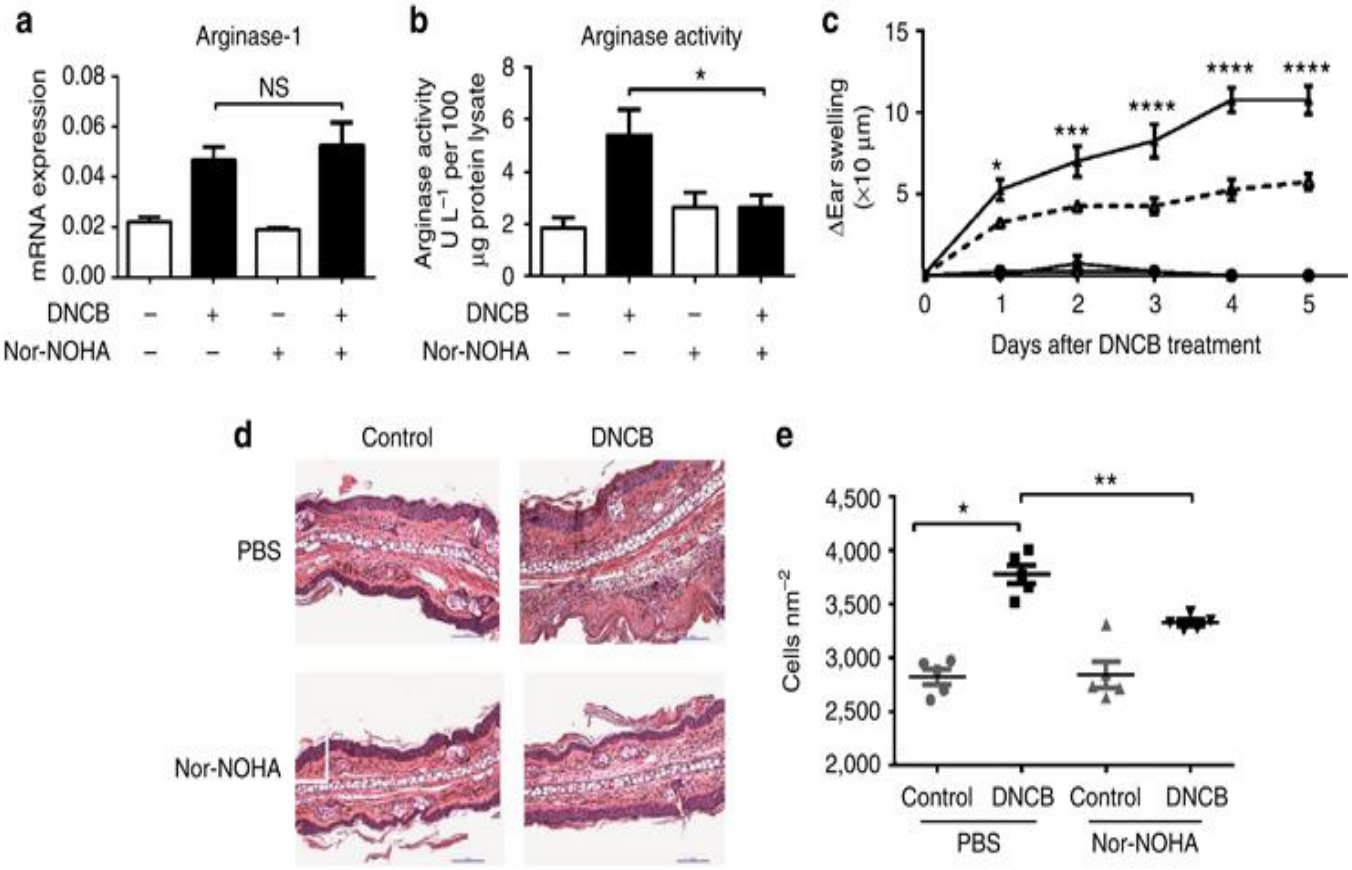

Figure 2.5- Inhibition of arginase ameliorates the ear swelling of dinitrochlorobenzene (DNCB)-treated K14.E7 mice. Mice were injected with 500 µg of arginase inhibitor (N^{ω}-hydroxy-nor-l-arginine (nor-NOHA)) or saline buffer 1 day before DNCB treatment and daily for 5 days. Arginase-1 messenger RNA (mRNA) expression (a) and arginase activity (b) in saline or nor-NOHA-treated K14.E7 mice after 24 hours of exposure to DNCB, determined by real-time PCR and arginase assay, respectively. Ear swelling of K14.E7 mice treated with saline (solid line) or nor-NOHA (dashed line) monitored during 5 days after DNCB treatment (c). Histological sections (d) and quantification of cell numbers infiltrating into the dermis from Nor-NOHA or saline-treated K14.E7 skins 1 day following DNCB application (e). Means±SEM, data show results from two independent experiments (n=5). NS, not significant; PBS, phosphate-buffered saline. *P<0.05, **P<0.01, ***P<0.001, ****P<0.0001.

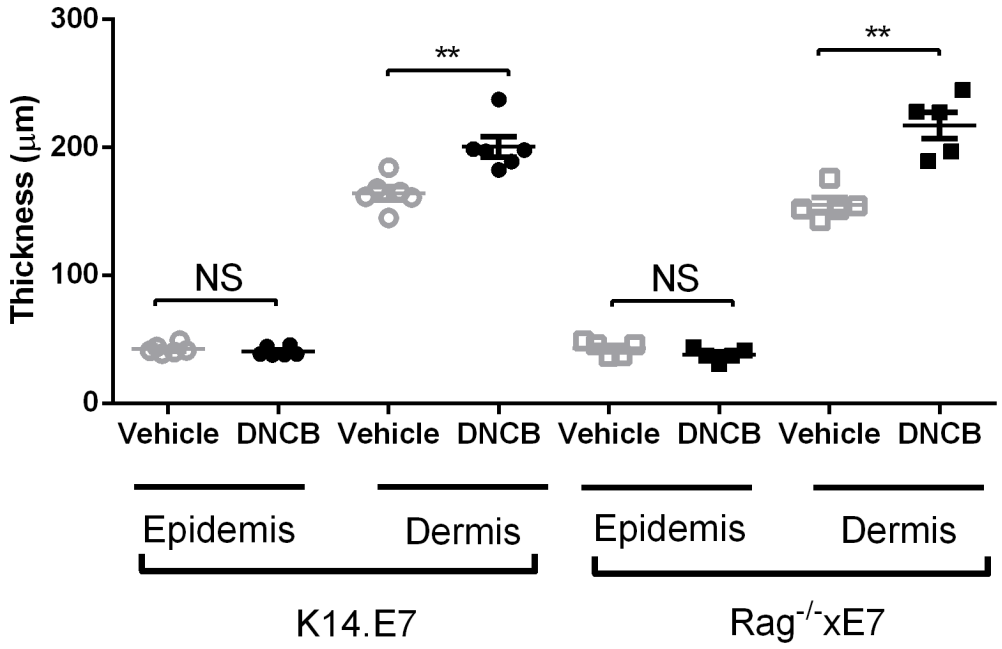

Supplementary figure 2.1- Dermal thickness but not epidermal thickness is augmented in both K14.E7 and Rag$^{-/-}$xE7 mice following DNCB application.

The average thickness of epidermis and dermis of vehicle or DNCB treated K14.E7 mice (n=6 mice) determined by using images of Hematoxylin and Eosin stained sections. Ten fields counted per mouse were selected randomly and the epidermal and dermal thickness were determined by using NIS Elements imaging software version 3.2 (Nikon). Data presented indicate means ± SEM. ** p<0.01, NS nonsignificant.

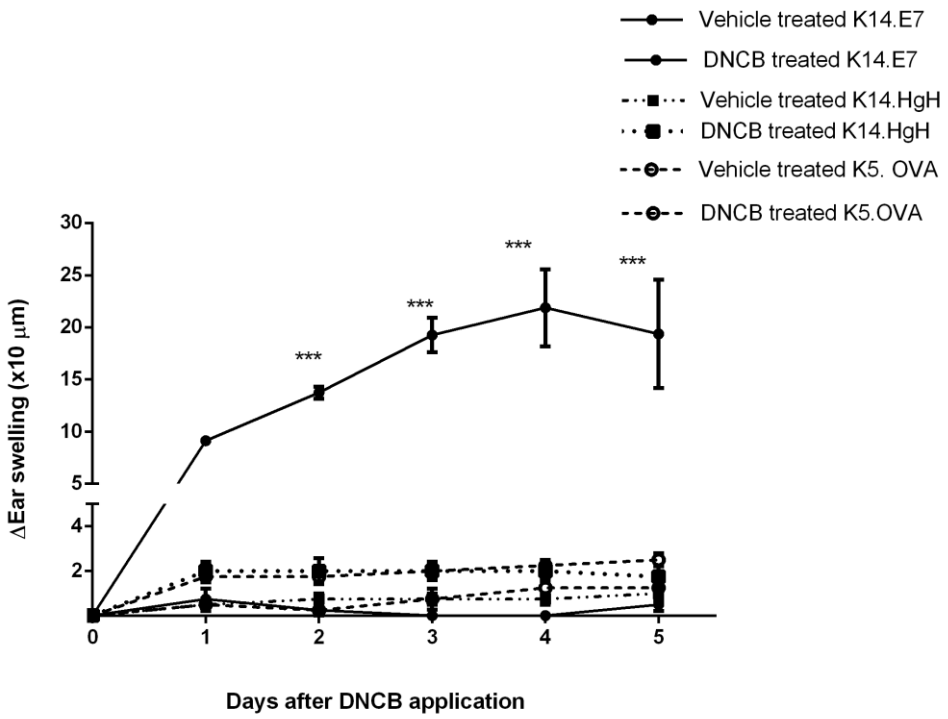

Supplementary figure 2.2- K14.E7; K14.HgH and K5.OVA mice displayed similar level of ear swelling following DNCB treatment.

The ear swelling of K14.E7; K14.HgH and K5.OVA mice (n=4 mice per group) within four consecutive days. Data presented indicate means ± SEM,** *P*<0.01, *** *P*<0.001.

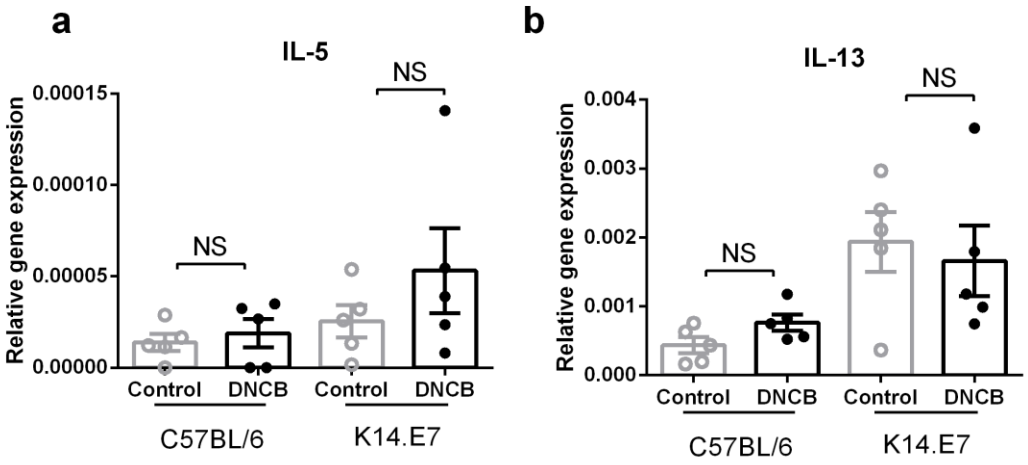

Supplementary figure 2.3- Th2 cytokine IL-5 and IL-13 production in K14.E7 skin remains unchanged following DNCB application. Relative gene expression levels of (**b**) IL-5 and (**c**) IL-13 messenger RNAs were determined by real-time PCR in the skin of C57BL/6, K14.E7 1 day following DNCB treatment, normalized against the housekeeping gene *RPL32*. Data are presented as means±SEM. NS, not significant. **P*<0.05.

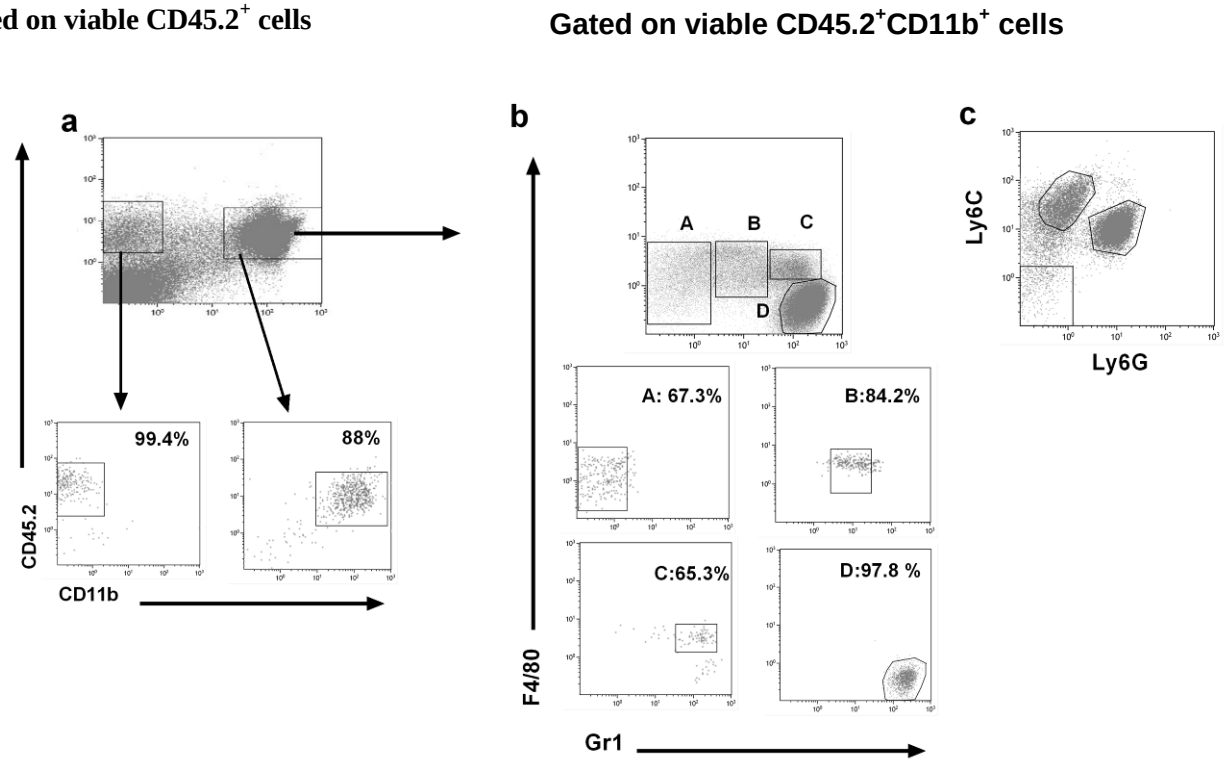

Supplementary figure 2.4- **Representative flow cytometry dot plots illustrating gating strategy and post-sort purity of CD45.2$^+$CD11b$^+$ and CD45.2$^+$CD11b$^+$ cell populations.** (a) Equal number of CD45.2$^+$CD11b$^+$ and CD45.2$^+$CD11b$^-$ subset was sorted from C57BL/6 or K14.E7 mice after one day of DNCB treatment (upper panel) and post-purity of each subset was accessed (lower panel). (b) and (c) Gating strategy and post-sort purity of different myeloid subsets based on the expression of F4/80 and Gr1 (b) or Ly6C and Ly6G antigens (c).

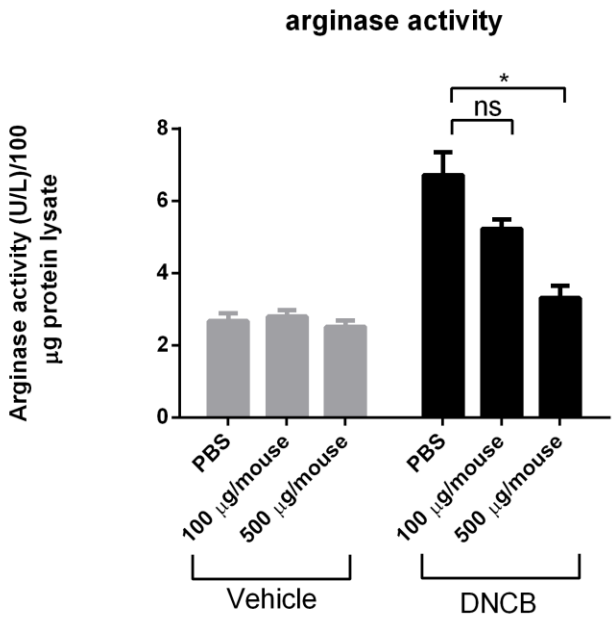

Supplementary figure 2.5- Concentration effect of nor-NOHA on arginase activity in DNCB treated K14.E7 skin. K14.E7 mice (n=4) were injected i.p. with 500 µg, 100 µg of nor-NOHA or saline buffer (PBS) alone. The treatment was repeated two hours prior DNCB/vehicle application. Arginase activity in ear tissues after 24 hours of exposure to DNCB was determined by arginase assay. Means ± SEM, *p<0.05, ns= not significant.

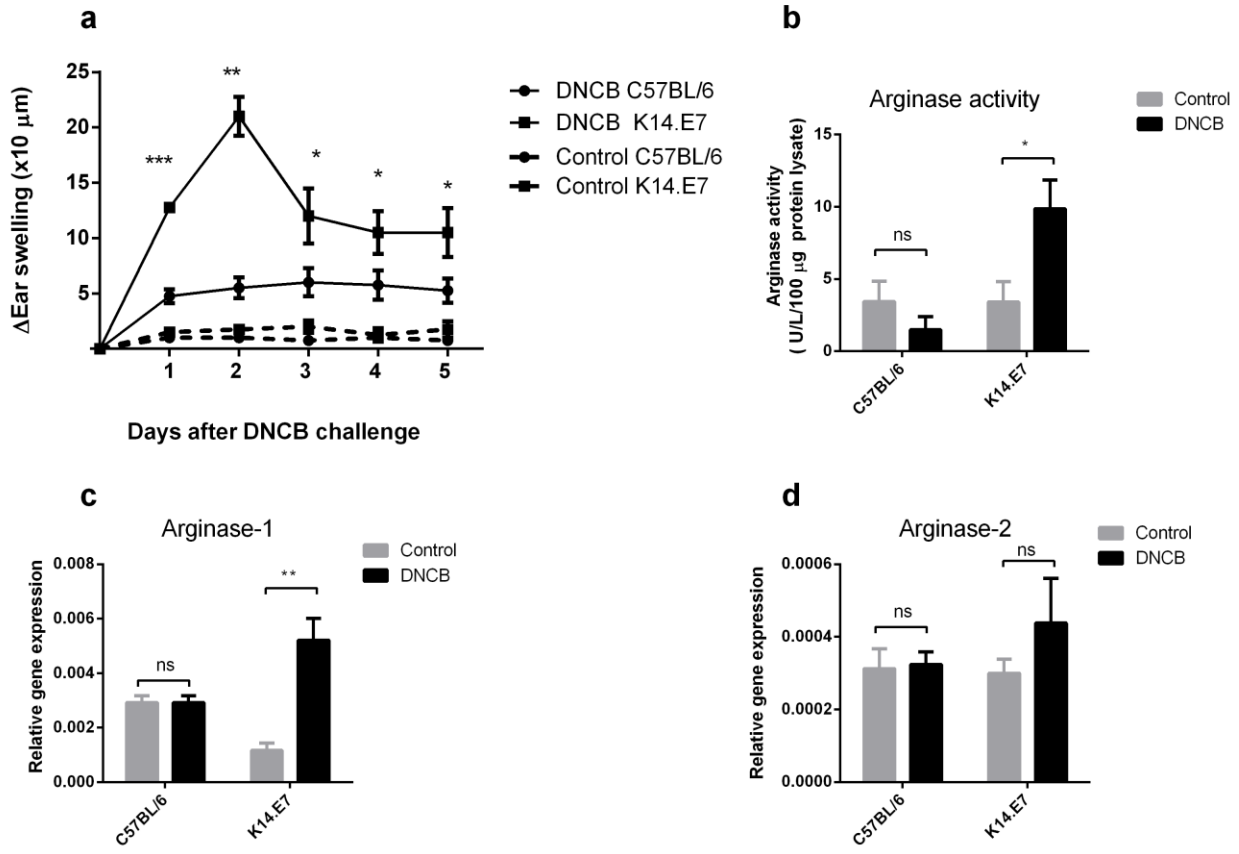

Supplementary figure 2.6- Sensitized K14.E7 mice exhibit enhanced ear swelling response, arginase-1 mRNA and arginase activity after DNCB challenge. K14.E7 and C57BL/6 mice were sensitized topically with 5% of DNCB on the abdomen. Five days later, all mice were challenged with 1% of DNCB (left ear) or vehicle (right ear). The ear swelling was measured within five day after DNCB challenge (a). Arginase activity in ear tissues harvested 24 hours after DNCB challenge was assessed by arginase assay (b). Relative gene expression of arginase (c) and arginase-2 (d) were determined by real-time PCR in ear tissues of C57BL/6 and K14.E7 mice 1 day after DNCB challenge. Means ± SEM, n= 5 mice per group, *p<0.05, **p<0.01, *** p<0.001, ns= not significant.

Discussion

DNCB triggers a T-cell–independent inflammatory response through the activation of the NALP-3 inflammasome in keratinocytes (147), and it has been used to treat HPV-associated genital warts. Despite its efficacy, this chemical is potentially mutagenic and carcinogenic (66). Therefore, we sought to understand the influence of the expression of the major oncogenic protein of HPV16, E7, on the inflammatory mechanism induced by DNCB using mice transgenic for the E7 protein expressed in keratinocytes. Here, we show that the acute response to DNCB in previously unexposed mice is significantly higher in K14.E7 transgenic mice than in nontransgenic mice. In response to DNCB-induced inflammasome activation, keratinocytes have been shown to produce a wide range of proinflammatory cytokines including IL-6 and IL-1β (148, 149), which are known to be responsible for the recruitment of polymorphonuclear cells (140, 141). We indeed found an increased number of inflammatory myeloid cells in the dermis and enhanced mRNA expression levels of IL-6 and IL-1β, in DNCB-treated K14E7 transgenic mice, and show further that DNCB-induced IL-1β and IL-6 production was greatly enhanced in K14E7 skin when compared with nontransgenic skin. We could not detect significant induction of IL-6 in nontransgenic skin. Therefore, we hypothesize that this cytokine might be a regulator of inflammatory cell infiltration in K14.E7 skin and its ear swelling. Premalignant skin of HPV16.E7 transgenic mice is characterized by hyperplastic epidermis and infiltration of innate immune cells of myeloid origin. The presence of these cells in K14.E7 skin might be responsible for the marked inflammatory response to short-term DNCB treatment and inflammasome activation. Interestingly, we were not able to detect these responses to DNCB in other transgenic skin including K14.hGh and K5.OVA (Supplementary figure 2.2), suggesting that they are unique to K14.E7 mice, a consequence of the presence of HPV.E7 oncoprotein in the skin.

DNCB treatment of K14.E7 mice significantly induced mRNA expression of Th2 cytokine IL-4 and IL-10, when compared with wild-type mice. This finding is consistent with the finding in a mouse model of allergic skin inflammation, in which Th2 cytokines are responsible for the amplification and chronicity of allergic skin inflammation (74), and with a study in which IL-4-deficient mice displayed an impaired ear swelling response to DNCB application (73). Furthermore, we show that DNCB-treated K14.E7 skin exhibited an accumulation of $CD11b^+$ myeloid cells, but not of non-myeloid bone marrow–derived cells,

which are mainly lymphocytes. Th2 cytokines induce arginase activity in myeloid cells including macrophages and dendritic cells (150, 151). Arginase-2 can be expressed by macrophages, and it has structural and enzyme characteristics similar to arginase-1 (152), but it remained unchanged in K14.E7 skin. Thus, the higher level of arginase activity in DNCB-treated K14.E7 mice is mainly contributed by arginase-1, and is promoted possibly by higher levels of Th2 cytokines and by accumulation of myeloid cells.

One predicted source of enhanced Th2 cytokine production in DNCB-treated K14E7 skin would be Th2 $CD4^+$ lymphocytes. Indeed, K14E7 skin has a large number of $CD4^+$ lymphocytes (139). However, we demonstrate here that the induction of arginase-1 and enhanced ear swelling response of K14.E7 skin are independent of lymphocytes. To confirm that, we performed experiments in sensitized animals and showed that following DNCB treatment, sensitized K14.E7 skins also displayed significantly enhanced ear swelling, arginase-1 mRNA and arginase activity production compared to non-transgenic skin as observed in non-sensitized mice (Supplementary figure 2.6). Th2 cytokines, which induce arginase-1 expression and hyperinflammatory response in DNCB-treated K14.E7, might therefore be derived from innate immune cells (153, 154) or epithelial cells (155). We also detected the induction of prostaglandin E2 synthase in DNCB-treated K14.E7 skin. Our data are consistent with a previous study that HPV16.E7 oncoprotein induced cyclooxygenase-2 transcription and prostaglandin E2 synthase production (156). Furthermore, the cyclooxygenase 2–Pteg2s synthase axis has been shown to induce arginase-1 in myeloid cells in a tumor environment (157). However, further studies are needed to address the induction mechanism of arginase-1 in DNCB-treated K14.E7 skin.

Cells producing arginase-1 in K14.E7 skin were positive for F4/80 and Ly6C antigen, and express Gr1 at the intermediate level. This population has been defined as monocytic myeloid suppressive cells or inflammatory monocytes, which appear to adopt an immune stimulatory or suppressive function depending on the local environment (158). Indeed, $CD11b^+Gr1^+$ cells during the early phase of polymicrobial sepsis exhibit proinflammatory phenotypes, whereas this cell population becomes immature and immune suppressive in the late phase (159). Apart from IL-4 and IL-10, the induction of other Th2 cytokines including IL-5 and IL-13 could not be detected in DNCB-treated K14.E7 skin (Supplementary figure 2.3).

To understand the role of arginase in the hyperinflammation in K14.E7 skin, we used the compound nor-NOHA, which efficiently suppresses arginase-1 and arginase-2 activity in *in vitro* and *in vivo* studies (145, 146). Nor-NOHA abrogates the function of arginase by modifying the structure of the enzyme, and it does not affect the transcription of the arginase gene, consistent with an unaltered arginase mRNA level (160). Arginase inhibitor treatment decreased the arginase activity and the level of leukocyte infiltrate and ear swelling in DNCB-treated K14.E7 mice. This suggests that enhanced arginase activity is critically required for the strong and sustained inflammatory response and that arginase inhibitor alleviates DNCB-induced inflammation by decreasing the recruitment of leukocytes in the skin. Arginase efficiently competes with inducible nitric oxide synthase for the common substrate, l-arginine, leading to the inhibition of inducible nitric oxide synthase expression and NO production. As endothelium-derived NO is reported to suppress the expression of adhesion molecules such as vascular cell adhesion molecule-1 and intercellular adhesion molecule-1 (123), limiting of NO bioavailability through arginase results in enhanced vascular inflammation (124). In a mouse model of atherogenesis, arginase-2 but not arginase-1 enhances monocyte adhesion to endothelial cells and triggers the production of proinflammatory cytokines through mitochondrial reactive oxygen species (126). Liu *et al.* (2013) show that infiltrating myeloid cells produce arginase-1, which promotes angiogenesis and further recruitment of monocytes in a laser-induced injury murine model (127).

Taken together, our findings demonstrate that HPV16.E7 oncoprotein–expressing skin develops a hyperinflammatory response to DNCB via an arginase-1-dependent mechanism. These findings provide insights into the proinflammatory role of arginase-1 in HPV16.E7-expressing skin in response to immunostimulation by DNCB.

Materials and Methods

Mice

K14.HPV16E7 (K14.E7) mice were generated from inbred strain C57BL/6 (161). K14.E7, K14.HgH, and $Rag^{-/-}$, all on a C57BL/6 background, were purchased from Animal Resources Center (Perth, Australia). K5.mOVA mice on a C57BL/6 background were kindly provided by H. Azukizawa (162). $Rag^{-/-}$ × E7 mice were generated by crossing male K14.E7 with female $Rag1^{-/-}$ knockout C57BL/6 mice; heterozygous K14E7 mice were crossed and then backcrossed with homozygous $Rag1^{-/-}$ mice to an F2 generation (161). All mice were maintained under specific pathogen-free conditions at Princess Alexandra Hospital Biological Research Facility. Experimental mice were sex-matched and used at 6–9 weeks of age. All animal procedures complied with guidelines approved by the University of Queensland Animal Ethics Committee.

DNCB treatment

DNCB (Sigma, Sydney, New South Wales, Australia) was dissolved in vehicle (acetone: olive oil (4:1)) immediately before use. Six- to nine-week-old mice were treated with 20 µl of 1% DNCB or vehicle on the left ear and right ear, respectively. After 24 hours, the ear tissues were collected for mRNA and protein analysis. Ear thickness was measured by using the digital caliper, and change in ear swelling was determined by calculating the mean increase in ear thickness compared with untreated ears.

Histological analysis

Ear tissues were fixed using 4% paraformaldehyde. Tissues were embedded in paraffin and 7-µm sections were prepared and stained with hematoxylin and eosin. Immune cell infiltration was evaluated by light microscopy and quantified by using the Nis-elements Br 3.2 software (Nikon Instruments, New York, NY).

Real-time PCR

RNA was isolated from homogenized tissues by using the RNaeasy Mini kit (Qiagen, Melbourne, Victoria, Australia). RNA extracts were quantified using absorption of light at 260 and 280 nm (A260/280). Details of the procedures and primers used for the quantitative real-time PCR are described in Supplementary Methods online.

Arginase activity

Arginase activity was measured by colorimetric determination of urea formed from l-arginine, as previously described (163). Details of the procedures are desbribed in Supplementary Methods.

Flow cytometry and cell sorting

Flow cytometry staining was performed as previously described (44). Details of flow cytometry and cell sorting are described in Supplementary Methods

Statistical analysis

Each data point represents the mean±SEM and is representative of two independent experiments with at least four mice per group.

Prism (Graph pad Software, La Jolla, CA) was used for graphs and statistical analysis: **P*<0.05;***P*<0.01; ****P*<<0.001; ****P<0.0001. Multiple comparisons of ear swelling data were derived by two-way analysis of variance. For other data, statistically significantly differences between groups were analyzed by non-parametric Mann–Whitney-Wilcoxon test.

Inhibition of arginase activity

Mice were injected i.p. with either 500 µg of Nor-NOHA/500 µl PBS or 500 µl of PBS alone one day prior to DNCB treatment. The treatment was repeated daily for 5 consecutive days. Nor-NOHA is a synthetic analog of NOHA, an intermediate of L-arginase pathway. The inhibitor specifically interacts with the manganese-cluster of the enzyme active site of arginase and does not function as a substrate or as an inhibitor for other factors (164). There

is extensive literature confirming specificity of nor-NOHA as a specific inhibitor of arginase *in-vitro* (145) and *in-vivo* (146).

Arginase activity

Briefly, ear tissues were homogenized in PBS buffer containing protease inhibitor cocktail (Roche Diagnostics, New South Wales, Australia), centrifuged and supernatants collected. Protein concentration was determined by using bicinchoninic acid (BCA) assay (Thermo Fisher Scientific, Victoria, Australia). 50 µl of tissue lysate was preactivated by adding 50 µl of 10 mM $MnCl_2$/50 mM Tris/HCl at pH 7.5 and heating for 10 min at 56^{o}C. 50 µl of 0.5 M L-arginine substrate (pH 9.5) was added to the samples and further incubated at 37oC for 120 min. The reaction was stopped by adding 400 µl of H_2SO_4: H_3PO_4: H_2O (1:3:7, v/v/v). After adding 25 µl of 9% 1-phenyl-1,2-propanedione-2-oxime, the samples were then boiled for 45 min at 100^{o}C. Urea concentration was determined using a spectrophotometer at 540 nm. Using a standard curve, arginase activity was calculated as units/ml/100 mg protein lysate. One unit of Arginase is the amount of enzyme that will convert 1.0 mmole of L-arginine to ornithine and urea per minute at pH 9.5 and 37 °C (165).

Real-time PCR reaction

For cDNA synthesis, 500 ng of total RNA was reverse transcribed in 20 µl reaction containing 5 mM $MgCl_2$; 1.6 mM dNTP mix, 2.5 mM oligo-dT, 1 µl of MuLv reverse transcriptase 5000U (Applied Biosystems, Victoria, Australia) and 10 units of RNaseOUT (Invitrogen, Victoria, Australia) at 42^{o}C for 60 min. The reactions were heated at 70oC for 15 min to inactivate reverse transcriptase enzyme. cDNA product was diluted at 1:4 and 2.5 µl was subjected to real-time PCR reaction using SYBR TAKA kit (Scientifix, Victoria, Australia) and primers (Integrated DNA Technologies, Iowa, United States) listed in supplementary table 1. The relative expression of arginase-1 and arginase-2 was determined by normalizing against the house keeping gene encoded ribosomal protein RPL32.

Supplementary Table 1- Primers used for real time PCR determinations

Gene	Forward 5’ – 3’	Reverse 3’ – 5’
Arginase-1	AAGAATGGAAGAGTCAGTGTGG	GGGAGTGTTGATGTCAGTGTG
Arginase-2	GATCTCTGTGTCATCTGGGTTG	AATCCTGGCAGTTGTGGTAC
IL-4	CGAATGTACCAGGAGCCATATC	TCTCTGTGGTGTTCTTCGTTG
IL-10	GGAGTCGGTTAGCAGTATGTTG	AGCCGGGAAGACAATAACTG
IFN-γ	GAACTGGCAAAAGGATGGTGA	TGTGGGTTGTTGACCTCAAAC
Ptge2s	CAGTATTACAGGAGTGACCCAG	AAATGTATCCAGGCGATCAGAG
IL-6	CAAAGCCAGAGTCCTTCAGAG	GTCCTTAGCCACTCCTTCTG
IL-1β	GTTGATTCAAGGGGACATTA	GTTGATTCAAGGGGACATTA

Flow cytometry and cell sorting

Single cell suspensions were prepared from ear tissues by using collagenaseD/dispase (Roche Diagnostics) and grinding through a 70µm cell strainer. After adding Fcγ receptor block (Fcγ III/II receptor; BD Biosciences, Auckland, New Zealand, 1/50) and incubating on ice for 10 min, cells were stained with live/dead aqua dyes (Live/Dead fixable aqua dead cell stain kit, Invitrogen, 1/1000) and antibodies specific for the following markers for 30 min at 4˚C: CD45.2-PE-Cy7 (BD Biosciences, 1/200); CD11b-PE (BD Biosciences, 1/100), F4/80-FITC (eBioscience, San Diego, United States 1/100), and Gr1(Ly6G/Ly6C)-APC (eBioscience, 1/200), Ly6G-Alexa 700 (Biolegend, San Diego, United State, 1/200), Ly6C-APC.Cy7 (Biolegend, 1/100). Stained cells were acquired on a LSIR II or FACSCanto flow cytometer (BD Biosciences) and analyzed using Kaluza software (version 1.2, Beckman Coulter, New South Wales, Australia).

For cell sorting, ear tissues were processed as described above. Cells were stained in FACS staining buffer with anti–CD11b-PE, anti–CD45.2-PeCy7, anti-F4/80-FITC and anti-Gr1 (Ly6G/Ly6C)-APC. Viable $CD45.2^{+}CD11b^{-}$; $CD45.2^{+}CD11b^{+}$; and 5 different subsets of $CD45.2^{+}CD11b^{+}$ cells (Gr1-; $F4/80^{hi}Gr1^{int}$; $F4/80^{low}Gr1int$; $F4/80^{hi}Gr1^{hi}$; $F4/80^{-}Gr1^{hi}$) were sorted under BSL2 conditions on MoFlo Astrios cell sorter (BD Biosciences).

RNA from sorted cells was isolated by the RNAzol method (Sigma).

Total protein was isolated from sorted cells by resuspending cells in 50 µl of lysis buffer (20 mM Tris, 100 mM NaCl, 1 mM EDTA, 0.5% Triton X100) and incubating for 20 min. After centrifugation at 13,000 g at $4^{o}C$ for 20 min, the supernatant was collected for protein quantification (BCA) and arginase assay.

Conflict of interest

The authors state no conflict of interest.

Acknowledgments

This work was supported by grants from the National Institutes of Health (5U01CA141583), National Health and Medical Research Council of Australia (569938), Australian Research Council, Cancer Council Queensland, and Australian Cancer Research Foundation. Tran is a recipient of University of Queensland fellowship for international students. We thank the staff of the Biological Research Facility at Princess Alexandra Hospital for excellent technical assistance with animal care.

2.3 Additional data not described in the article 1

Arginase enhances nitric oxide (NO) production in DNCB-treated K14.E7 skin

As mentioned in 1.6, arginase-1 efficiently competes with iNOS for the common substrate L-arginine, leading to the inhibition of iNOS expression and NO production. Since NO has been reported to play an important role during cutaneous inflammation (166), we examined a possible contribution of arginase to the regulation of iNOS mRNA expression and NO production in DNCB-treated C57BL/6 and K14.E7 skin. Compared to non-detectable values in wild-type skin, the levels of iNOS mRNA expression and NO production were significantly induced in K14.E7 skin after DNCB application (Figure 2.6a and b). Unexpectedly, we found that blockade of arginase activity resulted in a trend towards decreased iNOS mRNA expression (Figure 2.6a) and a significant reduction of NO production in DNCB-treated K14.E7 skin (Figure 2.6b). Thus, these data suggested that DNCB treatment of K14.E7 mice induced NO production in the skin and that arginase might promote, rather than suppress, NO production. Given that the inhibitor used in this study specifically targeted arginase (167), this paradox can be explained by the impact of arginase on the recruitment of innate immune cells, including NO-producing cells rather than the competition for L-arginine substrate. Indeed, NO can be produced by many innate immune cell types, including macrophages, neutrophils, DCs (168) raising the possibility that arginase-1 might indirectly promote iNOS gene expression and NO production by enhancing the infiltration of NO-producing cells. Taken together, stimulation of NO-producing cell infiltration might be a potent mechanism by which arginase drives the DNCB-induced hyperinflammation in K14.E7 skin. This hypothesis is supported by a previous study showing that NO-derived neutrophils is involved in stimulating further neutrophil accumulation into the skin, thereby promoting zymosan-induced cutaneous inflammation (166).

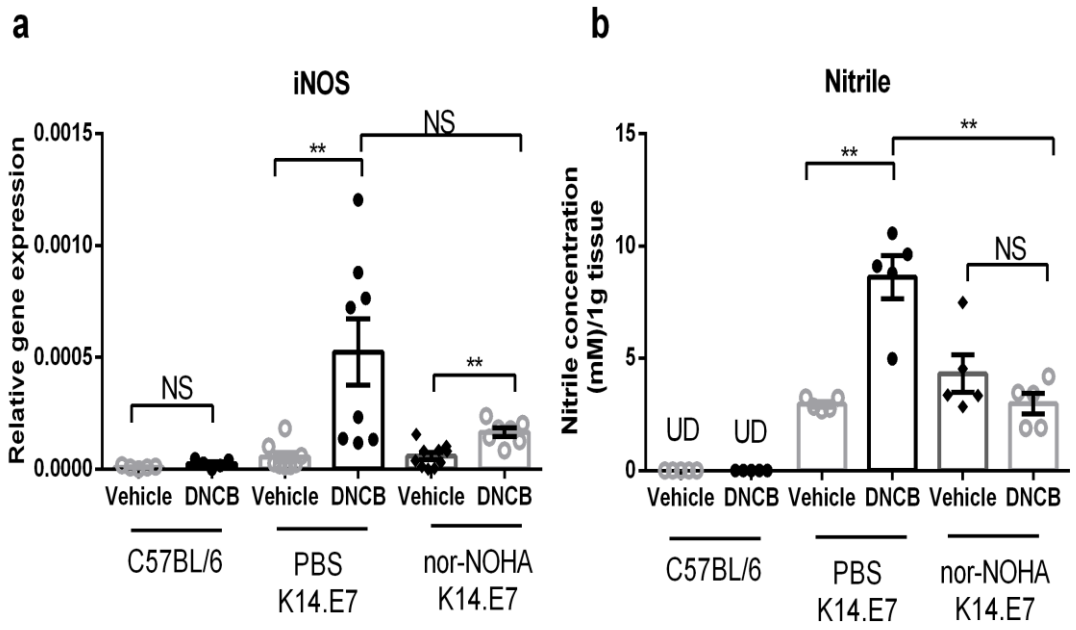

Figure 2.6- Suppression of arginase attenuates NO production in DNCB-treated K14.E7 skin. K14.E7 mice were injected with 500 µg of arginase inhibitor, nor-NOHA or saline buffer (PBS) 1 day before and 1 hour before DNCB treatment. Ear skin tissue was harvested for RNA isolation or skin explant culture. **(a)** iNOS mRNA expression in C57BL/6 and nor-NOHA or PBS-treated K14.E7 skins at day 1 following DNCB application, determined by real-time PCR. (b) NO production in the supernatants of these skin explants measured by the Griess reaction. Data are presented as means±SEM. UD, undetermined; NS, not significant. *, $P<0.05$.

2.4 Supplementary methods

iNOS gene expression

Relative expression of iNOS mRNA was determined by real-time PCR as described in materials and method in 2.1. The sequence of forward and reverse iNOS primers were: 5' GCAAACATCACATTCAGATCCC 3' and 5' TCAGCCTCATGGTAAACACG 3', respectively.

Griess assay-NO production

Nitrite concentration as a reflection of NO production was determined by the Griess reaction as previously described (169). Briefly, 24 hours after DNCB application, ears were excised, split into halves and placed dermis side down on 2 ml of complete DMEM (10% (v/v) fetal bovine serum, 1 mM penicillin/streptomycin/glutamine, 1mM sodium pyruvate and 10 mM HEPES (Gibco)) at 37^{o}C, 5% CO_2. After 24 hours, 100 µl of skin explant supernatant and or $NaNO_2$ standards were incubated in duplicate with 100µl Griess reagent (0.5% sulfanilamide, 0.05% naphthyldiamine dihydrochloride (Sigma) in 5% H_3PO_4) for 10 min. The plates were read at 550 nm.

2.5 Conclusion

In this chapter, I have shown that DNCB application to skin expressing HPV16.E7 as a transgene results in an acute hyperinflammatory response, which is not seen in nontransgenic control animals. The E7-associated hyperinflammation is manifested by the induction of Th2 cytokines and recruitment of $CD11b^{+}Gr1^{int}F4/80^{+}Ly6C^{hi}Ly6G^{low}$ myeloid cells, producing arginase-1. Consequently, arginase-1 mediates DNCB-induced acute inflammation by enhancing the recruitment of more leukocytes and production of NO.

However, many questions remain unanswered. First of all, as I have found that the regulation of arginase-1 and DNCB-induced hyperinflammation in K14.E7 skin are independent of T and B cell function, it would be interesting to address whether Th2 cytokines or other cytokines released from innate immune cells are involved in the induction of arginase-1. Secondly, how arginase and its inducers mediate DNCB-induced hyperinflammation in K14.E7 skin requires further study. Furthermore, whether innate immune activation mediated by DNCB can break the tolerance of HPV16.E7 oncoprotein. Lastly, is the induction of arginase in DNCB-induced hyperinflammation dependent on the expression of HPV16.E7 protein in the skin?

CHAPTER 3

IL-17A Mediates Arginase-1 induction and DNCB-induced inflammation in HPV16.E7 expressing skin

3.1 Foreword

Data shown in chapter 2 demonstrated the significant contribution of arginase-1 to the DNCB-induced acute hyperinflammation in HPV16.E7 expressing skin. However, the molecular basis regulating arginase-1 expression in association with HPV16.E7 oncoprotein has not been previously elucidated. It has been well established that the regulation of arginase-1 is dependent on the cytokine milieu in which arginase-1 is primarily induced in response to Th2 cytokines. In addition, recent studies have shown that IL-17A is implicated in the induction of arginase-1 by myeloid cells in epithelial inflammatory diseases including asthma and colitis. This chapter therefore aims to investigate the possible involvement of these cytokines in the regulation of arginase-1 and development of hyprerinflammatory response to DNCB. The study has been submitted to Journal of Immunology and formatted as requested by the journal.

Furthermore, it has been reported that immunization therapy with HPV16.E7 oncoprotein alone is not sufficient to induce rejection of K14.E7 skin graft. This chapter also addressed whether DNCB-induced inflammation combined with E7 specific vaccination therapy enables the rejection of K14.E7 skin graft.

.

3.2 Article 2

Interleukin-17A Promotes Arginase-1 Production And DNCB-Induced Acute Hyperinflammation In Human Papillomavirus E7 Oncoprotein Expressing Skin[1,2]

Running title: IL-17A in DNCB-induced hyperinflammation in Human Papillomavirus E7 oncoprotein expressing skin

Tran L.S.[*], Mittal D[†], Mattarollo S.R.[*], Frazer I.H.[*]

Author Affiliations

[*] The University of Queensland Diamantina Institute, Translational Research Institute, Woolloongabba, Brisbane, Queensland, Australia.

[†] QIMR Berghofer Medical Research Institute, Herston 4006, Queensland, Australia.

Corresponding Author: Prof. Ian Frazer, The University of Queensland Diamantina Institute, Translational Research Institute, 37 Kent Street, Woolloongabba, Brisbane, Qld 4102, Australia. Email: i.frazer@uq.edu.au; Phone: +61-7-3443 7711; Fax: +61-7-3443 7799.

Footnotes

[1]Abbreviations: IL-17A, Interleukin IL-17A; DNCB, 2,4-dinitrochlorobenzene; HPV, human papillomavirus; Nor-NOHA, N(omega)-hydroxy-nor-L-arginine; mRNA, messenger RNA; BMDM, bone marrow-derived macrophage.

[2]Grant support: this work was supported by grants from the NIH (5U01CA141583), National Health and Medical Research Council of Australia (569938) to I.H.F. I.H.F. was recipient of Queensland Government Premiers Fellowship. T.L.S is a recipient of University of Queensland fellowship for international students.

Abstract

Human Papillomaviruses (HPVs) have evoked numerous mechanisms to subvert host innate immunity and establish a local immunosuppressive environment to facilitate persistent virus infection. Topical application of 2,4-dinitrochlorobenzene (DNCB) was speculated to overcome this immune-suppressive environment and employed in the immunotherapy of HPV-associated lesions.

We have previously shown that DNCB treatment of skin expressing HPV16.E7 protein, the major oncogenic protein expressed in HPV-associated premalignant cervical epithelium, results in a hyperinflammatory response, with associated induction of Th2 cytokines and an infiltration of myeloid cells producing arginase-1 that also contributes to the hyperinflammation. However, the molecular mechanisms underlying arginase-1 induction and arginase-mediated hyperinflammation in K14.E7 skin have not been elucidated. Here, we show that HPV16.E7 protein expression as a transgene in skin is associated with enhanced IL-17A production by macrophages exposed to DNCB. Interestingly, induction of arginase by DNCB is not seen in K14.E7 animals unable to express IL-17A. Further, blockade of either IL-17A or arginase alleviates DNCB-induced hyperinflammation, through reduced recruitment of neutrophils, as a consequence of decreased CXCL1 and CXCL5 chemokine production. Thus, our findings suggest that increased IL-17A expression by macrophages in E7 expressing skin exposed to DNCB promotes arginase-1 induction and contributes directly to the observed hyperinflammation.

Introduction

Persistent infection of basal keratinocytes with oncogenic Human papillomavirus (HPV), particularly HPV type 16, causes epidermal dysplasia and eventually squamous cancers (1). Establishment of HPV persistence is associated with its ability to subvert effective innate immunity through the action of two major oncoproteins, E6 and E7 (21).

K14.E7 transgenic mice in which a single viral HPV type 16 E7 oncoprotein is expressed within the basal keratinocytes under the control of the keratin 14 transcriptional promoter, have been extensively employed as a model of HPV-associated premalignancy to study the mechanisms of immune-suppression mediated by this viral oncoprotein (13). Indeed, previous investigations using this model have revealed that HPV16.E7 oncoprotein induces a localized immune suppressive environment and that successful therapies need to circumvent or disrupt this environment (44, 54).

Stimulation of innate immunity by topical application of DNCB, a contact hypersensitizer, was recognized as a promising therapy for resistant warts caused by HPV (65). The effectiveness of this approach is ascribed to the activation of innate immune defense mechanisms through a strong cutaneous inflammation induced by DNCB (69). Although clinical application of DNCB has been discouraged due to its potent mutagenic, genotoxic and carcinogenic hazards (66), we hypothesised that understanding how DNCB-induced acute inflammation can alter the local immune suppressive environment generated by HPV16.E7 oncoprotein might lead to better treatment options for HPV persistently infected patients. Our recent study showed that treatment of K14.E7 skin with DNCB causes a hyperinflammatory response which is associated with enhanced recruitment of myeloid cells producing arginase-1, and that arginase-1 is required for the development of DNCB-induced hyperinflammation (170). However, the molecular basic of signaling axis regulating arginase-1 induction, as well as how arginase-1 regulates the hyperinflammation in K14.E7 skin, have not been elucidated.

Th2 cytokines including IL-4 and IL-13 drive the induction of arginase-1 in myeloid cells through STAT6 transcriptional factor (171, 172). In a murine asthma model, Th2 cytokines induced arginase-1 and allergic airway inflammation (74). In addition to Th2 cytokines, IL-17A, an important cytokine of innate immunity, has also been shown to induce arginase-1 production in inflammatory macrophages in a model of *Leishmania amazonensis* infection (173), in vascular inflammation (174) and in a tumor environment (175).

Although IL-17A is primarily produced by T helper 17 cells and other lymphocyte subsets (γδ T cells, invariant natural killer T cells), recent studies have reported that innate immune cells including neutrophils (176) and macrophages (177) are important cellular sources of IL-17A. IL-17A, which signals through a receptor complex composed of IL-17RA /IL-17RC, mediates skin lesions through induction of chemokines and recruitment of innate immune cells (178).

Since regulation of arginase is dependent on a cytokine milieu, the present study aimed to investigate the involvement of these cytokines in the induction of arginase-1 and the enhanced inflammation in K14.E7 skin. Here, we show that suppression of IL-17A and not Th2 cytokines caused a significant reduction in the production of arginase-1 in K14.E7 skin exposed to DNCB, indicating involvement of IL-17A in arginase-1-mediated hyperinflammation in K14.E7 skin.

In addition, we show that IL-17A is induced by $CD11b^{+}F4/80^{+}$ macrophages in the absence of lymphocytes and that IL-17A together with its down-stream mediator, arginase-1, participates in ongoing DNCB-induced hyperinflammation in K14.E7 skin through enhanced recruitment of neutrophils. Taken together, our findings demonstrate that IL-17A promotes DNCB-induced hyperinflammatory response in HPV16.E7 skin, concomitant with the induction of arginase activity.

Materials and Methods

Mice

HPV16.E7 transgenic C57BL/6 mice (designated K14.E7) which express HPV type 16 E7 oncoprotein under control of keratin 14 promoter were generated from inbreed strain, C57BL/6 mice (161). $Rag1^{-/-}$ and $IL\text{-}17A^{-/-}$ mice were obtained from the Animal Resources Center (Perth, Australia) and Professor Helen Thomas (The University of Melbourne), respectively. $E7.Rag^{-/-}$ and $E7.IL17^{-/-}$ were generated by crossing male K14.E7 mice with female $Rag1^{-/-}$ or $IL17^{-/-}$ knockout (KO) C57BL/6 mice, heterozygous K14E7 mice were crossed and then backcrossed with homozygous $Rag1^{-/-}$ or $IL17^{-/-}$ mice to an F2 generation (161). K14.hGH mice were purchased from the Animal Resources Center (Perth, Australia). All mice, on C57BL/6 background, were maintained under specific pathogen-free conditions at Translational Research Institute-Biological Research Facility. Experimental mice were sex-matched and used at 6-9 week of age. All animal procedures complied with guidelines approved by the University of Queensland Animal Ethics Committee (AEC#367/13).

Media and Reagents

Complete medium was DMEM supplemented with 10% heat inactivated fetal calf serum (FCS), 1% penicillin/streptomycin, 1% L-glutamine, 1% Sodium Pyruvate, 1% HEPES (Gibco, Victoria, Australia).

Neutralizing monoclonal antibodies (Mabs) against IL-4 (Rat IgG1, clone 11B11) and IL-10 (Rat IgG1, clone JES5-2A5) and matched-isotype control Mab (Rat IgG1, clone eBRG1) were purchased from eBioscience (California, USA). Mab, rat IgG1, against murine IL-17A (LA426), and control isotype-matched rat mAb (2405001) were obtained from Lilly Research Laboratories (Illinois, USA).

Mouse IL-17A (homodimer) enzyme-linked immunosorbent assay Ready-SET-Go kits (ELISA) with sensitivity limit of 4 pg/ml were purchased from eBioscience.

DNCB treatment

2,4-dinitrochlorobenzene (Sigma, New South Wales, Australia) was dissolved in acetone: olive oil (4:1) immediately prior to use. For IL-17A neutralization in vivo, six- to

nine-week-old mice were intraperitoneally administered at a dose of 10 mg/kg of anti-IL-17A blocking antibody or matched-isotype control antibody. After 24 hours, the treatment was repeated 30 min before applying 20 µl of 1% or 10% (m/v) DNCB on the left ear and 20 µl of vehicle (acetone:olive oil 4:1) on the right ear. The ear tissues were harvested for mRNA and protein analysis 24 hours following DNCB treatment. Ear thickness was measured within 5 consecutive days by using the digital caliper and change in ear swelling was determined by calculating the mean increase in ear thickness compared to untreated ears.

For arginase suppression, mice were injected with 500 µg of arginase inhibitor, nor-NOHA (Cayman, MI, USA) or saline buffer one day prior to DNCB treatment and daily for 5 days

Skin explant culture

Four hours after DNCB exposure, ear skin was excised and split into dorsal and ventral halves and each ear half was placed dermis side down on 2 ml of complete DMEM, 24-well tissue culture plates at 37^{o}C, 5% CO_2. To reduce the effect of cell-death related release of cytokines and danger signals, after 1 hour, the culture medium was exchanged with 2 ml of fresh complete DMEM. For in vitro cytokine neutralization, culture medium was supplemented with 10 ng/ml of anti-IL-4, anti-IL-10 or anti-IL-17A neutralizing mabs and matched Rat IgG1 isotype control mab. Ear skin explant supernatant was collected after 20 hours and used for BMDM stimulation or cytokine production analysis by ELISA.

Preparation and cultivation of BMDM

Bone marrow cells were flushed from femurs and tibias of C57BL/6 mice and cultivated in complete DMEM medium supplemented with 20% L-cell conditioned medium (kindly provided by Dr. Antje Blumenthal) and cultured at 37^{o}C, 5% CO_2. 5 ml of fresh medium was added to culture every 2 days. After 6 days, BMDM cells were harvested and seeded in complete DMEM medium at a concentration of $5x10^5$ cells/ml, then allowed to recover for two hours before performing in vitro stimulation. Monoclonal antibodies against IL-4, IL-10 or IL-17A and matched-isotype control antibodies were added to culture medium 30 minutes before stimulating BMDM cells with 20% skin explant supernatant. After 24 hours, BMDM cells were harvested by using cold 0.05% EDTA in PBS. Total protein was isolated from sorted cells by resuspending cells in 50 µl of lysis buffer

containing 20 mM Tris, 100 mM NaCl, 1 mM EDTA, 0.5% Triton X100, EDTA-Minicomplete protease inhibitor (Roche diagnostics, New South Wales, Australia) and incubating for 30 min. After centrifugating at 13,000 g at 4^{o}C for 20 min, the supernatant was collected for protein quantification determined by using Pierce^{TM} bicinchoninic acid (BCA) protein assay (Thermoscientific, Illinois, USA) and then 100 µg of protein lyaste was used to determine arginase activity.

Arginase enzymatic assay

Arginase activity was measured by colorimetric determination of urea formed from L-arginine as previously described (163).

IL-17A ELISA

IL-17A production in skin explant supernatant was determined following the manufacturer's instructions. IL-17A concentration in supernatant was normalized to weight of the skin explant and shown as pg/mg tissue.

Realtime-PCR

Table 3.1- Primer sequences

Gene	Forward 5' – 3'	Reverse 3' – 5'
RPL32	GGTGAAGCCCAAGATCGTC	TTGGGATTGGTGACTCTGATG
Arginase-1	AAGAATGGAAGAGTCAGTGTGG	GGGAGTGTTGATGTCAGTGTG
Arginase-2	GATCTCTGTGTCATCTGGGTTG	AATCCTGGCAGTTGTGGTAC
IL-4	CGAATGTACCAGGAGCCATATC	TCTCTGTGGTGTTCTTCGTTG
IL-10	GGAGTCGGTTAGCAGTATGTTG	AGCCGGGAAGACAATAACTG
IL-17A	TCCAGAATGTGAAGGTCAACC	TATCAGGGTCTTCATTGCGG
CXCL1	AACCGAAGTCATAGCCACAC	CAGACGGTGCCATCAGAG
CXCL2	GAAGTCATAGCCACTCTCAAGG	CTTCCGTTGAGGGACAGC
CXCL5	GTTCCATCTCGCCATTCATG	TTAAGCAAACACAACGCAGC

Total RNA was isolated from homogenized tissues by using RNaeasy Mini kit (Qiagen, Victoria, Australia). RNA extracts were quantified using absorption of light at 260

and 280 nm (A260/280). For cDNA synthesis, 500 ng of total RNA was reverse transcribed in 20 µl reaction containing 5 mM $MgCl_2$; 1.6 mM dNTP mix, 2.5 mM oligo-dT, 1 µl of MuLv reverse transcriptase 5000U (Applied Biosystems, Victoria, Australia) and 10 units of RNaseOUT (Invitrogen, Victoria, Australia) at 42^{o}C for 60 min. The reactions were heated at 70^{o}C for 15 min to inactivate reverse transcriptase enzyme. cDNA product was diluted at 1:4 and 2.5 µl was subjected to real-time PCR reaction using SYBR TAKA kit (Scientifix, Victoria, Australia) and primers (Integrated DNA Technologies, Iowa, United States) listed in table 2.1. The relative expression was determined by normalizing against the house keeping gene RPL32 (L32 ribosomal protein gene).

Flow cytometric analysis

Single cell suspensions were prepared by incubating minced ear skin tissue in 2 mg/ml dispase (Roche Diagnostics) for 1 hour and 0.3 mg/ml collagenaseD (Roche Diagnostics) for 30 min and grinding through a 70µm cell strainer. After adding Fcγ receptor block (Fcγ III/II receptor; BD Biosciences, Auckland, New Zealand, 1/50) and incubating on ice for 10 min, cells were stained with live/dead aqua dyes (Live/Dead fixable aqua dead cell stain kit, Invitrogen, 1/1000) and antibodies specific for the following surface markers for 30 min at 4˚C: CD45.2-PerCP5.5 (eBioscience, clone 30-F11) ; CD11b-Pacific Blue (eBioscience, clone M1/70) , F4/80-FITC (eBioscience, clone BM8), Gr1(Ly6G/Ly6C)-APC (eBioscience, clone RB6-8C5)), MHC-II-APC.Cy7 (Biolegend, clone M5/114.15,2) , CD11c-PE.Cy7 (BD Pharmingen, clone HL3) and CD3-PE (eBioscience, clone 17A2). Cells were fixed and permeabilized the BD Biosciences Cytofix/Cytoperm kit (BD Pharmingen) according to the manufacturer's instructions before stained intracellularly with mab against IL-17A or matched isotype control antibody (eBiosciences, 1/100) for 45 min. Flow-Count fluorospheres (Beckman Coulter) for absolute cell counting was added to stained cells before acquiring on a LSR fortessa II cytometer (BD Biosciences). Data was analyzed using Kaluza software (version 1.2, Beckman Coulter, New South Wales, Australia).

Histological analysis

Ear tissues were fixed in 4 % paraformaldehyde for 24 hours. Tissues were embedded in paraffin and 7 µm sections were prepared and stained with Hematoxylin and

Eosin. Immune cell infiltration was evaluated by light microscopy using Nis-elements Br 3.2 software (Nikon Instruments Inc., New York, United States).

Paraffin sections were dewaxed and rehydrated through xylol and descending graded alcohols to Tris buffered saline (TBS) pH 7.6. Endogenous peroxidase activity is blocked by incubating the sections in 2.0% hydrogen peroxide in TBS for 10 minutes. After rinsing slides in distilled water, sections were transferred to Biocare Medical Diva retrieval buffer pH and subjected to 15 minutes heat antigen retrieval at 105^{O}C using the Biocare Medical decloaking chamber. Samples were allowed to cool down for 20 min and washed three times in TBS before adding anti-mouse F4/80 (abcam, 1/350), was applied for 90 minutes at room temperature. Sections are washed in TBS before adding secondary antibody, Rat-on-Mouse HRP Polymer Kit (Biocare Medical, United States, CA). Colour is developed in DAB for 5 minutes and sections were lightly counterstained in Mayers' haematoxylin, then dehydrated through ascending graded alcohols, cleared in xylene, and mounted using DePeX.

Statistical Analysis

Data represents the mean ± SEM and are representative of two independent experiments with at least 4 mice per group. Prism (Graph pad Software, California, USA) was used for graphs and statistical analysis: *; $p<0.05$; **; $p<0.01$; ***, $p<0.001$; **** $p<0.0001$. Multiple comparisons of ear swelling data were derived by two-way ANOVA. For other data, statistically significantly differences between groups were analysed by non-parametric Mann-Whitney-Wilcoxon test.

Results

DNCB-induced IL-17A, but not IL-4 or IL-10, in K14.E7 skin promotes macrophage arginase production

We have previously shown that DNCB treatment of skin expressing the E7 protein of HPV.16 as a transgene induces hyperinflammation when compared with similar treatment of non-transgenic skin, and that this is associated with the induction of IL-4 and IL-10. These cytokines have been described as potent inducers of arginase-1 in monocytes/macrophages, so we assessed the link between each of these cytokines and arginase-1 production in DNCB-treated K14.E7 skin, using an *in-vitro* skin explant model. BMDM were cultured in supernatants harvested from explant cultures of vehicle or DNCB-treated skin from C57BL/6, $Rag^{-/-}$, K14.E7 or E7.$Rag^{-/-}$ mice. BMDM cells exposed to supernatant from DNCB-treated K14.E7 or E7.$Rag^{-/-}$ skin explants expressed more arginase activity than those exposed to supernatant from vehicle-treated skin explants. By contrast, there was no change in arginase activity when BMDM cells were stimulated with supernatants from DNCB-treated wild-type C57BL/6 and $Rag^{-/-}$ skin explants (Figure 3.1a). These observations confirmed in-vitro our previous ex-vivo observation that DNCB treatment of K14.E7 skin leads to enhanced arginase activity in inflammatory macrophages, by a mechanism independent of T- and B-lymphocytes (Figure 3.1a).

We next tested whether IL-4 or IL-10 released by DNCB-treated K14.E7 ear skin is involved in the induction of arginase-1 in BMDM, by exposing the BMDM cultures to anti-IL-4 and anti-IL-10 neutralizing antibodies. Neutralization of IL-4 and IL-10 did not change the level of arginase activity in BMDM stimulated with supernatant from DNCB-treated K14.E7 skin explant (Figure 3.1b), demonstrating that IL-4 and IL-10 were not necessary for the enhanced arginase activity in DNCB-treated K14.E7 skin.

Since IL-17A has been shown to induce arginase-1 expression by macrophages in recent studies (174, 175), we next investigated whether IL-17A played a role in the induction of arginase in our model. Depletion of IL-17A with neutralizing antibody, in contrast to depletion of IL-10 and IL4, significantly reduced the observed level of arginase activity (Figure 3.1b). In support of this observation, BMDM cells cultured in supernatant from skin explants from DNCB-treated E7.$IL17^{-/-}$ animals produced less arginase activity than those cultured in supernatants from E7.$IL17^{+/-}$ or from K14.E7 skin explants (Figure 3.1c).

To further confirm a key role for IL-17A in the enhancement of arginase production in response to DNCB, we assessed the in-vivo production of arginase in K14.E7 skin and E7.IL17$^{-/-}$ skin after DNCB application. Consistent with our *in-vitro* data, E7.IL17$^{-/-}$ mouse skin treated with DNCB demonstrated significantly less arginase activity, and arginase-1 transcription, than K14.E7 mouse skin (Figure 3.2a and 3.2b). Arginase-2 mRNA transcription was reduced to a much lesser extent (Figure 3.2c). Thus, IL-17A contributes to the induction of arginase-1 mRNA expression and arginase activity not only in BMDM cells *in-vitro* but also in K14.E7 skin following DNCB application.

IL-17A has been suggested to mediate recruitment of inflammatory macrophages (179). Therefore, we investigated whether IL-17A mediated the induction of arginase-1 in DNCB-treated K14.E7 skin by enhancing recruitment of the CD11b^{+}Gr1^{int}F4/80^{+} subset of macrophages, which we previously showed to be the main cell population producing arginase-1 in DNCB-treated K14.E7 skin. The expected extensive infiltrate of F4/80^{+} cells in K14.E7 skin in response to DNCB application, was much reduced in DNCB-treated E7.IL17$^{-/-}$ skin, demonstrating that IL-17A enhances recruitment of F4/80^{+} cells in K14.E7 skin in response to DNCB (Figure 3.2d). Consistent with this observation, flow cytometric analysis showed significantly lower numbers of CD11b^{+}F4/80^{+}Gr1^{int} cells in DNCB-treated E7.IL17$^{-/-}$ skin compared to K14.E7 skin (Figure 3.2e).

Taking these findings together, we conclude that IL-17A, by increasing the number of CD11b^{+}F4/80^{+}Gr1^{int} macrophages, is responsible for the increased arginase-1 mRNA expression and arginase activity in DNCB-treated K14.E7 skin.

IL-17A is specifically induced in DNCB-treated K14.E7 skin in the absence of lymphocytes

As IL-17A contributes to the enhanced induction of arginase-1 in DNCB-treated K14.E7 mouse skin, we investigated IL-17A expression in wild–type and K14.E7 mouse skin. Following DNCB application, IL-17A gene expression was significantly induced in DNCB-treated K14.E7 skin while it remained unchanged in DNCB-treated wild-type skin (Figure 3.3a). Additionally, DNCB-treated K14.E7 skin secreted more IL-17A into the skin explant supernatant than wild-type skin (Figure 3.3b). Base levels of IL-17A in untreated K14.E7 skin were also higher than that in C57BL/6 skin, as reported previously (35). Thus, in addition to Th2 cytokines, IL-17A was induced in K14.E7 skin in response to DNCB.

As we previously reported that hyperinflammatory response in K14.E7 mice exposed to DNCB is independent of lymphocyte function, we investigated the production

of IL-17A in E7.Rag$^{-/-}$ skin. Interestingly, IL-17A mRNA expression was significantly induced by DNCB in E7.Rag$^{-/-}$ skin, although at a lower level than in E7 skin, but not in Rag$^{-/-}$ skin (Figure 3.3a). Consistent with this, the level of IL-17A protein released into the skin explant supernatants from both Rag$^{-/-}$ and E7.Rag$^{-/-}$ mice was undetectable by ELISA (Figure 3.3b), suggesting a significant contribution of lymphocytes to the enhanced IL-17A production in DNCB-treated E7 transgenic skin.

To establish the role of E7 protein in the induction of IL-17A, we examined the induction of IL-17A in another K14 transgenic mouse line (K14.hGH) and in C57BL/6 mice, treated with a 10-fold higher dose of DNCB to induce ear swelling level comparable to that observed in K14.E7 mouse skin exposed to a lower level of DNCB (Figure 3.3c). In both the K14.hGH transgenic and the C57BL/6 mouse skin, no production of IL-17A was observed. Thus, induction of IL-17A by DNCB is dependent on expression of HPV16.E7 in skin.

Taken together, these data suggested that expression of HPV16.E7 in skin facilitates IL-17A induction in both lymphocyte and “non-lymphocyte” immune subsets in response to DNCB.

CD11b^{+}F4/80^{+} macrophages are the major producers of IL-17A in DNCB-treated K14.E7 skin

Recent studies have reported that in addition to Th17 cells, various myeloid cells including neutrophils (176), and macrophages (177) can produce IL-17A under inflammatory conditions. Our observation of induction of IL-17A by DNCB in E7.Rag$^{-/-}$ skin prompted us to test whether myeloid cell subsets as well as lymphocytes contributed to IL-17A production in this model. Intracellular staining confirmed expression of IL-17A in CD45.2^{+}CD11b^{+} myeloid cells and CD45.2^{+}CD11b^{-} cells isolated from C57BL/6, K14.E7, Rag$^{-/-}$ and E7.Rag$^{-/-}$ mice after DNCB treatment (Sup. figure 3.1a). As expected, flow cytometric analysis showed a significant increase in the percentage (Sup. figure 3.1b) as well as absolute number of IL-17A^{+}CD11b^{-} cells (Figure 3.4a) in K14.E7 skin after DNCB treatment, whereas the number of these cells remained unchanged in E7.Rag$^{-/-}$, C57BL/6 and Rag$^{-/-}$ mouse skin. Thus, while in K14.E7 skin, lymphocytes induced a significant amount of IL-17A after DNCB treatment, in both K14.E7 and E7.Rag$^{-/-}$ mice there was an increase in the proportion (Sup. figure 3.1c) and number of IL-17A^{+}CD11b^{+} cells compared to C57BL/6 and Rag$^{-/-}$ mice (Figure 3.4b). Also, DNCB-treated K14.E7 mice had approximately 6-fold more IL-17A^{+}CD11b^{+} cells (12,026 ± 1,234 cells/ear, mean ± SEM)

than IL-17A^{+} CD11b^{-} cells (1,925±354 cells/ear, mean ± SEM), indicating that CD11b^{+} myeloid cells were also a major source of IL-17A in these mice was also (Figure 3.4a and 3.4b). To further indentify which myeloid cell subsets produce IL-17A in DNCB-treated K14.E7 and E7.Rag$^{-/-}$ mice, we analyzed the expression of IL-17A in the macrophage (F4/80^{+}), neutrophil (Gr1^{hi}), and dendritic cells (CD11c^{+}MHCII^{+}) fraction of CD11b^{+} cell population. F4/80^{+} macrophages from both K14.E7 and E7.Rag$^{-/-}$ skin, but not from their counterpart controls (C57BL/6 and Rag$^{-/-}$) showed an increased production of IL-17A after DNCB treatment (Figure 3.4c and 3.4d). Interestingly, neither neutrophils nor dendritic cells in K14.E7 mice after DNCB treatment showed staining for IL-17A (Sup. figure 1d). Thus, CD11b^{+}F4/80^{+} macrophages were major contributors of IL-17A induction in DNCB-treated K14.E7 skin, and this increased production occurred in the absence of T and B lymphocytes.

Suppression of IL-17A or arginase-1 attenuates the DNCB-induced inflammation in K14.E7 skin

To address whether IL-17A expression is sufficient to trigger the enhanced acute inflammation in K14.E7 and E7.Rag$^{-/-}$ skin, we applied DNCB to E7.IL17$^{-/-}$ or IL-17A neutralizing antibody-treated K14.E7 and E7.Rag$^{-/-}$ mice. Pretreatment of mice with IL-17A neutralizing antibody, when compared to isotype control antibody, caused a significant reduction in the ear swelling (Figure 3.5a). Further, histological examination also showed a significant reduction in ear thickness and the number of infiltrating leukocytes within the dermis of E7.IL17$^{-/-}$ mice or K14.E7 and E7.Rag$^{-/-}$ mice pretreated with anti-IL-17A neutralizing antibody, as compared with K14.E7 and E7.Rag$^{-/-}$ mice, respectively one day after DNCB treatment (Figure 3.5b).

IL-17A and arginase-1 mediate the enhanced recruitment of neutrophils in DNCB -treated K14.E7 skin via CXCL1 and CXCL5 production

Neutralization of IL-17A in K14.E7 mice reduced the DNCB-induced ear swelling on day 5 post treatment to a greater extent than suppression of arginase activity (Figure 3.6). As IL-17A was shown to promote arginase production, we assessed whether simultaneous inhibition of arginase and IL-17A suppressed ear swelling to a greater extent compared to blockade of IL-17A alone. If both IL-17A and arginase were inhibited, ear swelling levels were similar to mice in which only IL-17A was depleted (Figure 3.6).

We have demonstrated that the hyperinflammatory response in K14.E7 skin is manifested by a large recruitment of myeloid cells, particularly neutrophils which account for a significant proportion of total infiltrating myeloid cells (Sup. figure 3.2). Deficiency in IL-17A or blockade of arginase-1 production significantly reduced the number of neutrophils ($CD11b^{+}Gr1^{hi}$ cells) but not of other cell types in K14.E7 skin after one day of DNCB application (Figure 3.7a-c). Recruitment of neutrophils is driven by chemokines including CXCL1, CXCL2, and CXCL5 (180). These chemokines are highly elevated in K14.E7 skin following DNCB treatment. Conversely, the expression level of CXCL1 and CXCL5, but not CXCL2, was significantly reduced in $E7.IL17^{-/-}$ skin, and in arginase inhibitor-treated K14.E7 skin, suggesting that both IL-17A and arginase were required for the induction of these chemokines (Figure 3.7d-f).

Taken together, our data show that IL-17A contributed to the enhanced production of arginase-1 and that IL-17A together with arginase-1, contributed to DNCB-induced hyper-inflammatory response in HPV16.E7 expressing skin, possibly by promoting the production of CXCL1 and CXCL5 chemokines-mediated recruitment of neutrophils.

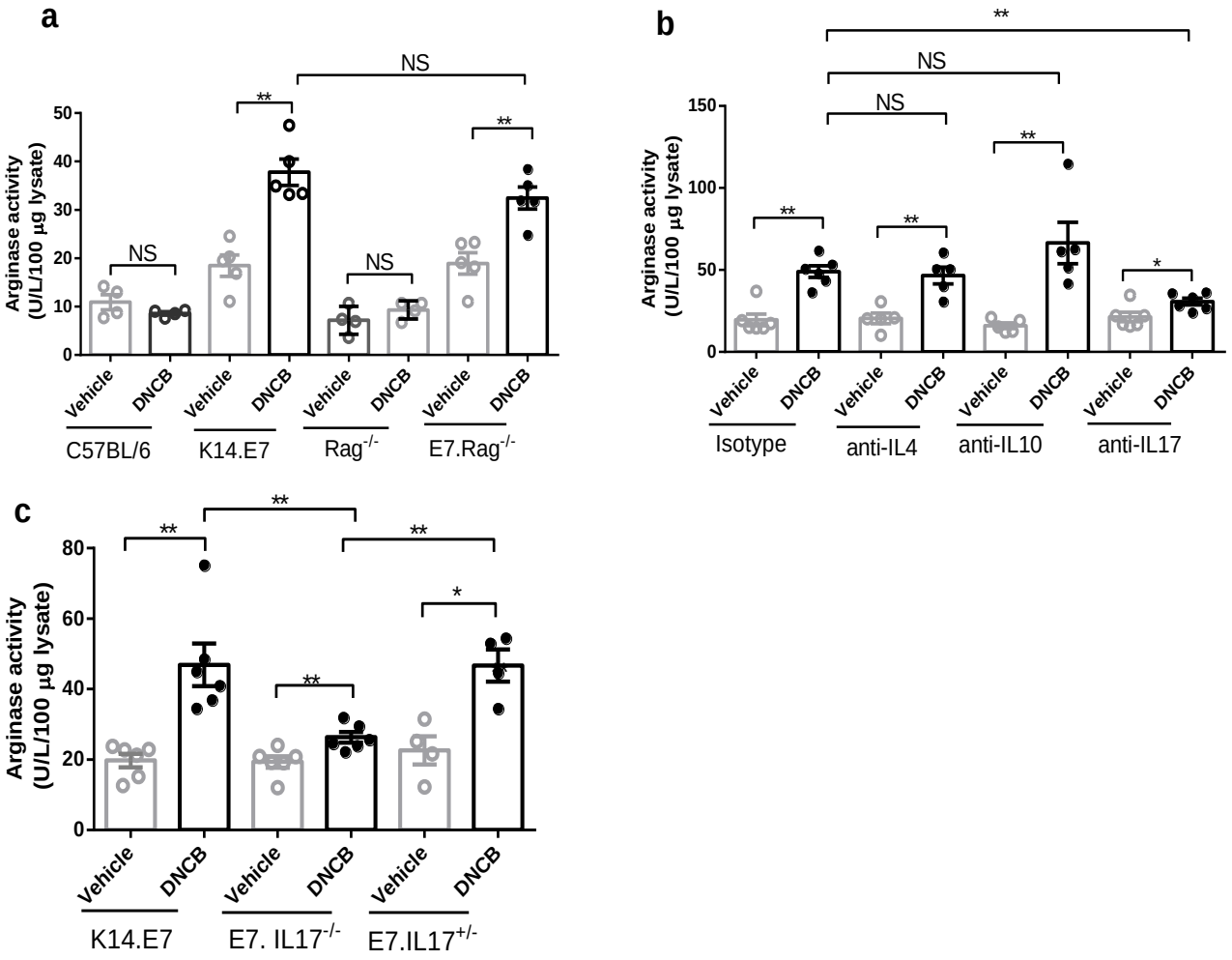

Figure 3.1- IL-17A from DNCB-treated E7 transgenic skin contributes to the induction of arginase in BMDM. (a) C57BL/6, K14.E7, Rag$^{-/-}$ and E7.Rag$^{-/-}$ mice were treated with vehicle or DNCB for 4 hours. Explanted skin was cultured for 24 hours and culture supernatant was assessed for induction of BMDM arginase activity **(b)** Arginase activity in BMDM cultured in vehicle or DNCB-treated K14.E7 skin explant supernatants and exposed to matched-isotype antibodies or neutralizing antibodies (10 ng/ml) against IL-4, IL-10 or IL-17A. **(c)** Arginase activity in BMDM cultured in supernatants from vehicle or DNCB-treated E7.IL17$^{-/-}$ or E7.IL17$^{+/-}$ skin explants. Data are means ± SEM, and are representative of two independent experiments, each with 4-6 mice per group.* $p<0.05$, ** $p<0.01$, NS not significant.

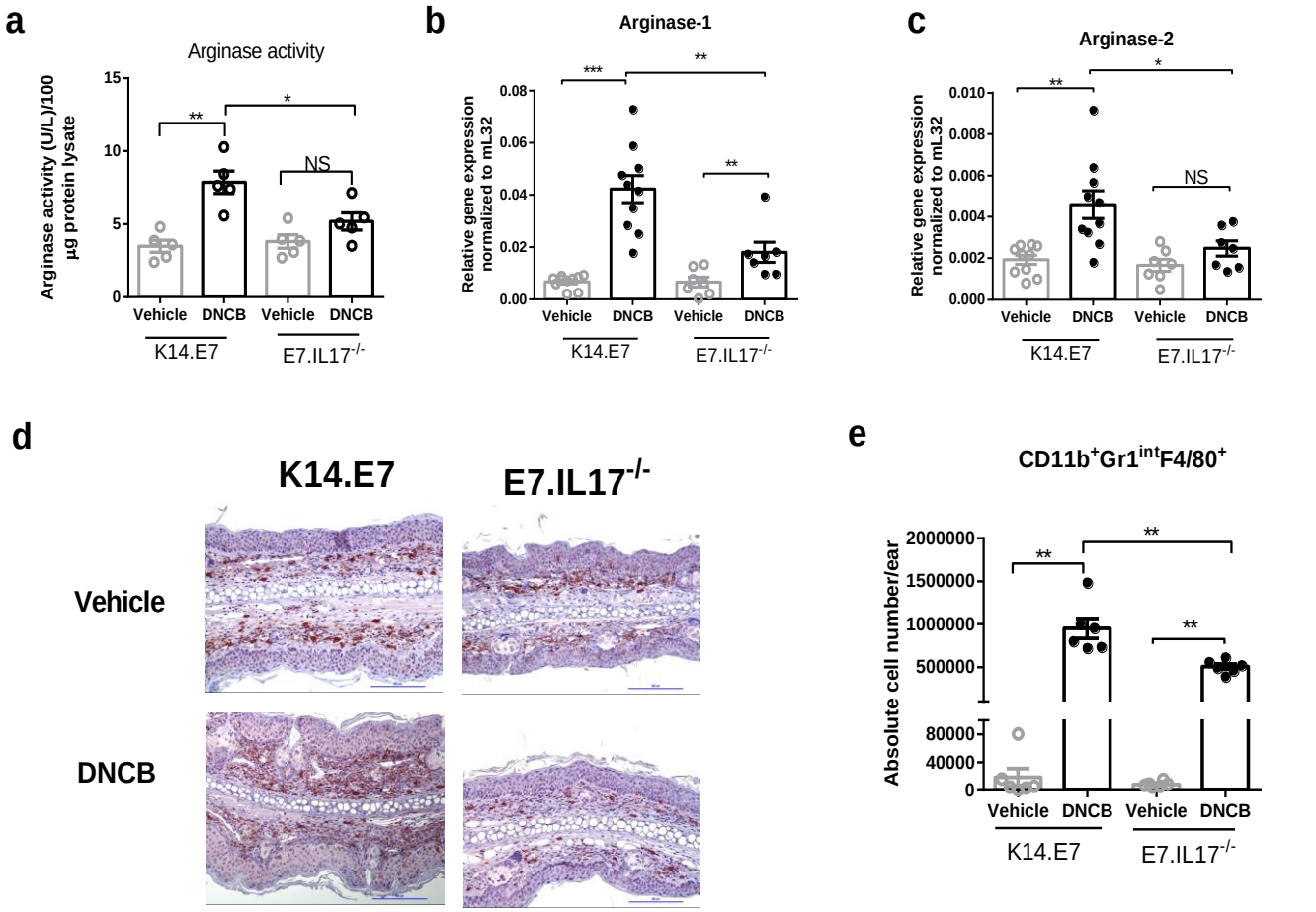

Figure 3.2- IL-17A enhances recruitment of arginase-1 producing CD11b^{+}Gr1^{int}F4/80^{+} cells to K14.E7 mouse skin following DNCB application. **(a)** Arginase activity in K14.E7 and E7.IL17$^{-/-}$ mouse skin after 24 hours of DNCB treatment. **(b) and (c)** Expression of arginase-1 and arginase-2 mRNA transcripts in K14.E7 and E7.IL17$^{-/-}$ mouse skin following DNCB application determined by real-time PCR. **(d)** Immunohistochemical analysis of F4/80^{+} macrophages in K14.E7 or E7.IL17$^{-/-}$ skin exposed to DNCB. Stained sections are representative of 4 mice per group, original magnification x200, scale bar =100 µm. **(e)** The absolute number of infiltrating CD11b^{+}Gr1^{+}F4/80^{+} cells in K14.E7 and E7.IL17$^{-/-}$ skin one day after DNCB treatment was determined by flow cytometry**.** Data are means ± SEM, and are pooled from two independent experiments, each with 4-7 mice per group.* $p<0.05$, ** $p<0.001$, *** $p<0.0001$, NS not significant.

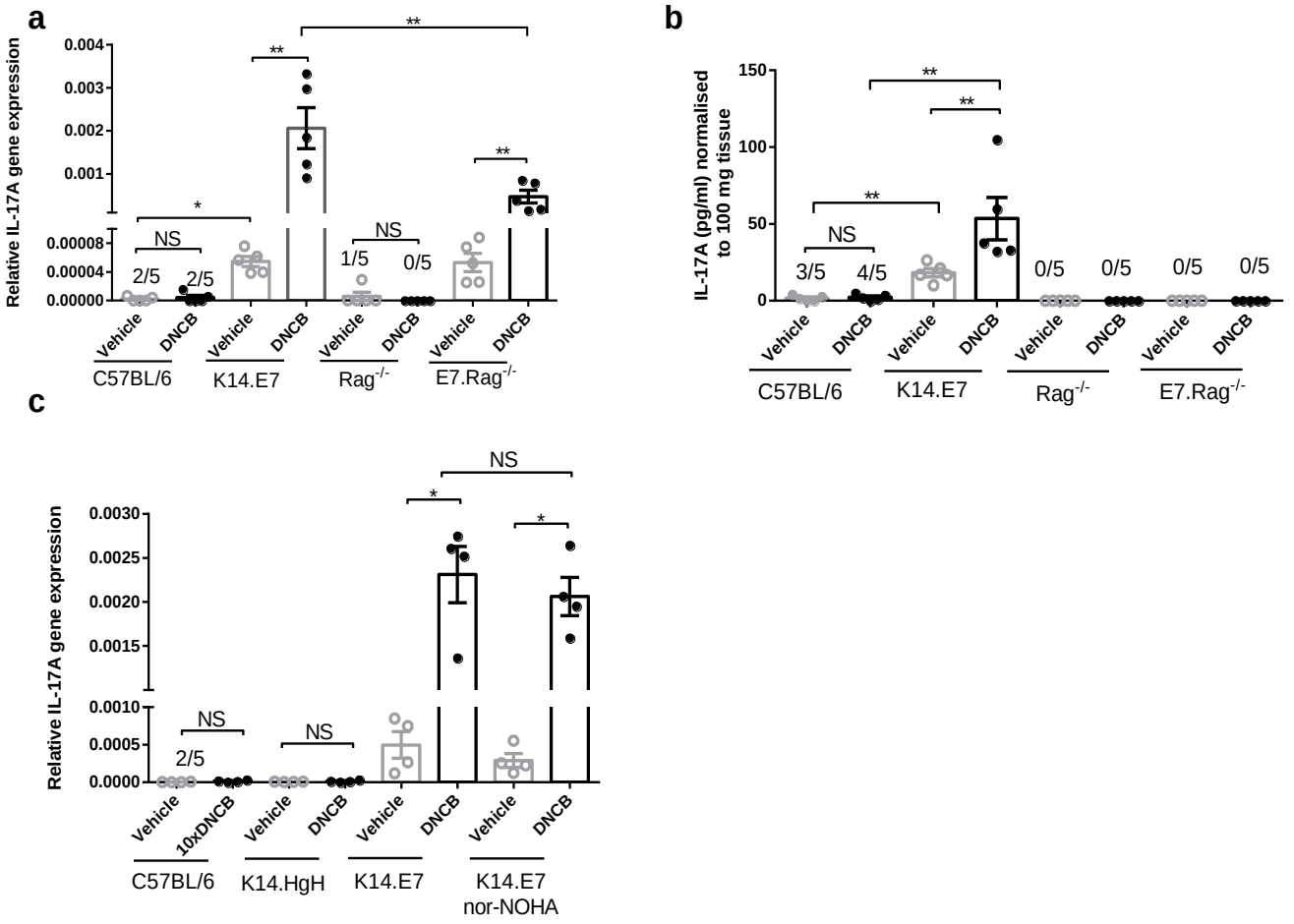

Figure 3.3- IL-17A is induced by DNCB in both K14.E7 and E7.Rag$^{-/-}$ transgenic skin. (a) Quantitative real-time PCR analysis of IL-17A mRNA transcripts in the skin and **(b)** IL-17A production by ELISA in the supernatants of skin explant cultures from C57BL/6, K14.E7, Rag$^{-/-}$ and E7.Rag$^{-/-}$ mice one day after DNCB (1% (w/v)) treatment or vehicle application. **(c)** Quantitative real-time PCR analysis of IL-17A mRNA transcripts in C57BL/6 treated with a 10% DNCB (w/v) or in K14.HgH, K14.E7, nor-NOHA treated K14.E7 skin after 1% DNCB (w/v) treatment. Data show the mean ± SEM and represent two independent experiments, each with 4-5 animals per group.* $p<0.05$,** $p<0.001$, NS not significant.

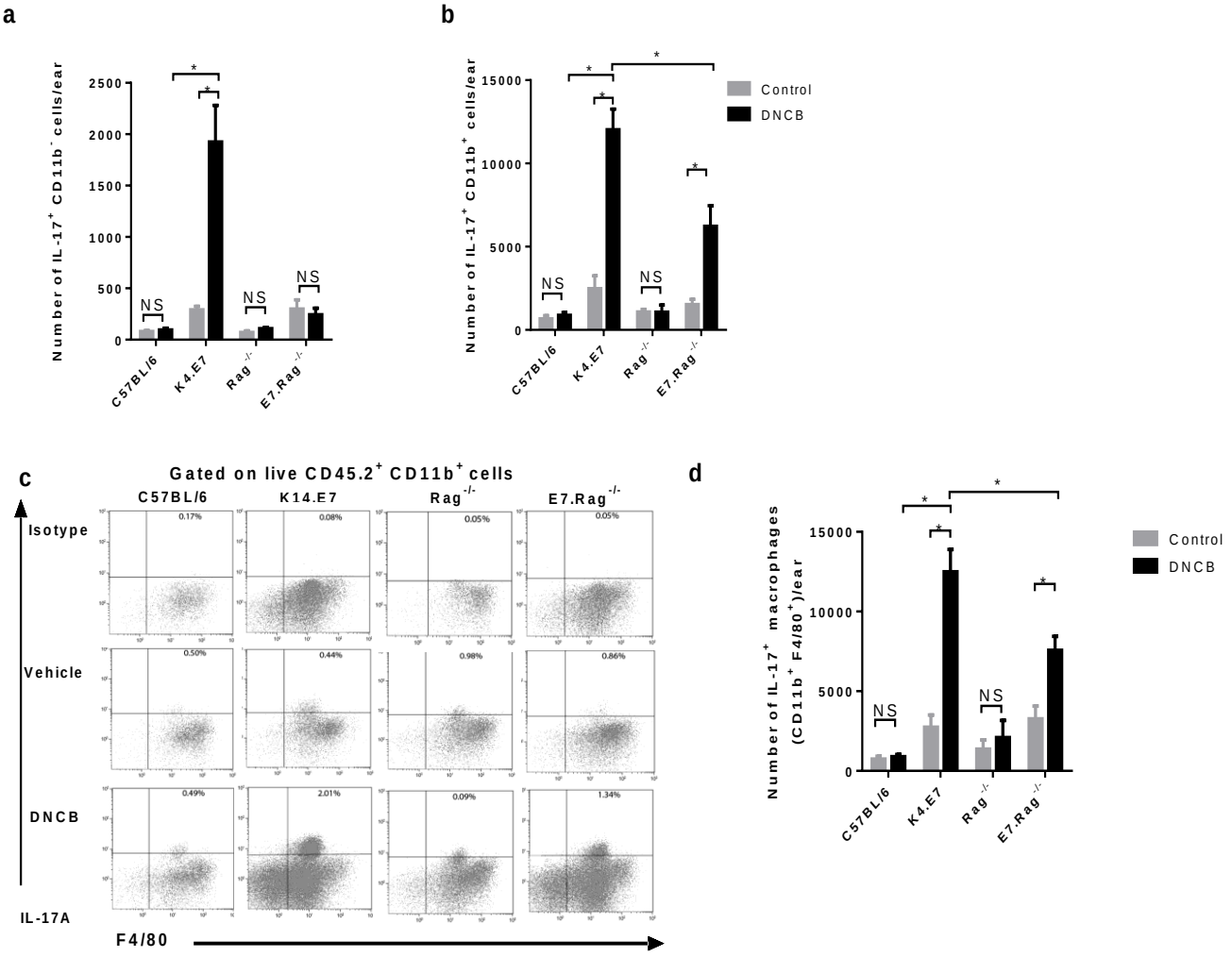

Figure 3.4- DNCB induced IL-17A is mostly produced by CD11b^{+}F4/80^{+} macrophages. C57BL/6, K14.E7, Rag$^{-/-}$ and E7.Rag$^{-/-}$ mice were treated with vehicle or DNCB, and after 24 hours cells were isolated from ear skin tissues and stained for IL-17A. **(a), (b) and (d)** The absolute number of IL17A^{+} CD11b^{-} (a) and IL-17A^{+} CD11b^{+} (b) and IL-17A^{+}CD11b^{+}F4/80^{+} (d) cells. **(c)-**Representative dot plots pre-gated on viable CD45.2^{+}CD11b^{+} cells and stained with F4/80 and IL-17A. Data shows the mean ± SEM and represent two independent experiments of 4 animals per experiment.* p<0.05, NS not significant.

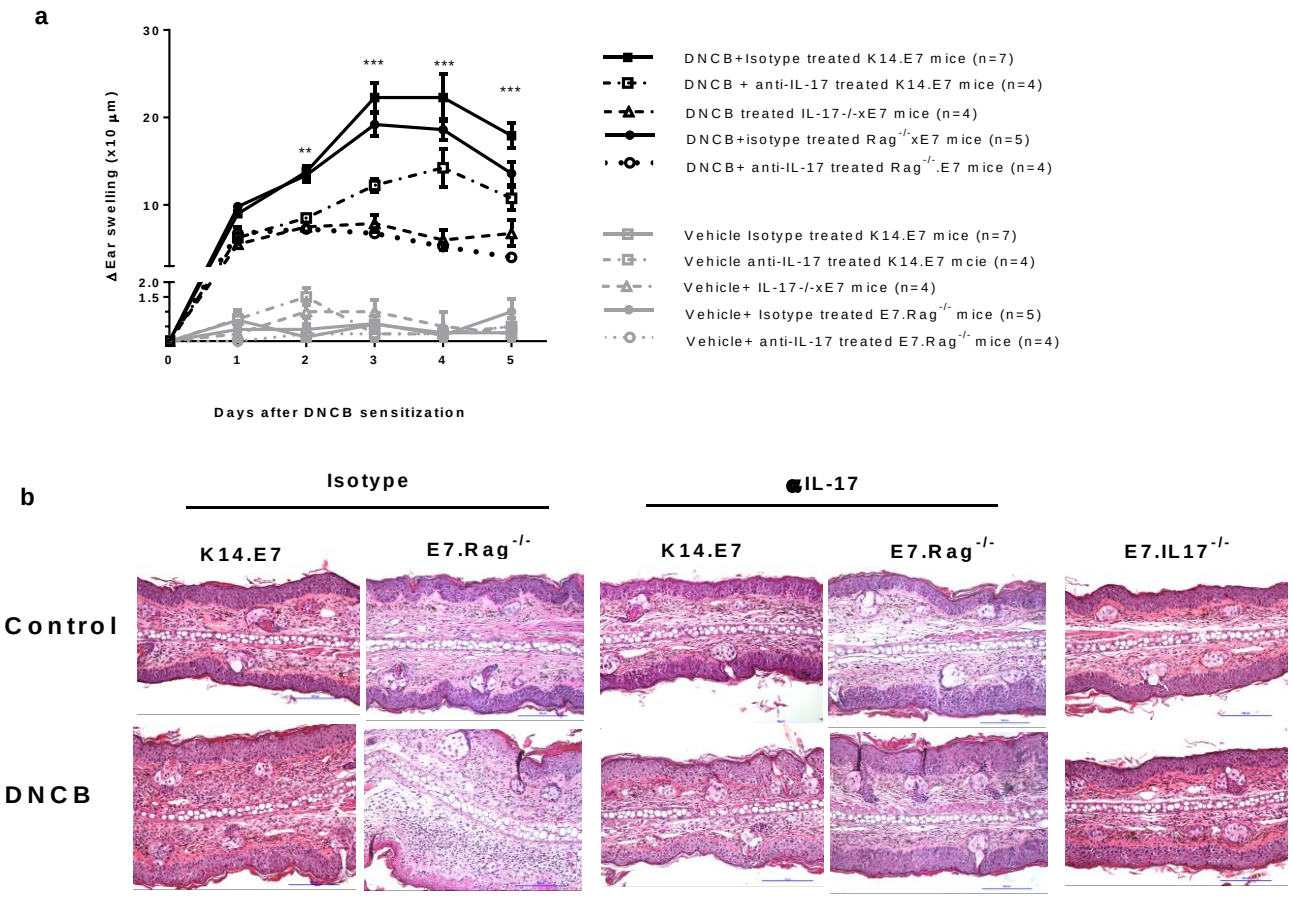

Figure 3.5- IL-17A promotes ear swelling induced by DNCB in K14.E7 skin. (a) Ear swelling of isotype or anti-IL-17 neutralizing antibody treated K14.E7 and E7.Rag$^{-/-}$ or E7.IL17$^{-/-}$ mice following DNCB application. Data are means ± SEM**,** and representative of 2 independent experiments, each with 4-7 animals per group,***** p <0.05, ** p< 0.01, *** p<0.001, NS not significant. **(b)** Histological analysis of isotype antibody or anti-IL-17A neutralizing antibody treated K14.E7 and E7.Rag$^{-/-}$ skin or E7.IL17$^{-/-}$ skin. Hematoxylin and eosin sections, original magnification x200, scale bar =100 µm (representative of four mice per group).

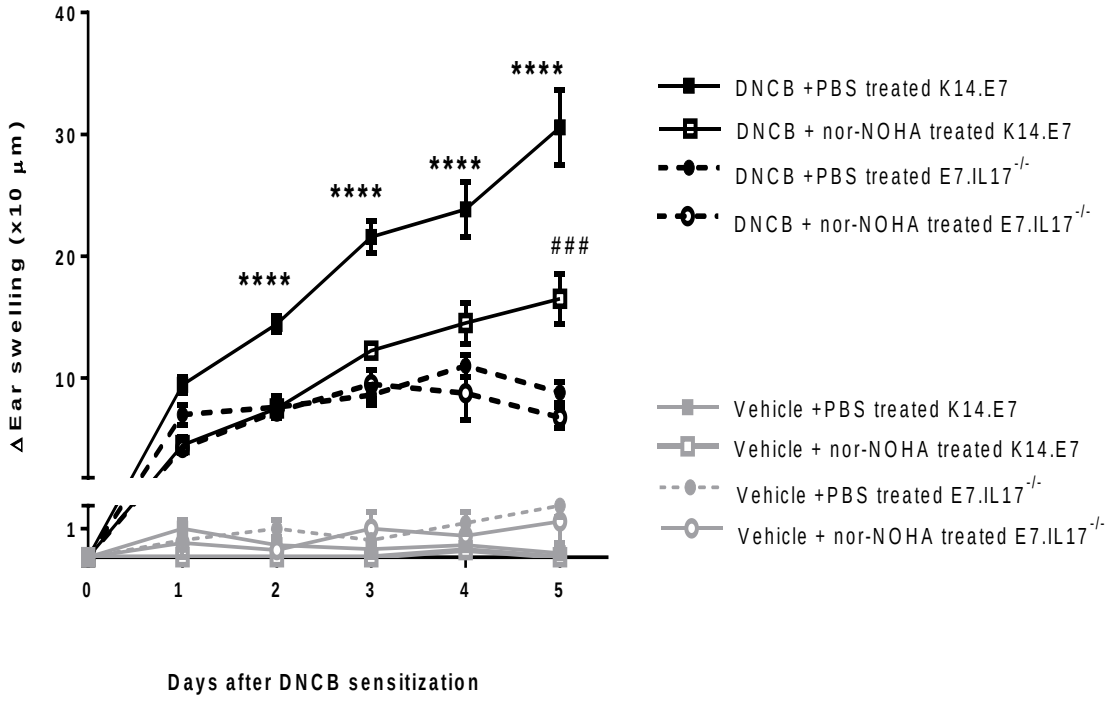

Figure 3.6- IL-17A and arginase blockade cause comparable suppression of ear swelling in DNCB-treated K14.E7 mouse skin. Ear swelling of K14.E7 and E7.IL-17$^{-/-}$ mice treated with PBS or 500 µg/mouse of nor-NOHA one day before DNCB or vehicle application and daily for 5 days. Data are means±SEM**,** and representative of 2 independent experiments, *** p< 0.001(DNCB and PBS-treated K14.E7 skin versus other treatment groups), ### p<0.001 (DNCB and nor-NOHA-treated K14.E7 skin versus DNCB-treated E7.IL17$^{-/-}$ or DNCB and IL-17A blocked K14.E7 group).

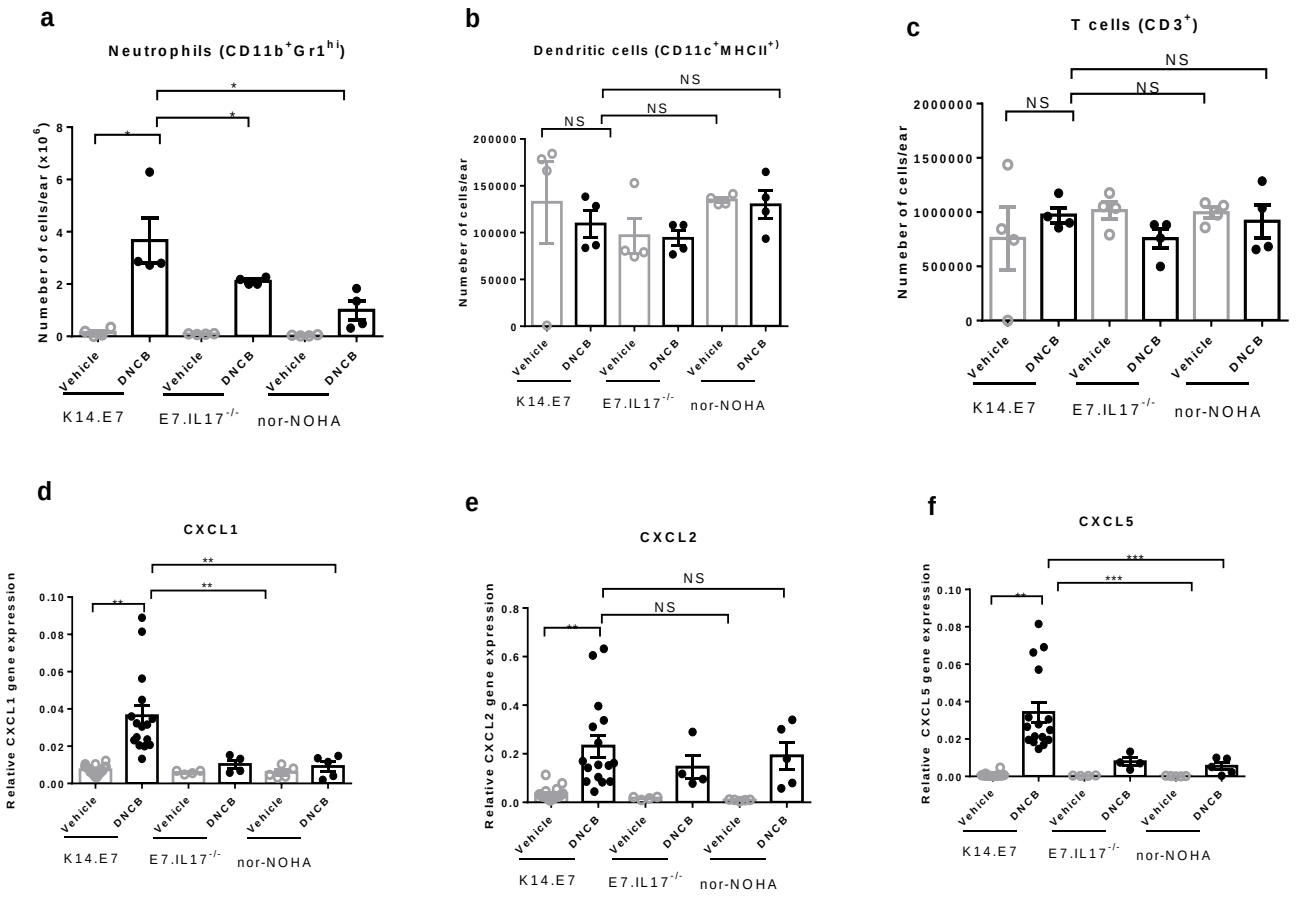

Figure 3.7- IL-17A and arginase induce chemokine production and neutrophil recruitment in DNCB-treated K14.E7 mouse skin **(a)-(c)** The absolute number of neutrophils ($CD11b^{+}Gr1^{hi}$) (a), dendritic cells ($CD11c^{+}MHCII^{+}$) (b) and T cells ($CD3^{+}$) (c) in K14.E7 mice, E7.IL17$^{-/-}$ mice and arginase inhibitor (nor-NOHA)- treated K14.E7 mice was determined by flow cytometry. **(d)-(f)** Quantitative real-time PCR analysis of CXCL1 (d), CXCL2 (e), and CXCL5 (f) transcripts in these mice. Data are means ± SEM, and are pooled from two independent experiments (n≥4 mice per group). ***** p<0.05,** p< 0.01, *** p<0.001, NS not significant.

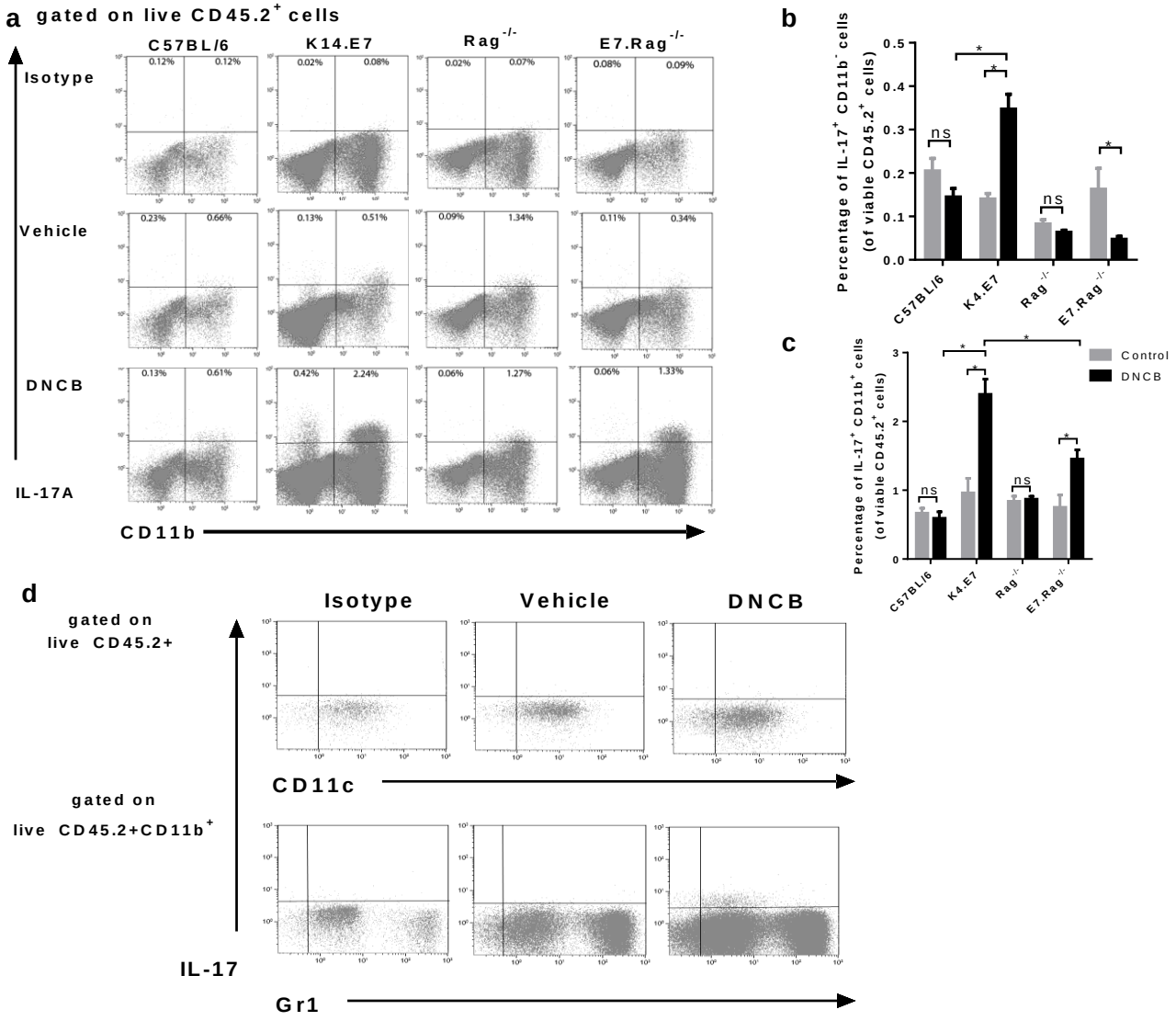

Supplementary figure 3.1- Myeloid cells are the major producers of IL-17A in DNCB-treated K14.E7 skin. (a) Representative dot plots pre-gated on viable CD45.2$^+$ cells and stained with CD11b and IL-17A**. (b)-(c)** The frequency of IL-17A$^+$ CD11b$^-$, IL-17A$^+$ CD11b$^+$ in C57BL/6, K14.E7, Rag$^{-/-}$ and E7.Rag$^{-/-}$ mice one day after DNCB treatment. Data are means ± SEM, and are pooled from two independent experiments (n= 4 mice per group).***** p<0.05, NS not significant. **(d)** Representative dot plot of IL-17A/CD11c or IL-17A/Gr1 populations. Cells were pre-gated on viable CD45.2$^+$ MHCII$^+$ cells for dendritic cell analysis and CD45.2$^+$ cells for neutrophil analysis.

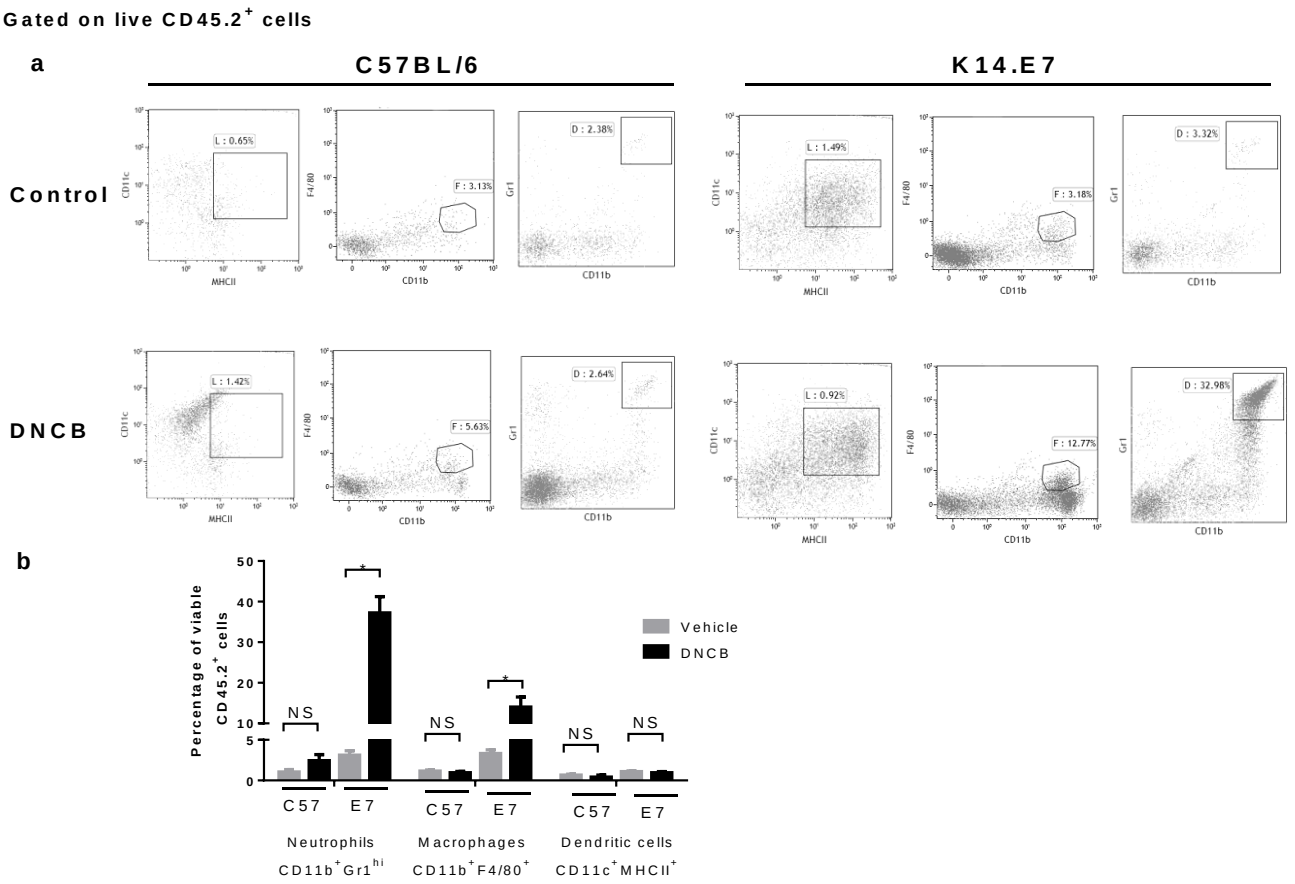

Supplementary figure 3.2- K14.E7 mouse skin exhibits enhanced recruitment of neutrophils and macrophages after DNCB treatment.

(a) Representative dot plot from vehicle/DNCB treated C57BL/6 and K14.E7 skin showing gating strategy for flow cytometric analysis of dendritic cells ($CD11c^+MHCII^+$), macrophages ($CD11b^+F4/80^+$) and neutrophils ($CD11b^+Gr1^{hi}$). Plots are representative of 4 mice per group. (b) The frequencies of these cell subsets in C57BL/6 and K14.E7 (n=4) skins after one day of DNCB treatment. Data are ploted as the mean % of viable $CD45.2^+$ cells ± SEM. * $p<0.05$, NS not significant.

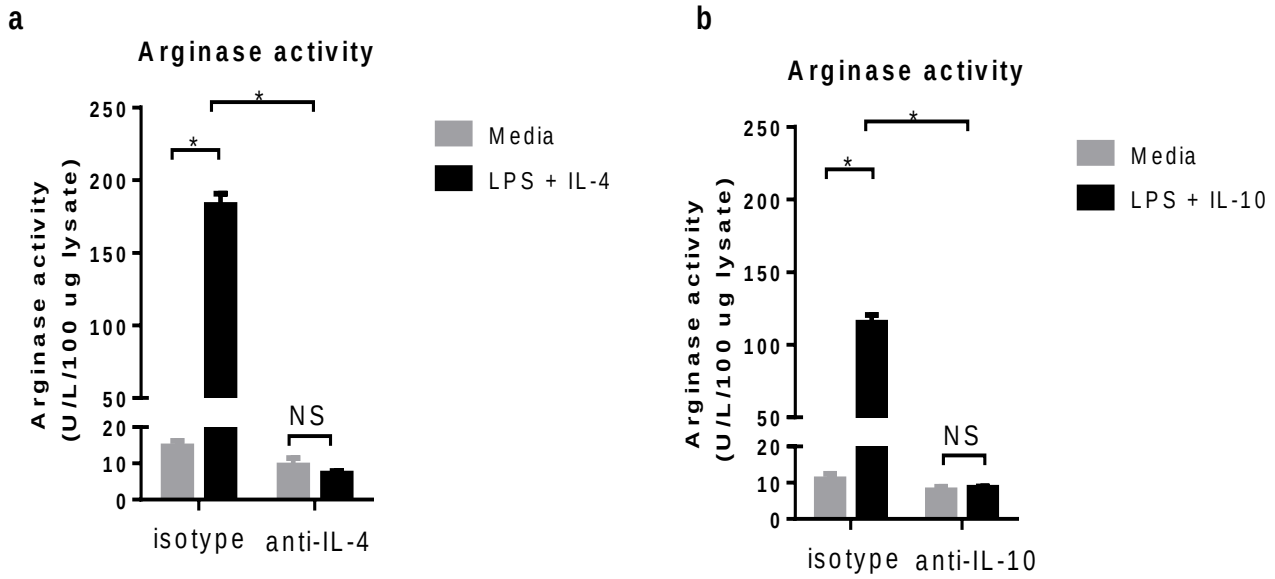

Supplementary figure 3.3- BMDM showed enhanced arginase production in response to LPS and IL-4 or IL-10 stimulation. (a)-(b) BMDM cells obtained from C57BL/6 mice were pretreated with 10 ng/ml of monoclonal antibody against IL-4 (a) or IL-10 (b) or matched-isotype control antibody before stimulation with LPS (100 ng/ml) and recombinant IL-4 or IL-10 (10 ng/ml) for 24 hours. Total protein was isolated and arginase activity was determined.

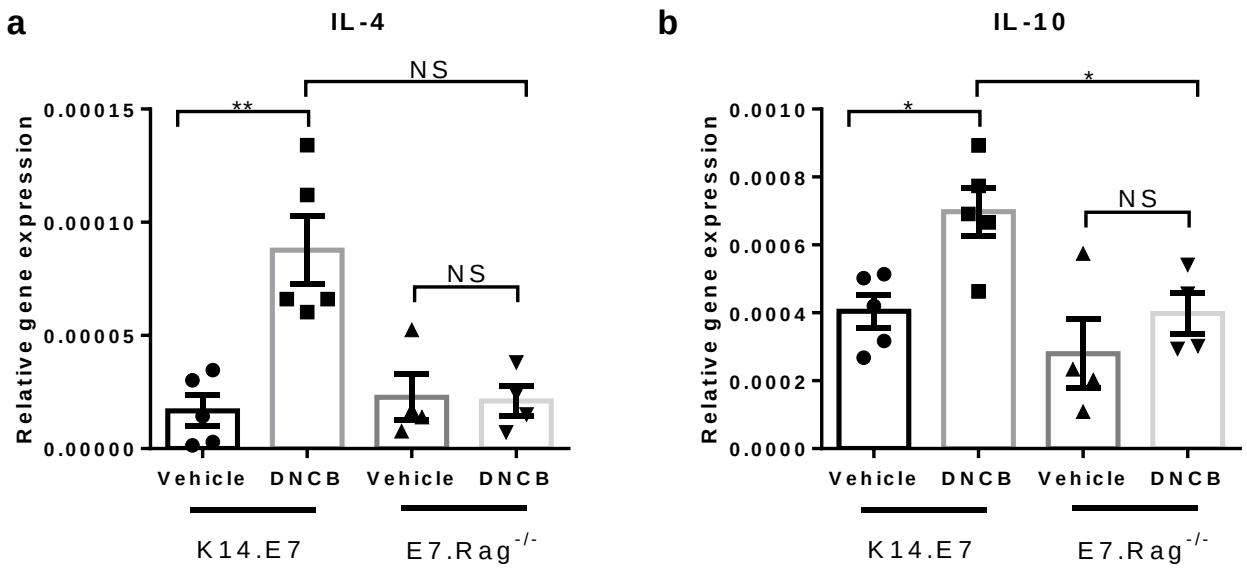

Supplementary figure 3.4- IL-4 and IL-10 are mainly produced by lymphocytes in DNCB -treated K14.E7 skin. (a)-(b) Quantitative real-time PCR analysis of IL-4 (a) and IL-10 (b) in K14.E7 or E7.Rag$^{-/-}$ skin one day after DNCB or vehicle treatment. Data are means ± SEM and representative of two independent experiments, each with n≥4 mice per group. $p<0.05$,** $p< 0.01$, NS not significant.

Discussion

Here, we show that induction of IL-17A contributes to a significantly enhanced chemokine-mediated recruitment of neutrophils and arginase-1 producing macrophages in skin expressing the E7 protein of HPV16 treated with DNCB, when compared with non-transgenic skin similarly treated with DNCB. We have previously demonstrated that HPV16.E7 expressing skin exposed to DNCB develops a hyperinflammatory response which is associated with recruitment of myeloid cells producing arginase-1 and that arginase-1 activity contributes to the enhanced inflammation (170). Here, ex-vivo skin explant culture supernatants induced enhanced arginase activity in BMDM in immune competent and $Rag^{-/-}$ mice, confirming that arginase-1 induction in K14.E7 skin exposed to DNCB was dependent on innate immune cells rather than T and B lymphocytes (170).

IL-4 and IL-10 which have been well described as potent inducers of arginase-1 in macrophages (171) and as well as important regulators of cutaneous inflammation (74) were found to be induced in K14.E7 skin, but not in wild-type C57BL/6 skin, suggesting possible involvement of these cytokines in arginase-1 regulation. Consistent with previous reports (172, 181), we found that BMDM treated with IL-4 and LPS significantly induced arginase activity and that arginase-1 induction was completely abrogated in the presence of anti-IL-4 or anti-IL-10 neutralizing antibody (Sup. figure 3.3). However, IL-4 and IL-10 blockade failed to reduce arginase-1 activity in BMDM treated with skin explant supernatant from DNCB -treated K14.E7 skin. Furthermore, the induction of Th2 cytokine IL-4 and IL-10 was abrogated in DNCB-treated E7.$Rag^{-/-}$ skin (Sup. figure 3.4), arguing against a role for these cytokines in arginase-1 induction in K14.E7 skin since the enhanced production of arginase-1 also occurred in the absence of lymphocytes.

Our observation that blockade of IL-17A caused a significant reduction in arginase-1 are consistent with a recent study which suggested that IL-17A indirectly mediates arginase-1 production in macrophages through inducing cyclooxygenase-2 (COX-2) production by human cervical cancer cell line HeLa (175). Moreover, IL-17A has been shown to mediate arginase-1 induction by promoting infiltration of inflammatory monocytes to the site of inflammation (182). In support of this, blockade of IL-17A in DNCB-treated K14.E7 skin significantly decreased the number of arginase producing $CD11b^{+}Gr1^{int}F4/80^{+}$ cells. IL-17A

might act as an up-stream enhancer of local arginase activity by enhancing recruitment of inflammatory macrophages.

IL-17A and arginase-1 were not induced in the hyperinflammation established in nontransgenic skin exposed to 10% DNCB, suggesting the involvement of HPV16.E7 oncoprotein or HPV16.E7-induced hyperproliferative epithelium in the induction of these molecules. A recent study in our laboratory suggested that expression of HPV16.E7 oncoprotein leads to elevated production of IL-17A in the skin of K14.E7 mice and hyperplastic cervical tissue (35). To date, there is no evidence in the literature that HPV16.E7 protein can directly affect the transcription of arginase. Furthermore, the E7-associated mechanisms that are responsible for IL-17A or arginase-1 induction in association with DNCB treatment remained unknown. It is speculated that E7 oncoprotein expression interacts with DNCB as an inflammasome activator, which subsequently drives the secretion of active IL-1β and IL-6 (91). These inflammasome-drived cytokines have been shown to promote IL-17A production by not only Th17 but also “non-T cells”, innate lymphoid cells (183). In support to this hypothesis, we previously demonstrated the induction of both IL-1β and IL-6 in K14.E7 skin and not in nontransgenic skin following DNCB treatment.

IL-17A production was produced by $CD11b^{+}F4/80^{+}$ macrophages in DNCB-treated $E7.Rag^{-/-}$ skin in which Th17 and γδT cells are absent, confirming the findings of others that lymphocyte subsets are not exclusive sources of IL-17A (177, 183). The proportion of IL-17A producing macrophages was significantly reduced in $E7.Rag^{-/-}$ skin compared to K14.E7 skin, suggesting that lymphocytes contributed significantly to the induction of IL-17A in these cells. However, this subset appeared to be a major producer of IL-17A in K14.E7 skin, as $IL\text{-}17A^{+}$ macrophages markedly outnumber $IL\text{-}17A^{+}$ T cells in K14.E7 skin. Thus, it is possible that IL-17A secreting macrophages might stimulate themselves in an autocrine manner leading to enhanced production of arginase-1. Alternatively, IL-17A and arginase-1 are produced by two different subsets of $CD11b^{+}Gr1^{int}F4/80^{+}$ cells. Indeed, further characterizing the IL-17A-producing subset showed that they do not express MHC-II, while arginase-1 producing cells express MHC-II (data not shown). Further, it is noted that suppression of IL-17A in K14.E7 mice could not completely abrogate arginase-1 induction, suggesting that IL-17A is not the only factor promoting arginase-1 induction.

IL-17A neutralization in K14.E7 skin as well as $E7.Rag^{-/-}$ resulted in reduced DNCB-induced ear swelling response, suggesting that macrophage-derived IL-17A contributed to the

hyperinflammation induced by DNCB in K14.E7 skin. Although Th17 and other lymphocyte subsets are regarded as primary sources of IL-17A and have been implicated as effector cells of cutaneous inflammation, our findings are in agreement with a recent study that shows that alveolar macrophages as a source of IL-17A which mediated allergic lung inflammation in a murine model of asthma (177).

The mechanisms driving the initiation of inflammation in this model remained unidentified so far, as the induction of ear swelling, measured at one day post DNCB application, did not change regardless of whether IL-17A or arginase was suppressed. However, our data clearly shows that IL-17A and arginase are significantly required for the ongoing hyper-inflammation in K14.E7 after the second day. Simultaneous blockade of both IL-17A and arginase activity did not further suppress the ear swelling response in DNCB-treated K14.E7, compared to blocking either alone. In addition, suppression of arginase activity did not reduce IL-17A production in DNCB-treated K14.E7 skin, further confirming that arginase-1 and IL-17A act in the same pathway and IL-17A is likely to be an up-stream mediator of arginase-1.

DNCB-induced hyperinflammation in K14.E7 skin is manifested by the infiltration of myeloid cells, particularly neutrophils. Blockade of either IL-17A or arginase resulted in a decrease in the number of infiltrating neutrophils, thereby reducing neutrophilic inflammation caused by DNCB in K14.E7 skin. CXCL1, CXCL2 (MIP2) and CXCL5, that signal through CXCR2 receptors, are the most potent neutrophil chemoattractants and appear to selectively promote neutrophil infiltration (178). These chemokines were all induced in K14.E7 skin after DNCB treatment, IL-17A deficiency and suppression of arginase-1 in K14.E7 skin significantly reduced the expression of CXCL1 and CXCL5, suggesting that CXCL1 and CXCL5 are important mediators for IL-17A and arginase to promote the hyperinflammation in K14.E7 skin. Our findings are supported by previous studies that IL-17A promotes neutrophil infiltration via CXCL1 (184) or CXCL5 (185) induction during acute inflammatory responses. Further, arginase specific inhibitor treatment significantly ameliorated pulmonary inflammation and airway fibrosis in guinea pig repeatedly exposed to LPS. The alleviated inflammation in these animals was concomitant with decreased neutrophil infiltration (122). However, whether IL-17A has a direct role in neutrophil recruitment and chemokine induction or acts through arginase-1 remains unknown.

In summary, the present study shows that DNCB application to HPV16.E7 expressing skin generates the acute hyperinflammation through a previously undescribed pathway at least involving IL-17A which enhances arginase-1 production. This study also identifies the E7-associated proinflammatory roles for IL-17A and arginase-1 that might be considered as potential targets to stimulate innate immunity which is speculated to support antigen specific immune-therapies for the treatment of HPV-associated diseases.

Disclosures

The authors state no conflict of interest

Acknowledgements

We would like to thank staff of the Biological Research Facility at Translational Research Institute for technical assistance and animal care. We also acknowledge Lilly Research Laboratories for providing anti-IL-17A neutralizing and matched-isotype control antibodies.

3.3 Additional data not described in the article 2

3.3.1 CCL2/MCP1 and CCL7/MCP3 are involved in IL-17A mediated-recruitment of macrophages

Data shown in article 2 demonstrated that IL-17A promoted monocyte/macrophage recruitment to DNCB-treated K14.E7 skin. Monocyte trafficking during inflammation can be guided by C-C motif chemokine ligands including CCL2, CCL7, CCL8 and CCL12 (186). DNCB application to K14.E7 skin caused a significant induction of CCL2 and CCL7 mRNA (Figure 3.8a and 3.8b). The mRNA expression levels of these chemokine were significantly reduced in IL-17A deficient K14.E7 skin, suggesting the contribution of IL-17A to the induction of CCL2 and CCL7. Conversely, there was no change in the mRNA expression levels of other chemokines including CCL8 and CCL12 in K14.E7 skin after DNCB treatment (Figure 3.8c and 3.8d). There are no chemokines or receptors which have been identified so far have a specific role in monocyte or macrophage infiltration (187). Nevertheless, CCL2 and its closely related analogue, CCL7, which can be produced by a variety of cell types including macrophages, neutrophils, fibroblasts and epithelial cells, have been identified as major mediators of the $CCR2^{+}$ monocyte infiltration during acute inflammation (188-190). Consistently, our finding suggests that IL-17A might promote macrophage/monocyte infiltration in DNCB-treated K14.E7 skin through the upregulation of CCL2 and CCL7.

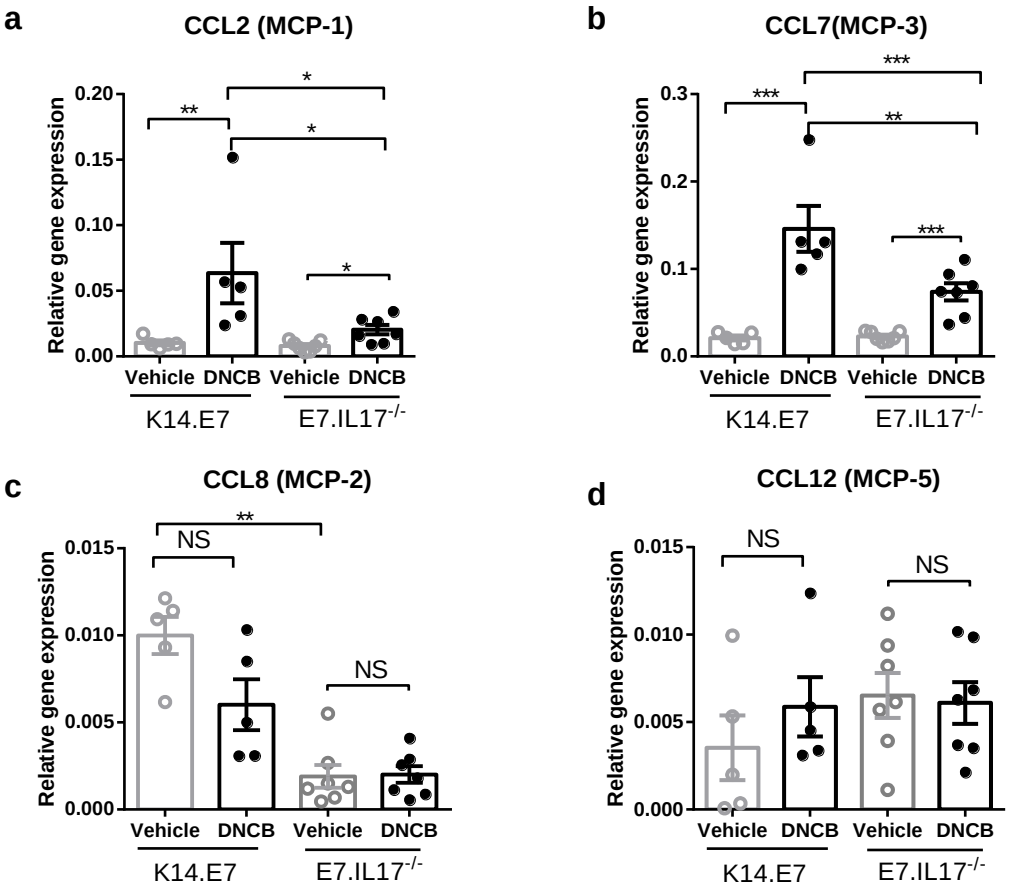

Figure 3.8- IL-17A promotes CCL2/MCP1 and CCL7/MCP3 production in K14.E7 skin after DNCB application. (a)-(d) CCL2, CCL7, CCL8 and CCL12 mRNA expression in K14.E7 and E7.IL$^{-/-}$ skin one day post vehicle or DNCB application. Data indicate SEM± mean, n≥ 5 mice per group.*, p<0.05; **, p<0.001; ***, p<0.0001; NS, not significant.

3.3.2 HPV16.E7 protein is required for IL-17A and aginase mediated-hyperinflammation

To establish the role of E7 protein in the induction of arginase-1, we examined the induction of this molecule in C57BL/6 mice treated with a 10-fold higher dose of DNCB. These animals developed ear swelling level comparable to that observed in K14.E7 mouse skin exposed to a lower level of DNCB (Figure 3.9b). However, they were unable to induce arginase-1 (Figure 3.9a) as well as IL-17A (Figure 3.3c) mRNA expression. Furthermore, blockade of IL-17A or arginase activity was unlikely to reduce the level of ear swelling of these animals (Figure 3.9b). These findings confirm that HPV16.E7 protein is required for the induction of IL-17A and arginase-1 and establishment of hyperinflammation mediated by these factors. However, the mechanism of action of E7 protein in the regulation of IL-17A and arginase-1 in response to DNCB application will require further studies.

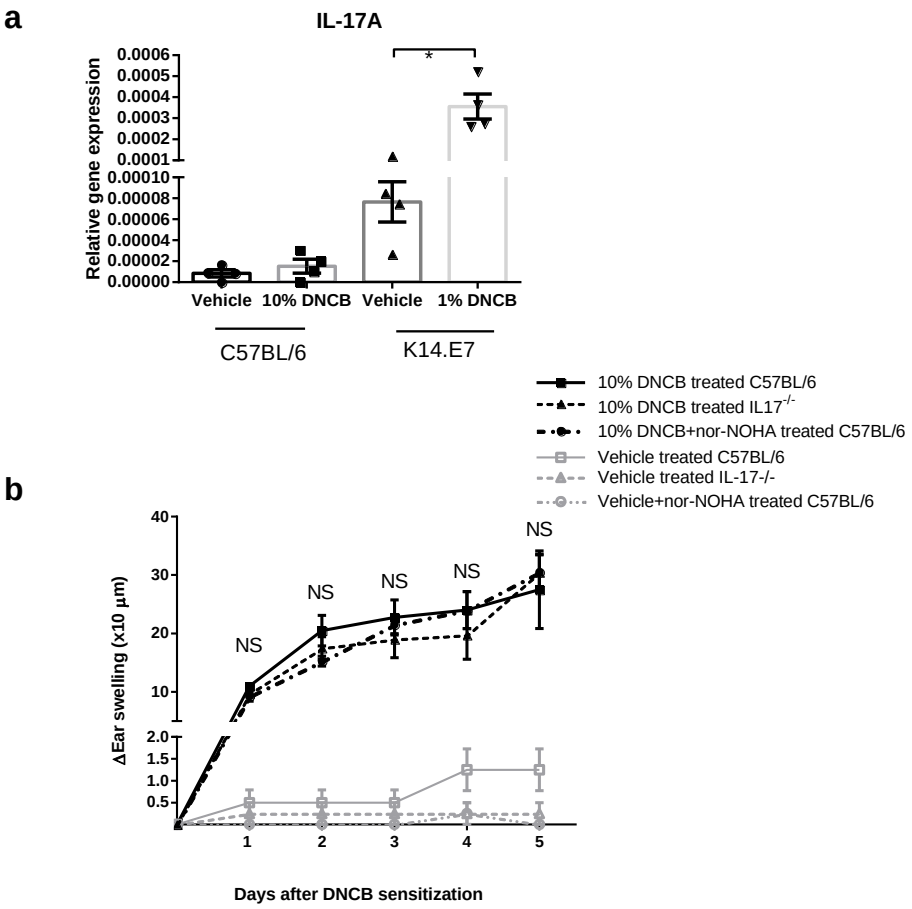

Figure 3.9- IL-17A and arginase-1 are not involved in DNCB-induced hyperinflammation in wild-type C57BL/6 transgenic skin. (a) Real-time PCR analysis of IL-17A gene expression in C57BL/6 and K14.E7 skin at day 1 post 10% or 1% of DNCB application, respectively. **(b)** Ear swealing of C57BL/6 mice pre-treated with PBS or arginase inhibitor and IL-17$^{-/-}$ mice before application with vehicle or 10% of DNCB. Data are means ± SEM, n= 4-6 mice per group.* *p<0.05*, NS not significant.

3.3.3 DNCB application results in induction of IL-1β and IL-6 in both K14.E7 and E7.Rag$^{-/-}$ skin

It has been shown that innate immune response to DNCB is initiated by the activation of inflammasome signaling pathways that drive the secretion of active IL-1β and IL-6 (91, 147). These inflammasome-drived cytokines were reported to promote IL-17A production by lymphocyte and “non-T cells”, innate lymphoid cells (183). Furthermore, IL-6 when combined with TGFβ was described as the strongest inducer of Th17 cell differentiation while IL-23 is thought to act on the expansion, maintenance of Th17 cells (83). However, little is known about the regulation of IL-17A in “non T cells”. As shown in the article 2 that the myeloid cells-derived IL-17A promoted lymphocyte independent inflammatory response to DNCB in K14.E7 skin, we sought to investigate the production of possible inducers of IL-17A in K14.E7 and E7.Rag$^{-/-}$ skin. IL-6 and IL-1β mRNA expression were significantly induced in K14.E7 and E7.Rag$^{-/-}$ skin and not in their wild-type counterpart controls (C57BL/6 and Rag$^{-/-}$) (Figure 3.10a and 3.10b). In contrast, the level of IL-23 mRNA was significantly reduced in both K14.E7 and E7.Rag$^{-/-}$ skin (Figure 3.10c). It is noted that E7.Rag$^{-/-}$ skin expressed a greater base level of IL-23 mRNA than K14.E7 skin. There was no change in the level of TGFβ mRNA expression in both K14.E7 and E7.Rag$^{-/-}$ skin following DNCB treatment (Figure 3.10d). These results suggest that the DNCB- associated induction of IL-1β and IL-6 is driven by innate immune cells in K14.E7 skin, indicating their possible involvements in the regulation of IL-17A or arginase-1 in myeloid cells.

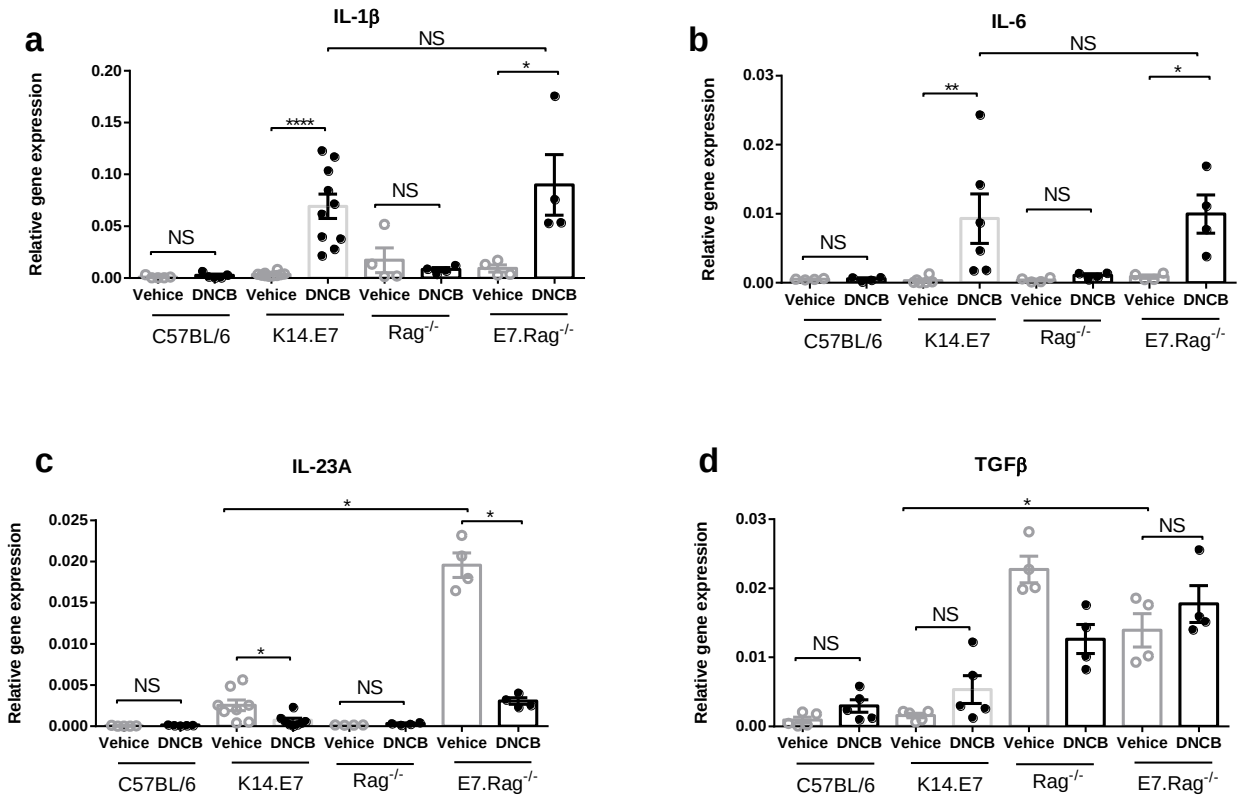

Figure 3.10- IL-1β or IL-6 and not IL-23 or TGF-β are induced by innate immune cells in K14.E7 skin. (a)-(d) Relative gene expression of IL-1β (a), IL-6(b), IL-23(c) and TGF-β (d) in C57BL/6, K14.E7, Rag$^{-/-}$ and E7.Rag$^{-/-}$ skin at one day following DNCB application. Data are means ± SEM, n= 4-9 mice per group.* *p<0.05*, *** p<0.0001, NS not significant.

3.3.4 DNCB-induced acute inflammation combined with HPV16.E7 peptide vaccination is unable to reject K14.E7 skin graft

Previous investigations have reported that K14.E7 skin is not spontaneously rejected when transplanted onto a syngeneic immunocompetent recipient animal which is capable of rejecting other non-self antigen expressing skins. Furthermore, vaccination with HPV16.E7 peptide or protein was unable to reject K14.E7 skin graft despite the induction of specific immune responses, including E7-specific $CD8^+$ T cells. Thus, these findings confirm that the expression of HPV16.E7 in the epithelium induces a local suppressive environment and the subversion of antigen-specific $CD8^+$ T cells (44, 54). Since topical application of DNCB was clinically used for the treatment of HPV-associated lesions, we speculated that stimulation of innate immunity by DNCB along with antigen-specific immunization might disrupt the local suppressive environment and restore the effector function of adaptive immunity. To address this hypothesis, we grafted wild-type C57BL/6 or K14.E7 skin onto C57BL/6 recipients, and subsequently performed vaccination with HPV16.E7 peptide and topical application with vehicle or DNCB (Figure 3.11a). As expected, graft rejection did not occur when vaccinated K14.E7 and C57BL/6 grafts were treated with vehicle. DNCB treatment along with vaccination caused moderate inflammation in C57BL/6 skin graft. Conversely, these treatments caused necrosis and dramatic shrinkage of K14.E7 skin graft on day 14 post-grafting (Figure 3.11b). Nevertheless, as the inflammation is resolved, at 20 days post grafting, the original border and shape of K14.E7 graft was retrieved despite of the loss of proximal half of the original graft. The graft is considered to be rejected if it showed the signs of ulceration or necrosis to >80% of the graft (44). Based on these criteria, DNCB-induced hyperinflammation combined with specific immunization was unable to completely reject K14.E7 skin graft even after a second treatment of DNCB and E7 vaccination (data not shown). Histologically, at 20 days post-grafting, DNCB-treated K14.E7 graft showed hyperplastic epidermis and increased infiltration of immune cells, as seen in normal K14.E7 skin (Figure 3.12), confirming that the combination therapy involving DNCB application and E7 immunization is unlikely to induce the complete rejection of K14.E7 skin graft.

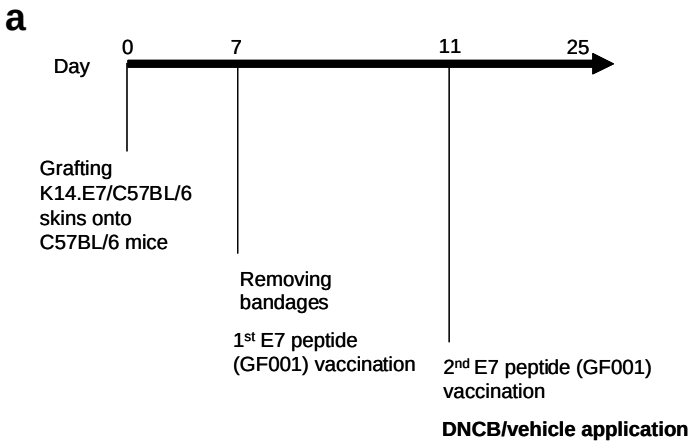

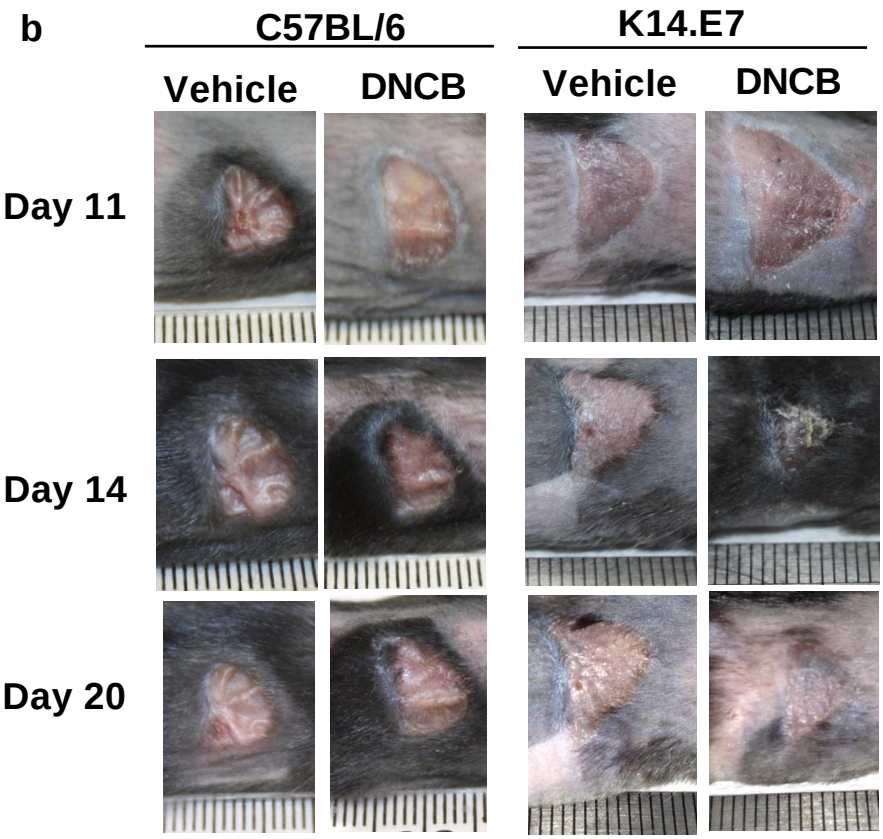

Figure 3.11- DNCB treatment combined with HPV16.E7 peptide vaccination fails to induce complete rejection of K14.E7 graft. (a) Schematic representation of peptide immunization with or without 50 µg of HPV16.E7 peptide per mouse and vehicle or DNCB (1% w/v) application of C57BL/6 and K14.E7 grafts (n=8 mice per group). **(b)** Representative photographs taken before (day 11 post-grafting), 3 days (day 14 post-grafting) and 9 days (day 20 post grafting) after vehicle or DNCB application.

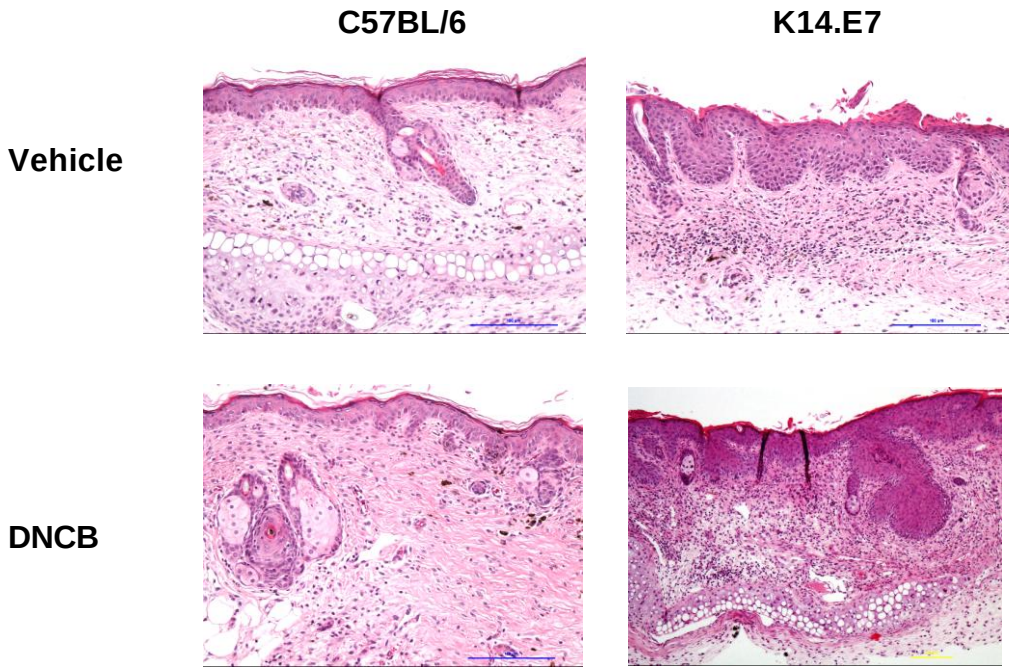

Figure 3.12- Histological sections showing epidermal hyperplasia and cellular infiltrate in E7-vaccinated and DNCB-treated K14.E7 graft. Hematoxylin and eosin stain of C57BL/6 and K14.E7 graft on day 25 post-grafting, original magnification × 200, scale bar=100 µm (Representative of at least 8 grafts per group).

3.4 Supplementary method

Skin grafting

Donor ear skin was transplanted onto recipient flanks as previously described (42, 53). Briefly, dorsal and ventral ear halves excised from donor mice were placed on the thoracic flanks of anesthetized recipient mice. Grafts were held in place with antibiotic-permeated gauze (Bactigras; Smith and Nephew, London, UK) and bandaged with micropore tape and Flex-wrap (Lyppard, Queensland, Australia). Bandages were removed 7 days after grafting, and grafts were monitored daily for loss of distinct border and visible signs of ulceration or necrosis to >80% of the graft, which was defined as graft rejection.

Immunization and DNCB treatment scheme

After removing bandages, grafted mice were immunized subcutaneously at the flank with 100 μg/mouse of GF001 peptide (H-2D^{b}–restricted minimal CTL epitope of HPV16 E7 protein, aa sequence = RAHYNIVTF) emulsified in Complere Freund's adjuvant as indicated (Sigma, MO, USA). Immunization was repeated with incomplete Fruend's adjuvant on day 11 post-grafting and 50 μl of 1% (v/v) DNCB was topically applied onto skin graft region. Photos of grafts were taken daily to monitor graft rejection.

3.5 Conclusion

Chapter 2 demonstrated the significant contribution of arginase-1 to the DNCB-induced inflammation in K14.E7 skin. In this third chapter, my results showed that HPV16.E7 expressing skin developed a hyperinflammatory response to DNCB through a pathway at least involving IL-17A which promotes arginase-1 production. Furthermore, this study identified the E7 associated- proinflammatory role of macrophage-derived IL-17A and arginase-1 in the stimulation of neutrophil infiltration via CXCL1 and CXCL5.

Additionally, I observed the lymphocyte- independent induction of IL-1β and IL-6 which might be associated with activation of inflammasome signaling in K14.E7 skin in response to DNCB, thereby leading to the induction of IL-17A and arginase-1.

Lastly, I have shown that the combination therapy involving HPV oncoprotein specific immunization and DNCB mediated-innate immune activation was insufficient to break the tolerance of HPV16.E7 oncoprotein.

CHAPTER 4

Conclusion and Discussion

4.1. Topical application of DNCB to HPV16.E7 expressing skin causes lymphocyte-independent hyperinflammation

Previous studies using the K14.E7 skin transplantation model of HPV-associated human squamous cancer, have shown that a 14.E7 skin graft is not spontaneously rejected by an immunocompetent recipient animal despite the induction of specific immune response by immunization with E7 protein. This finding indicates that the HPV16.E7 oncoprotein induces a locally immunosuppressive environment which subverts the host innate immunity, thereby leading to viral persistent infection and carcinogenesis. Effective immune-therapies targeting HPV-associate cancer are thus required to overcome the local suppressive environment.

Topical application of DNCB, an immune-enhancer, resulted in a greater than 80% regression of HPV-associated lesions including alopecia areata, viral warts, and basal and squamous cell carcinomas (191). In line with these clinical findings, a previous study using a mouse model of melanoma showed that combination therapy involving the simultaneous application of DNCB with systemic administration of decarbazine, a DNA alkylating agent, caused an enhanced cytolytic effector function of $CD8^+$ T cells and tumor regression (192).

Although clinical use of DNCB has been limited due to its mutagenic and carcinogenic effects, understanding the underlying mechanisms of how DNCB treatment alters the local immune environment induced by HPV16.E7 oncoprotein might lead to better treatment options for HPV persistently infected patients. The present study shows that a single exposure to DNCB causes an acute hyperinflammatory response in K14.E7 skin which is not seen in non-transgenic mice. This finding is consistent with the clinical observation that DNCB application evokes more vigorous inflammation in tumor tissues than in surrounding normal skin (193).

It has been well established that the clinical effect of DNCB is attributable to its ability to boost the T cell-mediated immune responses (69). Interestingly, data shown in chapter 2 demonstrated that the hyperinflammation after a single exposure to DNCB also occurred in E7.$Rag^{-/-}$ skin and is therefore independent of antigen specific cell-mediated immunity.

4.2 HPV16.E7-induced cutaneous hyperinflammation to DNCB is associated with enhanced myeloid cell infiltration and IL-4, IL-10 and IL-17A production

There is limited data concerning the topical DNCB effect on the innate immunity. DNCB has been described as a “danger signal” which can trigger the NALP-3 inflammasome in keratinocytes or DC (91, 147, 194), resulting in production of proinflammatory cytokines including IL-6, IL-1β during early inflammatory response (148, 149). We indeed detected T and B lymphocyte-independent induction of IL-6 and IL-1β mRNA in DNCB-treated K14E7 skin, indicating the possible contribution of these cytokines in regulating the hyperinflammation.

Furthermore, it has been shown that these molecules exert their immune-stimulatory effects through recruitment of leukocytes and further induction of a wide range of cytokines including Th1, Th2 cytokines, IL-17A and IL-22 in these cells (195-197). In support of this notion, the hyperinflammation in K14.E7 skin was manifested by an increased number of inflammatory myeloid cells in the dermis and the induction of IL-4, IL-10, IL-17A, but not Th1 cytokines including IFNγ and TNFα. Although Th2 cytokines and IL-17A have been previously reported to correlate with HPV-associate tumor progression, the mechanisms of action of these molecules have not been elucidated yet (198, 199). In contrast, a recent study has demonstrated that Listeria-based immune therapy induces IL-17A production which fosters the regression of tumor in HPV transplantable mouse model (32). In addition, IL-17A-derived-γδ T cells is critically required for optimal anti-tumor function of $CD8^+$ T cells and chemotherapeutic efficacy (200).

4.3 DNCB-induced IL-17A, but not IL-4 and IL-10 mediates arginase-1 induction by macrophages in K14.E7 skin

Findings in chapter 2 showed that arginase-1 and arginase activity were significantly induced in $CD11b^+F4/80^+Gr1^{int}Ly6C^+Ly6G^-$ monocyte/macrophages infiltrating to DNCB-treated K14.E7 skin but not in nontransgenic control animals. Cytokines including IL-4, IL-10 and IL-17A have been reported as important inducers of arginase-1 by myeloid cells, an important regulator of innate immunity (150, 175). The induction of Th2 cytokines including IL-14 and IL-10 was entirely diminished in DNCB-treated $E7.Rag^{-/-}$ skin in which arginase

induction occurred, arguing against a role for these cytokines in the regulation of arginase-1 in K14.E7 skin. Furthermore, we showed in chapter 3 that blockade of IL-4 or IL-10 was unlikely to abrogate the induction of arginase-1 in BMDM stimulated with supernatant from DNCB-treated K14.E7 skin explants. In contrast, IL-17A mRNA expression was shown to be induced in E7.Rag$^{-/-}$ skin and contributed to the induction of arginase-1 in BMDM as well as K14.E7 skin following DNCB application. In line with this finding, IL-17A has been recently shown to promote arginase-1 expression in macrophages through activation of the COX-2/PGE2 pathway in HPV-positive cancer cells. Indeed, we also detected the induction of PGE2 synthase (Table 2.1) in K14.E7 skin but not in nontransgenic skin after DNCB application, suggesting that additional studies are required to dissect the link of IL-17A and this molecule.

Furthermore, Nishikawa *et al.* (2014) reported that IL-17A was involved in the enhanced recruitment of CD11b^{+}Ly6C^{+}MHCII^{+} macrophages which produce arginase-1 during intestinal inflammatory response in a mouse model of colitis (201). Consistent with this observation, data shown in chapter 3 demonstrated a significant reduction in the number of CD11b^{+}Gr1^{int} cells in E7.IL17$^{-/-}$ skin after DNCB application, suggesting one action of IL-17A on the induction of arginase in K14.E7 skin is to increase recruitment of arginase-1 producing myeloid cells. Inflammatory monocytes which express the CCR2 receptor are recruited from the peripheral blood circulation to the site of inflammation in K14.E7 skin in response to CCR2 ligands including CCL2 (MCP1), CCL7 (MCP3), CCL8 (MCP2) and CCL12 (MCP5) (186). The present study showed that CCL2 and CCL7 (but not CCL8 and CCL12) were upregulated in K14.E7 after DNCB application and that IL-17A significantly contributes to the induction of these chemokines. These findings were supported by a previous study of airway inflammation showing that IL-17A stimulated monocyte chemotaxis occurs through induction of CCL2 and CCL5 in lung epithelial cells (202).

It is noted that suppression of IL-17A in K14.E7 mice could not completely abrogate arginase-1 induction, suggesting that IL-17A is not the only factor promoting arginase-1 induction. IL-6 or COX-2/PGE2 has each been shown to induce IL-17A and arginase production in macrophage (103, 203-205). Therefore, further studies are required to examine the link of these molecules with IL-17A or arginase induction in K14.E7 skin.

4.4 Macrophage derived-IL-17A and arginase mediate DNCB-induced hyperinflammation in K14.E7 skin

HPV16.E7-associated $CD11b^{+}F4/80^{+}$ macrophages induced a greater level of IL-17A in response to DNCB than lymphocytes, suggesting that this cell population is the dominant source of IL-17A in this response. Furthermore, deficiency in IL-17A production caused a significant reduction in the level of DNCB-induced inflammation in both K14.E7 and $Rag.E7^{-/-}$ skin, demonstrating that macrophage-derived IL-17A is important for DNCB-induced hyperinflammation in the absence of T and B cells. Although Th17 and other lymphocyte subsets are regarded as primary sources of IL-17A and have been implicated as effector cells of cutaneous inflammation, our findings are in agreement with a recent study showing that alveolar macrophages as a source of IL-17A mediated allergic lung inflammation in a murine model of asthma (177).

Arginase can function either as a proinflammatory or immunosuppressive mediator depending on the inflammatory context. Lepique *et al* (2009) showed that in a HPV-16 induced transplantable tumor model, macrophages expressing high levels of arginase-1 facilitate tumor growth by dampening antitumor T cell function (116). Data shown in chapter 2 demonstrated the proinflammatory function of arginase-1 in K14.E7 skin exposed to DNCB was blocked in the presence of a specific arginase inhibitor, alleviating DNCB-induced inflammation. In line with these findings, arginase-1 produced by macrophages has been shown to be responsible for the pathophysiology of asthma which is a complex disease manifested by allergic airway inflammation and airway hyperreactivity. In mouse models of asthma, arginase-1 drives allergic inflammatory response in lung epithelial cells through the modulation of NFκB signaling pathway (120, 121). Furthermore, treatment with an arginase specific inhibitor, ABH, significantly ameliorated pulmonary inflammation and airway fibrosis in guinea pigs repeatedly exposed to LPS. The alleviated inflammation in these animals was concomitant with decreased IL-8 production and neutrophil infiltration (122). In accordance with this study, we found that blockade of either IL-17A or arginase activity resulted in a decrease in the number of infiltrating neutrophils, thereby reducing neutrophilic inflammation caused by DNCB in the K14.E7 skin. CXCL1, CXCL2 and CXCL5, which signal through CXCR2 receptors, are the most potent neutrophil chemoattractants and appear to selectively promote neutrophil infiltration (178). These chemokines were all induced in K14.E7 skin after DNCB treatment, However, IL-17A deficiency and suppression of arginase-1 in K14.E7 skin significantly reduced the expression of CXCL1 and CXCL5, suggesting that CXCL1 and

CXCL5 are important mediators for IL-17A and arginase to promote the hyperinflammation in K14.E7 skin. Our findings are supported by previous studies that IL-17A promotes neutrophil infiltration via CXCL1 (184) or CXCL5 (185) induction during acute inflammatory responses. However, whether IL-17A has a direct role in neutrophil recruitment and chemokine induction or acts through arginase-1 remains unknown.

Suppression of NO production by iNOS is one possible mechanism by which arginase-1 mediates hyperinflammation. Endothelium-derived NO was reported to suppress the expression of adhesion molecules such as vascular cell adhesion molecule-1 and intercellular adhesion molecule-1 (123), thereby inhibiting vascular inflammation. Paradoxically, NO produced by neutrophils has been shown to enhance vascular permeability, erythema and infiltration of innate immune cells to the site of inflammation (206). As shown in chapter 2, iNOS was induced in K14.E7 skin following DNCB treatment despite the induction of arginase activity. Furthermore, DNCB-induced arginase activity in K14.E7 skin favored, rather than suppressed, NO production. Thus, we speculated that arginase enhanced NO production in DNCB treated K14.E7 skin, possibly through promoting recruitment of neutrophils which were previously described as major producers of NO during cutaneous inflammation (166).

Simultaneous blockade of IL-17A and arginase was unable to further suppress DNCB-induced ear swelling compared to suppression either arginase or IL-17A alone. Furthermore, suppression of arginase did not have an impact on IL-17A expression in DNCB-treated K14.E7 skin. Together, these findings suggested that arginase -1 is a downtream effector molecule of IL-17A and that IL-17A and arginase mediated DNCB-induced hyperinflammation in K14.E7 skin.

4.5 The involvement of HPV16.E7 protein in IL-17A and arginase induction

The present study showed that a single exposure to DNCB causes an acute hyperinflammatory response in K14.E7 skin which is not seen in non-transgenic mice or in other transgenic skins including K14.hGh and K5.OVA, suggesting the involvement of the HPV16.E7 oncoprotein in the generation of the hyperinflammation. Additionally, data shown in chapter 3 reported that IL-17A and arginase-1 were not induced in the hyperinflammation established in nontransgenic skin by exposure to 10% DNCB, further demonstrating the crosstalk between HPV16.E7 oncoprotein expressed in the epithelium and the induction of

these innate immune molecules. There is no evidence in the literature that HPV.E7 protein can directly affect the transcription of arginase, and we have shown RNA data to that effect from the mouse model. Likewise, RNAseq data (data in preparation for publication) showed the impact of E7 expression on a wide range of genes but not on Arginase-1 or 2. A recent study in our laboratory suggested that expression of the HPV16.E7 oncoprotein leads to the elevated production of IL-17A in the skin of K14.E7 mice and hyperplastic cervical tissue (35). However, the E7-associated mechanism of IL-17A and arginase-1 induction in response to DNCB application remains unknown. It is speculated that E7 expression interacts with DNCB as an inflammasome activator to alter arginase induction in myeloid cells. Indeed, it has been reported that the acute cutaneous inflammatory response to DNCB is initiated by the activation of inflammasome signaling pathways, which drive the secretion of active IL-1β and IL-6 (91). These inflammasome-driven cytokines were reported to promote IL-17A production by not only Th17 but also “non-T cells”, innate lymphoid cells (183). In support of this hypothesis, in chapter 3, we demonstrated the induction IL-1β and IL-6 in both K14.E7 and E7.Rag$^{-/-}$ skin following DNCB treatment. Of note, the precise mechanisms driving the initiation of inflammation in this model remain unidentified so far, as the induction of ear swelling, measured at one day post DNCB application, did not change regardless of whether IL-17A or arginase was suppressed. Further, studies are thus required to dissect the implication of these cytokines in the induction of IL-17A and arginase-1 in macrophages.

4.6 Conclusion and Clinical implication

Current therapeutic strategies targeting HPV-associated diseases have largely failed at clinical stages, despite promising results in animal models. One possible explanation for failure is that although these approaches induce HPV oncoprotein specific CD4^{+} and CD8^{+} T cell responses, they do not target the virus-driven immunosuppressive environment that inhibits the effector functions of T cells. The present study using the HPV16.E7 transgenic mouse model shows that DNCB application generates the lymphocyte-independent acute cutaneous hyperinflammation that might support antigen specific immune therapies. Furthermore, results presented in this thesis demonstrated a previously undescribed molecular and cellular pathway for the development of DNCB-induced hyperinflammation in which IL-17A and arginase play pro-inflammatory roles (Figure 4.1).

Thus, induction of IL-17A or arginase-1 by administrating recombinant IL-17A and arginase-1 protein might be considered as a supplementary strategy to establish acute hyperinflammation in HPV-infected patients. Although, there are numerous reports regarding IL-17A and arginase-1 showing their contributions to immunosuppression, our findings are consistent with recent studies suggesting that these molecules are involved in the activation of innate immune response in asthma. Furthermore, although numerous studies have suggested that arginase-1 expression is restricted to neutrophils in humans, recent studies have proposed the presence of arginase-1 macrophages in mycobacterial granulomas following clinical use of pegylated human recombinant arginase for cancer treatment in humans.

4.7 Future directions

The following questions would be addressed in prospective studies:

1. To what extent our observation is relevant to HPV infection in humans?

HPV16.E7 transgenic mouse reflects the biology of human squamous cancers associated with HPV oncoprotein induced-immune suppression, in which only E7 genes of the papillomavirus are expressed (13). However, this model does not reflect the complete immunobiology of HPV infection in humans. Indeed, previous studies have shown that not only E7 but also the E6 oncoprotein plays an important role in the local inflammatory responses and tumour specific immunity (42, 99, 207). Therefore, further studies will investigate the inflammatory response to DNCB in both the E6 and E7 and E6xE7 transgenic animals to dissect the role of these two oncoproteins in driving innate immunity to DNCB.

2. Is E7-driven epidermal hyperplasia responsible for the enhanced recruitment of myeloid cells and induction of IL-17A and arginase-1 in response to DNCB application?

Numerous studies have highlighted the crosstalk between hyperproliferative epithelium and innate immune cells (208, 209). We speculated that the activation of IL-17A and arginase-1 might be dependent on HPV16.E7 oncoprotein-induced epidermal hyperplasia. Therefore, it would be interesting to assess the effect of DNCB application on the recruitment of immune cells and production of arginase and IL-17A in Rb^{mut}xK14.E7 knock-in mice. These animals will allow us to compare the role for hyperplasia in DNCB-induced inflammation as

they express mutant retinoblastoma protein which is unable to be bound by E7 protein and thus remains functional for the control of the cell cycle and display normal skin without epidermal hyperplasia.

3. Whether arginase induction is driven by macrophage-derived IL-17A?

The induction of both IL-17A and arginase-1 in DNCB-treated E7.Rag$^{-/-}$ skin observed in chapter 3 prompted us to speculate that macrophage-derived IL-17A is an important inducer of arginase-1. To address this hypothesis, the level of arginase-1/arginase activity will be examined in E7.Rag$^{-/-}$ skin following administration of IL-17A neutralizing antibody or matched-isotype control antibody.

4. Why did DNCB-induced inflammation cause hyperinflammaton and shrinkage in K14.E7 grafts but fail to induce complete graft rejection?

The rejection of E7 skin graft is believed to be mediated by a strong cell-mediated immunity, particularly cytotoxic CD8^{+} T cells (210). The results shown in chapter 3 demonstrated that DNCB application combined with E7 peptide immunization was unable to induce complete rejection of K14.E7 grafts in HPV16.E7-immunized recipient animals despite induction of hyperinflammation and significant shrinkage of the graft. This raised the question of whether the failure of rejection might be due to insufficient effector CD8^{+} T cells. First of all, the ability of DNCB treatment to enhance the recruitment or effector function of E7-specific CD8^{+} T cells in immunized recipient mice will be assessed by performing flow cytometric analysis of infiltrating graft lymphocytes. Furthermore, we wish to address whether combination therapy involving adoptive transfer of E7^{+} specific CD8^{+} T cells and DNCB application can enhance K14.E7 graft rejection. Alternatively, does DNCB-associated IL-17A and arginase not only play a proinflammatory role but also exert their immunosuppressive functions which might be responsible for the failure of K14.E7 graft rejection? Therefore, further studies will investigate the extent to which these molecules drive the function of effector CD8^{+} T cells. Collectively, dissecting these questions will enable us to understand the requirements that must be met to break the tolerance of HPV16.E7 oncoprotein.

5. Whether a safer immune adjuvant such as aluminium hydroxide (alum) which also acts by activating inflammasome can be used as a suitable substitute for DNCB?

Alum has widely been used as a principle vaccine adjuvant for several clinical applications due to its ability to stimulate the innate immunity. Recent studies have reported that alum can activate the NLRP3 inflammasome, thereby inducing IL1β production and promoting innate cell infiltration (211, 212). Therefore, it will be interesting to investigate whether alum treatment can provoke hyperinflammatory response in HPV16 E7 transgenic mouse model as DNCB application. Nonetheless, it is also noted that alum is a poor inducer of cell-mediated immunity while DNCB application can activate both innate and cellular immunity. Therefore, aditional signals are required for particulates to effectively promote cell-mediated immunity (213). Therefore, further studies will examine whether the combination of this adjuvant and E7-specific vaccine can induce the rejection of E7 expressing skin grafts.

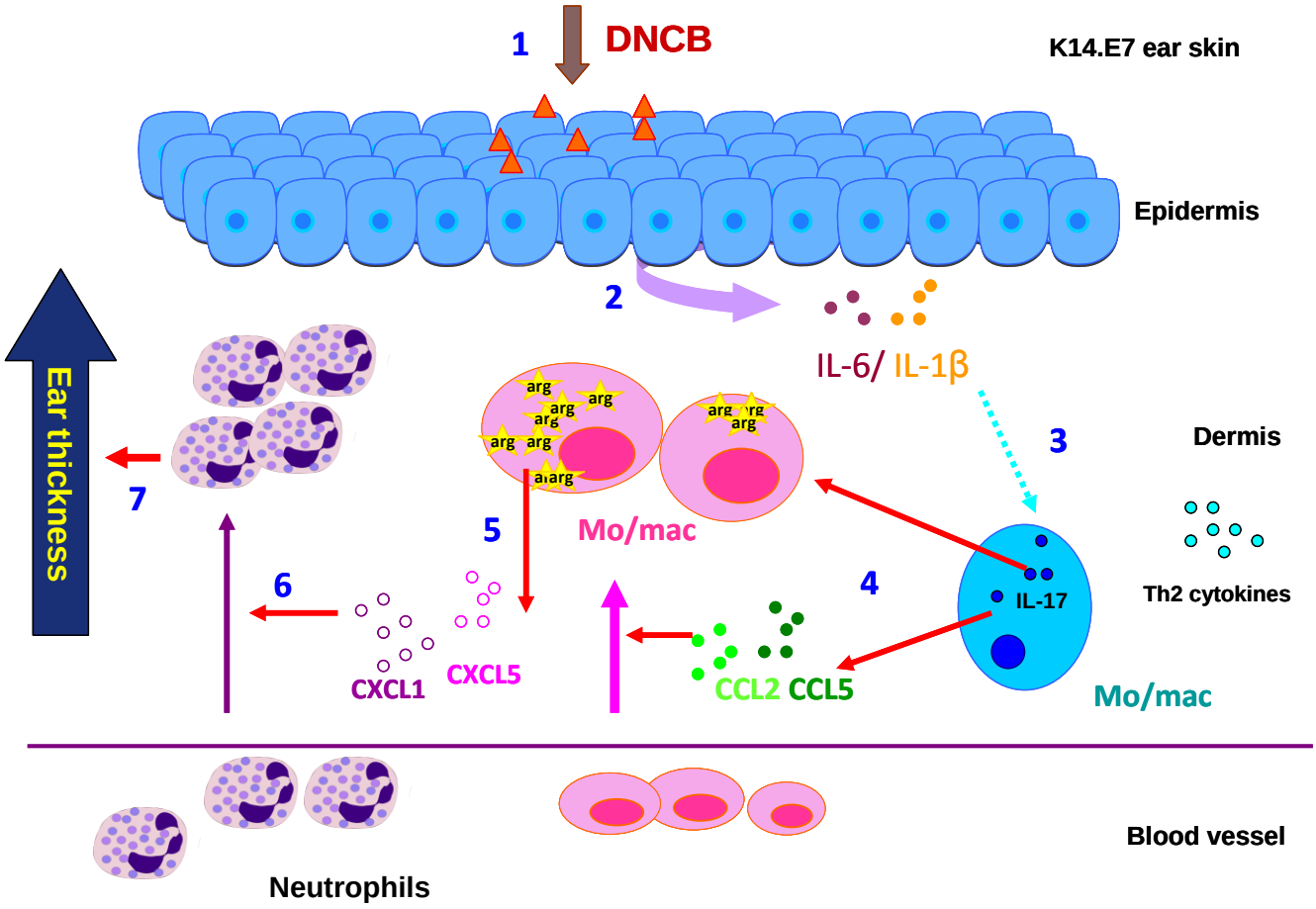

Figure 4.1- The proposed mechanism of DNCB-induced hyperinflammation in HPV16.E7 expressing skin. 1) and 2) DNCB application to the skin results in induction of inflammasome-driven cytokines including IL-6 and IL-1β. 3) These molecules might be responsible for the induction of IL-17A, IL-4 and IL-10. 4) IL-17A promotes the recruitment of arginase-1 producing macrophages through induction of CCL2 and CCL7. 5); 6) and 7) Arginase-1 and IL-17A enhance neutrophil infiltration through inducing CXCL1 and and CXCL5 production, thereby mediating DNCB-induced hyperinflammation. Mo/Mac: monocyte/macrophage

Bibliography

1. Stanley, M. A. 2012. Epithelial cell responses to infection with human papillomavirus. *Clin Microbiol Rev* 25: 215-222.
2. Boccardo, E., A. P. Lepique, and L. L. Villa. 2010. The role of inflammation in HPV carcinogenesis. *Carcinogenesis* 31: 1905-1912.
3. Quint, K. D., R. E. Genders, M. N. de Koning, C. Borgogna, M. Gariglio, J. N. Bouwes Bavinck, J. Doorbar, and M. C. Feltkamp. 2014. Human Beta-Papillomavirus Infection and Keratinocyte Carcinomas. *J Pathol*.
4. Favre, M., S. Majewski, N. De Jesus, M. Malejczyk, G. Orth, and S. Jablonska. 1998. A possible vertical transmission of human papillomavirus genotypes associated with epidermodysplasia verruciformis. *J Invest Dermatol* 111: 333-336.
5. Wang, J., B. Aldabagh, J. Yu, and S. T. Arron. 2014. Role of human papillomavirus in cutaneous squamous cell carcinoma: a meta-analysis. *J Am Acad Dermatol* 70: 621-629.
6. Aldabagh, B., J. G. Angeles, A. R. Cardones, and S. T. Arron. 2013. Cutaneous squamous cell carcinoma and human papillomavirus: is there an association? *Dermatol Surg* 39: 1-23.
7. zur Hausen, H. 2002. Papillomaviruses and cancer: from basic studies to clinical application. *Nat Rev Cancer* 2: 342-350.
8. Schiller, J. T., P. M. Day, and R. C. Kines. 2010. Current understanding of the mechanism of HPV infection. *Gynecol Oncol* 118: S12-17.
9. Frazer, I. H. 2004. Prevention of cervical cancer through papillomavirus vaccination. *Nat Rev Immunol* 4: 46-54.
10. Dyson, N., P. M. Howley, K. Munger, and E. Harlow. 1989. The human papilloma virus-16 E7 oncoprotein is able to bind to the retinoblastoma gene product. *Science* 243: 934-937.
11. Scheffner, M., B. A. Werness, J. M. Huibregtse, A. J. Levine, and P. M. Howley. 1990. The E6 oncoprotein encoded by human papillomavirus types 16 and 18 promotes the degradation of p53. *Cell* 63: 1129-1136.
12. Mazumder Indra, D., R. K. Singh, S. Mitra, S. Dutta, C. Chakraborty, P. S. Basu, R. K. Mondal, S. Roychoudhury, and C. K. Panda. 2011. Genetic and epigenetic changes of HPV16 in cervical cancer differentially regulate E6/E7 expression and associate with disease progression. *Gynecol Oncol* 123: 597-604.

13. Frazer, I. H., G. R. Leggatt, and S. R. Mattarollo. 2011. Prevention and treatment of papillomavirus-related cancers through immunization. *Annu Rev Immunol* 29: 111-138.
14. Schiffman, M., and P. E. Castle. 2005. The promise of global cervical-cancer prevention. *N Engl J Med* 353: 2101-2104.
15. Monnier-Benoit, S., F. Mauny, D. Riethmuller, J. S. Guerrini, M. Capilna, S. Felix, E. Seilles, C. Mougin, and J. L. Pretet. 2006. Immunohistochemical analysis of CD4+ and CD8+ T-cell subsets in high risk human papillomavirus-associated pre-malignant and malignant lesions of the uterine cervix. *Gynecol Oncol* 102: 22-31.
16. Dominiecki, M. E., G. L. Beatty, Z. K. Pan, P. Neeson, and Y. Paterson. 2005. Tumor sensitivity to IFN-gamma is required for successful antigen-specific immunotherapy of a transplantable mouse tumor model for HPV-transformed tumors. *Cancer Immunol Immunother* 54: 477-488.
17. Garnett, T. O., M. Filippova, and P. J. Duerksen-Hughes. 2006. Accelerated degradation of FADD and procaspase 8 in cells expressing human papilloma virus 16 E6 impairs TRAIL-mediated apoptosis. *Cell Death Differ* 13: 1915-1926.
18. Amador-Molina, A., J. F. Hernandez-Valencia, E. Lamoyi, A. Contreras-Paredes, and M. Lizano. 2013. Role of innate immunity against human papillomavirus (HPV) infections and effect of adjuvants in promoting specific immune response. *Viruses* 5: 2624-2642.
19. Nicholls, P. K., B. A. Klaunberg, R. A. Moore, E. B. Santos, N. R. Parry, G. W. Gough, and M. A. Stanley. 1999. Naturally occurring, nonregressing canine oral papillomavirus infection: host immunity, virus characterization, and experimental infection. *Virology* 265: 365-374.
20. Hernandez, B. Y., T. Ton, Y. B. Shvetsov, M. T. Goodman, and X. Zhu. 2012. Human papillomavirus (HPV) L1 and L1-L2 virus-like particle-based multiplex assays for measurement of HPV virion antibodies. *Clin Vaccine Immunol* 19: 1348-1352.
21. Bhat, P., S. R. Mattarollo, C. Gosmann, I. H. Frazer, and G. R. Leggatt. 2011. Regulation of immune responses to HPV infection and during HPV-directed immunotherapy. *Immunol Rev* 239: 85-98.
22. Hasan, U. A., E. Bates, F. Takeshita, A. Biliato, R. Accardi, V. Bouvard, M. Mansour, I. Vincent, L. Gissmann, T. Iftner, M. Sideri, F. Stubenrauch, and M. Tommasino. 2007. TLR9 expression and function is abolished by the cervical cancer-associated human papillomavirus type 16. *J Immunol* 178: 3186-3197.

23. Barnard, P., E. Payne, and N. A. McMillan. 2000. The human papillomavirus E7 protein is able to inhibit the antiviral and anti-growth functions of interferon-alpha. *Virology* 277: 411-419.
24. Zhou, F., J. Chen, and K. N. Zhao. 2013. Human papillomavirus 16-encoded E7 protein inhibits IFN-gamma-mediated MHC class I antigen presentation and CTL-induced lysis by blocking IRF-1 expression in mouse keratinocytes. *J Gen Virol* 94: 2504-2514.
25. Um, S. J., J. W. Rhyu, E. J. Kim, K. C. Jeon, E. S. Hwang, and J. S. Park. 2002. Abrogation of IRF-1 response by high-risk HPV E7 protein in vivo. *Cancer Lett* 179: 205-212.
26. Leong, C. M., J. Doorbar, I. Nindl, H. S. Yoon, and M. H. Hibma. 2010. Loss of epidermal Langerhans cells occurs in human papillomavirus alpha, gamma, and mu but not beta genus infections. *J Invest Dermatol* 130: 472-480.
27. Tindle, R. W. 2002. Immune evasion in human papillomavirus-associated cervical cancer. *Nat Rev Cancer* 2: 59-65.
28. Frazer, I. H., R. Thomas, J. Zhou, G. R. Leggatt, L. Dunn, N. McMillan, R. W. Tindle, L. Filgueira, P. Manders, P. Barnard, and M. Sharkey. 1999. Potential strategies utilised by papillomavirus to evade host immunity. *Immunol Rev* 168: 131-142.
29. Bais, A. G., I. Beckmann, J. Lindemans, P. C. Ewing, C. J. Meijer, P. J. Snijders, and T. J. Helmerhorst. 2005. A shift to a peripheral Th2-type cytokine pattern during the carcinogenesis of cervical cancer becomes manifest in CIN III lesions. *J Clin Pathol* 58: 1096-1100.
30. Kobayashi, A., V. Weinberg, T. Darragh, and K. Smith-McCune. 2008. Evolving immunosuppressive microenvironment during human cervical carcinogenesis. *Mucosal Immunol* 1: 412-420.
31. Peghini, B. C., D. R. Abdalla, A. C. Barcelos, L. Teodoro, E. F. Murta, and M. A. Michelin. 2012. Local cytokine profiles of patients with cervical intraepithelial and invasive neoplasia. *Hum Immunol* 73: 920-926.
32. Guirnalda, P. D., and Y. Paterson. 2012. Vaccination with immunotherapeutic Listeria monocytogenes induces IL-17(+) gammadelta T cells in a murine model for HPV associated cancer. *Oncoimmunology* 1: 822-828.
33. Zhou, L., and D. R. Littman. 2009. Transcriptional regulatory networks in Th17 cell differentiation. *Curr Opin Immunol* 21: 146-152.

34. Kowli, S., R. Velidandla, K. E. Creek, and L. Pirisi. 2013. TGF-beta regulation of gene expression at early and late stages of HPV16-mediated transformation of human keratinocytes. *Virology* 447: 63-73.
35. Gosmann, C., S. R. Mattarollo, J. A. Bridge, I. H. Frazer, and A. Blumenthal. 2014. IL-17 Suppresses Immune Effector Functions in Human Papillomavirus-Associated Epithelial Hyperplasia. *J Immunol* 193: 2248-2257.
36. Torres-Poveda, K., M. Bahena-Roman, C. Madrid-Gonzalez, A. I. Burguete-Garcia, V. H. Bermudez-Morales, O. Peralta-Zaragoza, and V. Madrid-Marina. 2014. Role of IL-10 and TGF-beta1 in local immunosuppression in HPV-associated cervical neoplasia. *World J Clin Oncol* 5: 753-763.
37. Lee, J. H., S. M. Yi, M. E. Anderson, K. L. Berger, M. J. Welsh, A. J. Klingelhutz, and M. A. Ozbun. 2004. Propagation of infectious human papillomavirus type 16 by using an adenovirus and Cre/LoxP mechanism. *Proc Natl Acad Sci U S A* 101: 2094-2099.
38. Campo, M. S. 2002. Animal models of papillomavirus pathogenesis. *Virus Res* 89: 249-261.
39. Buitrago-Perez, A., M. Hachimi, M. Duenas, B. Lloveras, A. Santos, A. Holguin, B. Duarte, J. L. Santiago, B. Akgul, J. L. Rodriguez-Peralto, A. Storey, C. Ribas, F. Larcher, M. del Rio, J. M. Paramio, and R. Garcia-Escudero. 2012. A humanized mouse model of HPV-associated pathology driven by E7 expression. *PLoS One* 7: e41743.
40. Lin, K. Y., F. G. Guarnieri, K. F. Staveley-O'Carroll, H. I. Levitsky, J. T. August, D. M. Pardoll, and T. C. Wu. 1996. Treatment of established tumors with a novel vaccine that enhances major histocompatibility class II presentation of tumor antigen. *Cancer Res* 56: 21-26.
41. Arbeit, J. M., K. Munger, P. M. Howley, and D. Hanahan. 1994. Progressive squamous epithelial neoplasia in K14-human papillomavirus type 16 transgenic mice. *J Virol* 68: 4358-4368.
42. Matsumoto, K., G. R. Leggatt, J. Zhong, X. Liu, R. L. de Kluyver, T. Peters, G. J. Fernando, A. Liem, P. F. Lambert, and I. H. Frazer. 2004. Impaired antigen presentation and effectiveness of combined active/passive immunotherapy for epithelial tumors. *J Natl Cancer Inst* 96: 1611-1619.
43. Herber, R., A. Liem, H. Pitot, and P. F. Lambert. 1996. Squamous epithelial hyperplasia and carcinoma in mice transgenic for the human papillomavirus type 16 E7 oncogene. *J Virol* 70: 1873-1881.

44. Mattarollo, S. R., A. Rahimpour, A. Choyce, D. I. Godfrey, G. R. Leggatt, and I. H. Frazer. 2010. Invariant NKT cells in hyperplastic skin induce a local immune suppressive environment by IFN-gamma production. *J Immunol* 184: 1242-1250.
45. Trimble, C. L., and I. H. Frazer. 2009. Development of therapeutic HPV vaccines. *Lancet Oncol* 10: 975-980.
46. Kalos, M. 2003. Tumor antigen-specific T cells and cancer immunotherapy: current issues and future prospects. *Vaccine* 21: 781-786.
47. Sethi, N., and J. Palefsky. 2004. Transcriptional profiling of dysplastic lesions in K14-HPV16 transgenic mice using laser microdissection. *FASEB J* 18: 1243-1245.
48. Agosti, J. M., and S. J. Goldie. 2007. Introducing HPV vaccine in developing countries--key challenges and issues. *N Engl J Med* 356: 1908-1910.
49. Hung, C. F., B. Ma, A. Monie, S. W. Tsen, and T. C. Wu. 2008. Therapeutic human papillomavirus vaccines: current clinical trials and future directions. *Expert Opin Biol Ther* 8: 421-439.
50. de Vos van Steenwijk, P. J., T. H. Ramwadhdoebe, M. J. Lowik, C. E. van der Minne, D. M. Berends-van der Meer, L. M. Fathers, A. R. Valentijn, J. Oostendorp, G. J. Fleuren, B. W. Hellebrekers, M. J. Welters, M. I. van Poelgeest, C. J. Melief, G. G. Kenter, and S. H. van der Burg. 2012. A placebo-controlled randomized HPV16 synthetic long-peptide vaccination study in women with high-grade cervical squamous intraepithelial lesions. *Cancer Immunol Immunother* 61: 1485-1492.
51. Chu, N. R., H. B. Wu, T. Wu, L. J. Boux, M. I. Siegel, and L. A. Mizzen. 2000. Immunotherapy of a human papillomavirus (HPV) type 16 E7-expressing tumour by administration of fusion protein comprising Mycobacterium bovis bacille Calmette-Guerin (BCG) hsp65 and HPV16 E7. *Clin Exp Immunol* 121: 216-225.
52. Barrios, K., and E. Celis. 2012. TriVax-HPV: an improved peptide-based therapeutic vaccination strategy against human papillomavirus-induced cancers. *Cancer Immunol Immunother* 61: 1307-1317.
53. Dunn, L. A., M. Evander, R. W. Tindle, A. L. Bulloch, R. L. de Kluyver, G. J. Fernando, P. F. Lambert, and I. H. Frazer. 1997. Presentation of the HPV16E7 protein by skin grafts is insufficient to allow graft rejection in an E7-primed animal. *Virology* 235: 94-103.
54. Mittal, D., A. J. Kassianos, L. S. Tran, A. S. Bergot, C. Gosmann, J. Hofmann, A. Blumenthal, G. R. Leggatt, and I. H. Frazer. 2013. Indoleamine 2,3-Dioxygenase Activity Contributes to Local Immune Suppression in the Skin Expressing Human Papillomavirus Oncoprotein E7. *J Invest Dermatol*.

55. Bahrami, A. A., A. Ghaemi, A. Tabarraei, A. Sajadian, A. Gorji, and H. Soleimanjahi. 2014. DNA vaccine encoding HPV-16 E7 with mutation in L-Y-C-Y-E pRb-binding motif induces potent anti-tumor responses in mice. *J Virol Methods* 206: 12-18.
56. Bellone, S., S. Pecorelli, M. J. Cannon, and A. D. Santin. 2007. Advances in dendritic-cell-based therapeutic vaccines for cervical cancer. *Expert Rev Anticancer Ther* 7: 1473-1486.
57. Adams, M., H. Navabi, B. Jasani, S. Man, A. Fiander, A. S. Evans, C. Donninger, and M. Mason. 2003. Dendritic cell (DC) based therapy for cervical cancer: use of DC pulsed with tumour lysate and matured with a novel synthetic clinically non-toxic double stranded RNA analogue poly [I]:poly [C(12)U] (Ampligen R). *Vaccine* 21: 787-790.
58. Rothman, J., and Y. Paterson. 2013. Live-attenuated Listeria-based immunotherapy. *Expert Rev Vaccines* 12: 493-504.
59. Guirnalda, P., L. Wood, R. Goenka, J. Crespo, and Y. Paterson. 2013. Interferon gamma-induced intratumoral expression of CXCL9 alters the local distribution of T cells following immunotherapy with. *Oncoimmunology* 2: e25752.
60. Maciag, P. C., S. Radulovic, and J. Rothman. 2009. The first clinical use of a live-attenuated Listeria monocytogenes vaccine: a Phase I safety study of Lm-LLO-E7 in patients with advanced carcinoma of the cervix. *Vaccine* 27: 3975-3983.
61. Brockstedt, D. G., and T. W. Dubensky. 2008. Promises and challenges for the development of Listeria monocytogenes-based immunotherapies. *Expert Rev Vaccines* 7: 1069-1084.
62. Stanley, M. A. 2002. Imiquimod and the imidazoquinolones: mechanism of action and therapeutic potential. *Clin Exp Dermatol* 27: 571-577.
63. Moore, R. A., J. E. Edwards, J. Hopwood, and D. Hicks. 2001. Imiquimod for the treatment of genital warts: a quantitative systematic review. *BMC Infect Dis* 1: 3.
64. Malek-Mansour, S. 1973. Remission of melanoma with D.N.C.B. treatment. *Lancet* 2: 503-504.
65. Georgala, S., I. Danopoulou, and A. Katsarou. 1989. Dinitrochlorobenzene treatment of condylomata acuminata. *Australas J Dermatol* 30: 103-105.
66. Black, H. S., F. F. Castrow, 2nd, and J. Gerguis. 1985. The mutagenicity of dinitrochlorobenzene. *Arch Dermatol* 121: 348-349.
67. Christensen, A. D., and C. Haase. 2012. Immunological mechanisms of contact hypersensitivity in mice. *APMIS* 120: 1-27.

68. Allen, I. C. 2013. Contact hypersensitivity models in mice. *Methods Mol Biol* 1032: 139-144.
69. Belij, S., A. Popov, L. Zolotarevski, I. Mirkov, J. Djokic, D. Kataranovski, and M. Kataranovski. 2012. Systemic immunomodulatory effects of topical dinitrochlorobenzene (DNCB) in rats. Activity of peripheral blood polymorphonuclear cells. *Environ Toxicol Pharmacol* 33: 168-180.
70. Wang, B., H. Fujisawa, L. Zhuang, I. Freed, B. G. Howell, S. Shahid, G. M. Shivji, T. W. Mak, and D. N. Sauder. 2000. CD4+ Th1 and CD8+ type 1 cytotoxic T cells both play a crucial role in the full development of contact hypersensitivity. *J Immunol* 165: 6783-6790.
71. Xu, H., N. A. DiIulio, and R. L. Fairchild. 1996. T cell populations primed by hapten sensitization in contact sensitivity are distinguished by polarized patterns of cytokine production: interferon gamma-producing (Tc1) effector CD8+ T cells and interleukin (Il) 4/Il-10-producing (Th2) negative regulatory CD4+ T cells. *J Exp Med* 183: 1001-1012.
72. Gautam, S. C., N. F. Chikkala, and T. A. Hamilton. 1992. Anti-inflammatory action of IL-4. Negative regulation of contact sensitivity to trinitrochlorobenzene. *J Immunol* 148: 1411-1415.
73. Traidl, C., F. Jugert, T. Krieg, H. Merk, and N. Hunzelmann. 1999. Inhibition of allergic contact dermatitis to DNCB but not to oxazolone in interleukin-4-deficient mice. *J Invest Dermatol* 112: 476-482.
74. Masuoka, M., H. Shiraishi, S. Ohta, S. Suzuki, K. Arima, S. Aoki, S. Toda, N. Inagaki, Y. Kurihara, S. Hayashida, S. Takeuchi, K. Koike, J. Ono, H. Noshiro, M. Furue, S. J. Conway, Y. Narisawa, and K. Izuhara. 2012. Periostin promotes chronic allergic inflammation in response to Th2 cytokines. *J Clin Invest* 122: 2590-2600.
75. Kish, D. D., A. V. Gorbachev, and R. L. Fairchild. 2005. CD8+ T cells produce IL-2, which is required for CD(4+)CD25+ T cell regulation of effector CD8+ T cell development for contact hypersensitivity responses. *J Leukoc Biol* 78: 725-735.
76. Tomura, M., T. Honda, H. Tanizaki, A. Otsuka, G. Egawa, Y. Tokura, H. Waldmann, S. Hori, J. G. Cyster, T. Watanabe, Y. Miyachi, O. Kanagawa, and K. Kabashima. 2010. Activated regulatory T cells are the major T cell type emigrating from the skin during a cutaneous immune response in mice. *J Clin Invest* 120: 883-893.
77. Vocanson, M., A. Hennino, C. Chavagnac, P. Saint-Mezard, B. Dubois, D. Kaiserlian, and J. F. Nicolas. 2005. Contribution of CD4(+)and CD8(+) T-cells in

contact hypersensitivity and allergic contact dermatitis. *Expert Rev Clin Immunol* 1: 75-86.

78. Peiser, M. 2013. Role of Th17 cells in skin inflammation of allergic contact dermatitis. *Clin Dev Immunol* 2013: 261037.
79. Korn, T., E. Bettelli, M. Oukka, and V. K. Kuchroo. 2009. IL-17 and Th17 Cells. *Annu Rev Immunol* 27: 485-517.
80. Dyring-Andersen, B., L. Skov, M. B. Lovendorf, M. Bzorek, K. Sondergaard, J. P. Lauritsen, S. Dabelsteen, C. Geisler, and C. M. Bonefeld. 2013. CD4(+) T cells producing interleukin (IL)-17, IL-22 and interferon-gamma are major effector T cells in nickel allergy. *Contact Dermatitis* 68: 339-347.
81. Tanaka, S., A. Suto, T. Iwamoto, D. Kashiwakuma, S. Kagami, K. Suzuki, H. Takatori, T. Tamachi, K. Hirose, A. Onodera, J. Suzuki, O. Ohara, M. Yamashita, T. Nakayama, and H. Nakajima. 2014. Sox5 and c-Maf cooperatively induce Th17 cell differentiation via RORgammat induction as downstream targets of Stat3. *J Exp Med* 211: 1857-1874.
82. Lalor, S. J., L. S. Dungan, C. E. Sutton, S. A. Basdeo, J. M. Fletcher, and K. H. Mills. 2011. Caspase-1-processed cytokines IL-1beta and IL-18 promote IL-17 production by gammadelta and CD4 T cells that mediate autoimmunity. *J Immunol* 186: 5738-5748.
83. McGeachy, M. J., K. S. Bak-Jensen, Y. Chen, C. M. Tato, W. Blumenschein, T. McClanahan, and D. J. Cua. 2007. TGF-beta and IL-6 drive the production of IL-17 and IL-10 by T cells and restrain T(H)-17 cell-mediated pathology. *Nat Immunol* 8: 1390-1397.
84. Nakae, S., Y. Komiyama, A. Nambu, K. Sudo, M. Iwase, I. Homma, K. Sekikawa, M. Asano, and Y. Iwakura. 2002. Antigen-specific T cell sensitization is impaired in IL-17-deficient mice, causing suppression of allergic cellular and humoral responses. *Immunity* 17: 375-387.
85. He, D., L. Wu, H. K. Kim, H. Li, C. A. Elmets, and H. Xu. 2009. IL-17 and IFN-gamma mediate the elicitation of contact hypersensitivity responses by different mechanisms and both are required for optimal responses. *J Immunol* 183: 1463-1470.
86. Larsen, J. M., C. M. Bonefeld, S. S. Poulsen, C. Geisler, and L. Skov. 2009. IL-23 and T(H)17-mediated inflammation in human allergic contact dermatitis. *J Allergy Clin Immunol* 123: 486-492.

87. Albanesi, C., C. Scarponi, A. Cavani, M. Federici, F. Nasorri, and G. Girolomoni. 2000. Interleukin-17 is produced by both Th1 and Th2 lymphocytes, and modulates interferon-gamma- and interleukin-4-induced activation of human keratinocytes. *J Invest Dermatol* 115: 81-87.
88. Dhingra, N., and E. Guttman-Yassky. 2014. A possible role for IL-17A in establishing Th2 inflammation in murine models of atopic dermatitis. *J Invest Dermatol* 134: 2071-2074.
89. Weber, F. C., P. R. Esser, T. Muller, J. Ganesan, P. Pellegatti, M. M. Simon, R. Zeiser, M. Idzko, T. Jakob, and S. F. Martin. 2010. Lack of the purinergic receptor P2X(7) results in resistance to contact hypersensitivity. *J Exp Med* 207: 2609-2619.
90. Corsini, E., V. Galbiati, D. Nikitovic, and A. M. Tsatsakis. 2013. Role of oxidative stress in chemical allergens induced skin cells activation. *Food Chem Toxicol* 61: 74-81.
91. Watanabe, H., O. Gaide, V. Petrilli, F. Martinon, E. Contassot, S. Roques, J. A. Kummer, J. Tschopp, and L. E. French. 2007. Activation of the IL-1beta-processing inflammasome is involved in contact hypersensitivity. *J Invest Dermatol* 127: 1956-1963.
92. Popov, A., I. Mirkov, D. Miljkovic, S. Belij, L. Zolotarevski, D. Kataranovski, and M. Kataranovski. 2011. Contact allergic response to dinitrochlorobenzene (DNCB) in rats: insight from sensitization phase. *Immunobiology* 216: 763-770.
93. Guarda, G., M. Braun, F. Staehli, A. Tardivel, C. Mattmann, I. Forster, M. Farlik, T. Decker, R. A. Du Pasquier, P. Romero, and J. Tschopp. 2011. Type I interferon inhibits interleukin-1 production and inflammasome activation. *Immunity* 34: 213-223.
94. Aiba, S., and H. Tagami. 1999. Dendritic cells play a crucial role in innate immunity to simple chemicals. *J Investig Dermatol Symp Proc* 4: 158-163.
95. Bronte, V., and P. Zanovello. 2005. Regulation of immune responses by L-arginine metabolism. *Nat Rev Immunol* 5: 641-654.
96. Kavalukas, S. L., A. R. Uzgare, T. J. Bivalacqua, and A. Barbul. 2012. Arginase inhibition promotes wound healing in mice. *Surgery* 151: 287-295.
97. ishihara, N. 1965. Arginase activity in epidermis following ultraviolet exposure. *The Rkurume medical journal* 12: 77-85.
98. Serafini, P., I. Borrello, and V. Bronte. 2006. Myeloid suppressor cells in cancer: recruitment, phenotype, properties, and mechanisms of immune suppression. *Semin Cancer Biol* 16: 53-65.

99. Frazer, I. H., D. M. Leippe, L. A. Dunn, A. Liem, R. W. Tindle, G. J. Fernando, W. C. Phelps, and P. F. Lambert. 1995. Immunological responses in human papillomavirus 16 E6/E7-transgenic mice to E7 protein correlate with the presence of skin disease. *Cancer Res* 55: 2635-2639.

100. El Kasmi, K. C., J. E. Qualls, J. T. Pesce, A. M. Smith, R. W. Thompson, M. Henao-Tamayo, R. J. Basaraba, T. Konig, U. Schleicher, M. S. Koo, G. Kaplan, K. A. Fitzgerald, E. I. Tuomanen, I. M. Orme, T. D. Kanneganti, C. Bogdan, T. A. Wynn, and P. J. Murray. 2008. Toll-like receptor-induced arginase 1 in macrophages thwarts effective immunity against intracellular pathogens. *Nat Immunol* 9: 1399-1406.

101. Morris, S. M., Jr., D. Kepka-Lenhart, and L. C. Chen. 1998. Differential regulation of arginases and inducible nitric oxide synthase in murine macrophage cells. *Am J Physiol* 275: E740-747.

102. Liscovsky, M. V., R. P. Ranocchia, C. V. Gorlino, D. O. Alignani, G. Moron, B. A. Maletto, and M. C. Pistoresi-Palencia. 2009. Interferon-gamma priming is involved in the activation of arginase by oligodeoxinucleotides containing CpG motifs in murine macrophages. *Immunology* 128: e159-169.

103. Rodriguez, P. C., and A. C. Ochoa. 2008. Arginine regulation by myeloid derived suppressor cells and tolerance in cancer: mechanisms and therapeutic perspectives. *Immunol Rev* 222: 180-191.

104. Ostrand-Rosenberg, S., and P. Sinha. 2009. Myeloid-derived suppressor cells: linking inflammation and cancer. *J Immunol* 182: 4499-4506.

105. Huang, B., P. Y. Pan, Q. Li, A. I. Sato, D. E. Levy, J. Bromberg, C. M. Divino, and S. H. Chen. 2006. Gr-1+CD115+ immature myeloid suppressor cells mediate the development of tumor-induced T regulatory cells and T-cell anergy in tumor-bearing host. *Cancer Res* 66: 1123-1131.

106. Parikh, F., D. Duluc, N. Imai, A. Clark, K. Misiukiewicz, M. Bonomi, V. Gupta, A. Patsias, M. Parides, E. G. Demicco, D. Y. Zhang, S. Kim-Schulze, J. Kao, S. Gnjatic, S. Oh, M. R. Posner, and A. G. Sikora. 2014. Chemoradiotherapy-Induced Upregulation of PD-1 Antagonizes Immunity to HPV-Related Oropharyngeal Cancer. *Cancer Res* 74: 7205-7216.

107. Hammes, L. S., R. R. Tekmal, P. Naud, M. I. Edelweiss, N. Kirma, P. T. Valente, K. J. Syrjanen, and J. S. Cunha-Filho. 2007. Macrophages, inflammation and risk of cervical intraepithelial neoplasia (CIN) progression--clinicopathological correlation. *Gynecol Oncol* 105: 157-165.

108. Sunthamala, N., C. Pientong, T. Ohno, C. Zhang, A. Bhingare, Y. Kondo, M. Azuma, and T. Ekalaksananan. 2014. HPV16 E2 protein promotes innate immunity by modulating immunosuppressive status. *Biochem Biophys Res Commun* 446: 977-982.

109. Bronte, V., P. Serafini, A. Mazzoni, D. M. Segal, and P. Zanovello. 2003. L-arginine metabolism in myeloid cells controls T-lymphocyte functions. *Trends Immunol* 24: 302-306.

110. Gabrilovich, D. I., S. Ostrand-Rosenberg, and V. Bronte. 2012. Coordinated regulation of myeloid cells by tumours. *Nat Rev Immunol* 12: 253-268.

111. Kampfer, H., J. Pfeilschifter, and S. Frank. 2003. Expression and activity of arginase isoenzymes during normal and diabetes-impaired skin repair. *J Invest Dermatol* 121: 1544-1551.

112. Ariel, A., and C. N. Serhan. 2012. New Lives Given by Cell Death: Macrophage Differentiation Following Their Encounter with Apoptotic Leukocytes during the Resolution of Inflammation. *Front Immunol* 3: 4.

113. Ha, H. L., H. Wang, P. Pisitkun, J. C. Kim, I. Tassi, W. Tang, M. I. Morasso, M. C. Udey, and U. Siebenlist. 2014. IL-17 drives psoriatic inflammation via distinct, target cell-specific mechanisms. *Proc Natl Acad Sci U S A* 111: E3422-3431.

114. Bruch-Gerharz, D., O. Schnorr, C. Suschek, K. F. Beck, J. Pfeilschifter, T. Ruzicka, and V. Kolb-Bachofen. 2003. Arginase 1 overexpression in psoriasis: limitation of inducible nitric oxide synthase activity as a molecular mechanism for keratinocyte hyperproliferation. *Am J Pathol* 162: 203-211.

115. Bedoya, A. M., D. J. Tate, A. Baena, C. M. Cordoba, M. Borrero, R. Pareja, F. Rojas, J. R. Patterson, R. Herrero, A. H. Zea, and G. I. Sanchez. 2014. Immunosuppression in cervical cancer with special reference to arginase activity. *Gynecol Oncol*.

116. Lepique, A. P., K. R. Daghastanli, I. M. Cuccovia, and L. L. Villa. 2009. HPV16 tumor associated macrophages suppress antitumor T cell responses. *Clin Cancer Res* 15: 4391-4400.

117. Coussens, L. M., C. L. Tinkle, D. Hanahan, and Z. Werb. 2000. MMP-9 supplied by bone marrow-derived cells contributes to skin carcinogenesis. *Cell* 103: 481-490.

118. Terabe, M., S. Matsui, N. Noben-Trauth, H. Chen, C. Watson, D. D. Donaldson, D. P. Carbone, W. E. Paul, and J. A. Berzofsky. 2000. NKT cell-mediated repression of tumor immunosurveillance by IL-13 and the IL-4R-STAT6 pathway. *Nat Immunol* 1: 515-520.

119. De Marco, F., E. Bucaj, C. Foppoli, A. Fiorini, C. Blarzino, K. Filipi, A. Giorgi, M. E. Schinina, F. Di Domenico, R. Coccia, D. A. Butterfield, and M. Perluigi. 2012. Oxidative Stress in HPV-Driven Viral Carcinogenesis: Redox Proteomics Analysis of HPV-16 Dysplastic and Neoplastic Tissues. *PLoS One* 7: e34366.
120. Ckless, K., A. van der Vliet, and Y. Janssen-Heininger. 2007. Oxidative-nitrosative stress and post-translational protein modifications: implications to lung structure-function relations. Arginase modulates NF-kappaB activity via a nitric oxide-dependent mechanism. *Am J Respir Cell Mol Biol* 36: 645-653.
121. Takahashi, N., K. Ogino, K. Takemoto, S. Hamanishi, D. H. Wang, T. Takigawa, M. Shibamori, H. Ishiyama, and Y. Fujikura. 2010. Direct inhibition of arginase attenuated airway allergic reactions and inflammation in a Dermatophagoides farinae-induced NC/Nga mouse model. *Am J Physiol Lung Cell Mol Physiol* 299: L17-24.
122. Pera, T., A. B. Zuidhof, M. Smit, M. H. Menzen, T. Klein, G. Flik, J. Zaagsma, H. Meurs, and H. Maarsingh. 2014. Arginase inhibition prevents inflammation and remodeling in a guinea pig model of chronic obstructive pulmonary disease. *J Pharmacol Exp Ther* 349: 229-238.
123. Peng, H. B., M. Spiecker, and J. K. Liao. 1998. Inducible nitric oxide: an autoregulatory feedback inhibitor of vascular inflammation. *J Immunol* 161: 1970-1976.
124. White, A. R., S. Ryoo, D. Li, H. C. Champion, J. Steppan, D. Wang, D. Nyhan, A. A. Shoukas, J. M. Hare, and D. E. Berkowitz. 2006. Knockdown of arginase I restores NO signaling in the vasculature of old rats. *Hypertension* 47: 245-251.
125. Akazawa, Y., M. Kubo, R. Zhang, K. Matsumoto, F. Yan, H. Setiawan, H. Takahashi, Y. Fujikura, and K. Ogino. 2013. Inhibition of arginase ameliorates experimental ulcerative colitis in mice. *Free Radic Res* 47: 137-145.
126. Ming, X. F., A. G. Rajapakse, G. Yepuri, Y. Xiong, J. M. Carvas, J. Ruffieux, I. Scerri, Z. Wu, K. Popp, J. Li, C. Sartori, U. Scherrer, B. R. Kwak, J. P. Montani, and Z. Yang. 2012. Arginase II Promotes Macrophage Inflammatory Responses Through Mitochondrial Reactive Oxygen Species, Contributing to Insulin Resistance and Atherogenesis. *J Am Heart Assoc* 1: e000992.
127. Liu, J., D. A. Copland, S. Horie, W. K. Wu, M. Chen, Y. Xu, B. Paul Morgan, M. Mack, H. Xu, L. B. Nicholson, and A. D. Dick. 2013. Myeloid cells expressing VEGF and arginase-1 following uptake of damaged retinal pigment epithelium suggests

potential mechanism that drives the onset of choroidal angiogenesis in mice. *PLoS One* 8: e72935.

128. Anderson, L. A. 2012. Prophylactic human papillomavirus vaccines: past, present and future. *Pathology* 44: 1-6.
129. Frazer, I. H., G. J. Fernando, N. Fowler, G. R. Leggatt, P. F. Lambert, A. Liem, K. Malcolm, and R. W. Tindle. 1998. Split tolerance to a viral antigen expressed in thymic epithelium and keratinocytes. *Eur J Immunol* 28: 2791-2800.
130. Hengge, U. R., B. Benninghoff, T. Ruzicka, and M. Goos. 2001. Topical immunomodulators--progress towards treating inflammation, infection, and cancer. *Lancet Infect Dis* 1: 189-198.
131. Ochoa, A. C., A. H. Zea, C. Hernandez, and P. C. Rodriguez. 2007. Arginase, prostaglandins, and myeloid-derived suppressor cells in renal cell carcinoma. *Clin Cancer Res* 13: 721s-726s.
132. Tacke, R. S., H. C. Lee, C. Goh, J. Courtney, S. J. Polyak, H. R. Rosen, and Y. S. Hahn. 2012. Myeloid suppressor cells induced by hepatitis C virus suppress T-cell responses through the production of reactive oxygen species. *Hepatology* 55: 343-353.
133. Mou, Z., H. M. Muleme, D. Liu, P. Jia, I. B. Okwor, S. M. Kuriakose, S. M. Beverley, and J. E. Uzonna. 2013. Parasite-derived arginase influences secondary anti-Leishmania immunity by regulating programmed cell death-1-mediated CD4+ T cell exhaustion. *J Immunol* 190: 3380-3389.
134. Kenyon, N. J., J. M. Bratt, A. L. Linderholm, M. S. Last, and J. A. Last. 2008. Arginases I and II in lungs of ovalbumin-sensitized mice exposed to ovalbumin: sources and consequences. *Toxicol Appl Pharmacol* 230: 269-275.
135. Zhang, W., B. Baban, M. Rojas, S. Tofigh, S. K. Virmani, C. Patel, M. A. Behzadian, M. J. Romero, R. W. Caldwell, and R. B. Caldwell. 2009. Arginase activity mediates retinal inflammation in endotoxin-induced uveitis. *Am J Pathol* 175: 891-902.
136. Stoermer, K. A., A. Burrack, L. Oko, S. A. Montgomery, L. B. Borst, R. G. Gill, and T. E. Morrison. 2012. Genetic ablation of arginase 1 in macrophages and neutrophils enhances clearance of an arthritogenic alphavirus. *J Immunol* 189: 4047-4059.
137. Pinto, N. B., T. C. Morais, K. M. Carvalho, C. R. Silva, G. M. Andrade, G. A. Brito, M. L. Veras, O. D. Pessoa, V. S. Rao, and F. A. Santos. 2010. Topical anti-inflammatory potential of Physalin E from Physalis angulata on experimental dermatitis in mice. *Phytomedicine* 17: 740-743.

138. Bromley, S. K., R. P. Larson, S. F. Ziegler, and A. D. Luster. 2013. IL-23 induces atopic dermatitis-like inflammation instead of psoriasis-like inflammation in CCR2-deficient mice. *PLoS One* 8: e58196.
139. Choyce, A., M. Yong, S. Narayan, S. R. Mattarollo, A. Liem, P. F. Lambert, I. H. Frazer, and G. R. Leggatt. 2013. Expression of a single, viral oncoprotein in skin epithelium is sufficient to recruit lymphocytes. *PLoS One* 8: e57798.
140. Zohlnhofer, D., K. Brand, K. Schipek, G. Pogatsa-Murray, A. Schomig, and F. J. Neumann. 2000. Adhesion of monocyte very late antigen-4 to endothelial vascular cell adhesion molecule-1 induces interleukin-1beta-dependent expression of interleukin-6 in endothelial cells. *Arterioscler Thromb Vasc Biol* 20: 353-359.
141. Fielding, C. A., R. M. McLoughlin, L. McLeod, C. S. Colmont, M. Najdovska, D. Grail, M. Ernst, S. A. Jones, N. Topley, and B. J. Jenkins. 2008. IL-6 regulates neutrophil trafficking during acute inflammation via STAT3. *J Immunol* 181: 2189-2195.
142. Sindrilaru, A., T. Peters, S. Wieschalka, C. Baican, A. Baican, H. Peter, A. Hainzl, S. Schatz, Y. Qi, A. Schlecht, J. M. Weiss, M. Wlaschek, C. Sunderkotter, and K. Scharffetter-Kochanek. 2011. An unrestrained proinflammatory M1 macrophage population induced by iron impairs wound healing in humans and mice. *J Clin Invest* 121: 985-997.
143. Chang, J., S. Thangamani, M. H. Kim, B. Ulrich, S. M. Morris, Jr., and C. H. Kim. 2013. Retinoic acid promotes the development of Arg1-expressing dendritic cells for the regulation of T-cell differentiation. *Eur J Immunol* 43: 967-978.
144. Hammad, H., and B. N. Lambrecht. 2008. Dendritic cells and epithelial cells: linking innate and adaptive immunity in asthma. *Nat Rev Immunol* 8: 193-204.
145. Tenu, J. P., M. Lepoivre, C. Moali, M. Brollo, D. Mansuy, and J. L. Boucher. 1999. Effects of the new arginase inhibitor N(omega)-hydroxy-nor-L-arginine on NO synthase activity in murine macrophages. *Nitric Oxide* 3: 427-438.
146. Bratt, J. M., L. M. Franzi, A. L. Linderholm, M. S. Last, N. J. Kenyon, and J. A. Last. 2009. Arginase enzymes in isolated airways from normal and nitric oxide synthase 2-knockout mice exposed to ovalbumin. *Toxicol Appl Pharmacol* 234: 273-280.
147. Schuepbach-Mallepell, S., V. Philippe, M. C. Bruggen, H. Watanabe, S. Roques, C. Baldeschi, and O. Gaide. 2013. Antagonistic effect of the inflammasome on thymic stromal lymphopoietin expression in the skin. *J Allergy Clin Immunol* 132: 1348-1357.

148. Enk, A. H., and S. I. Katz. 1992. Early molecular events in the induction phase of contact sensitivity. *Proc Natl Acad Sci U S A* 89: 1398-1402.
149. Rambukkana, A., F. H. Pistoor, J. D. Bos, M. L. Kapsenberg, and P. K. Das. 1996. Effects of contact allergens on human Langerhans cells in skin organ culture: migration, modulation of cell surface molecules, and early expression of interleukin-1 beta protein. *Lab Invest* 74: 422-436.
150. Munder, M., K. Eichmann, J. M. Moran, F. Centeno, G. Soler, and M. Modolell. 1999. Th1/Th2-regulated expression of arginase isoforms in murine macrophages and dendritic cells. *J Immunol* 163: 3771-3777.
151. Barron, L., A. M. Smith, K. C. El Kasmi, J. E. Qualls, X. Huang, A. Cheever, L. A. Borthwick, M. S. Wilson, P. J. Murray, and T. A. Wynn. 2013. Role of arginase 1 from myeloid cells in th2-dominated lung inflammation. *PLoS One* 8: e61961.
152. Khallou-Laschet, J., A. Varthaman, G. Fornasa, C. Compain, A. T. Gaston, M. Clement, M. Dussiot, O. Levillain, S. Graff-Dubois, A. Nicoletti, and G. Caligiuri. 2010. Macrophage plasticity in experimental atherosclerosis. *PLoS One* 5: e8852.
153. Bradding, P., I. H. Feather, P. H. Howarth, R. Mueller, J. A. Roberts, K. Britten, J. P. Bews, T. C. Hunt, Y. Okayama, C. H. Heusser, and et al. 1992. Interleukin 4 is localized to and released by human mast cells. *J Exp Med* 176: 1381-1386.
154. Kuroda, E., V. Ho, J. Ruschmann, F. Antignano, M. Hamilton, M. J. Rauh, A. Antov, R. A. Flavell, L. M. Sly, and G. Krystal. 2009. SHIP represses the generation of IL-3-induced M2 macrophages by inhibiting IL-4 production from basophils. *J Immunol* 183: 3652-3660.
155. Balato, A., S. Lembo, M. Mattii, M. Schiattarella, R. Marino, A. De Paulis, N. Balato, and F. Ayala. 2012. IL-33 is secreted by psoriatic keratinocytes and induces pro-inflammatory cytokines via keratinocyte and mast cell activation. *Exp Dermatol* 21: 892-894.
156. Subbaramaiah, K., and A. J. Dannenberg. 2007. Cyclooxygenase-2 transcription is regulated by human papillomavirus 16 E6 and E7 oncoproteins: evidence of a corepressor/coactivator exchange. *Cancer Res* 67: 3976-3985.
157. Rodriguez, P. C., C. P. Hernandez, D. Quiceno, S. M. Dubinett, J. Zabaleta, J. B. Ochoa, J. Gilbert, and A. C. Ochoa. 2005. Arginase I in myeloid suppressor cells is induced by COX-2 in lung carcinoma. *J Exp Med* 202: 931-939.
158. Kallberg, E., M. Stenstrom, D. Liberg, F. Ivars, and T. Leanderson. 2012. CD11b+Ly6C++Ly6G- cells show distinct function in mice with chronic inflammation or tumor burden. *BMC Immunol* 13: 69.

159. Brudecki, L., D. A. Ferguson, C. E. McCall, and M. El Gazzar. 2012. Myeloid-derived suppressor cells evolve during sepsis and can enhance or attenuate the systemic inflammatory response. *Infect Immun* 80: 2026-2034.

160. Krotova, K., J. M. Patel, E. R. Block, and S. Zharikov. 2010. Endothelial arginase II responds to pharmacological inhibition by elevation in protein level. *Mol Cell Biochem* 343: 211-216.

161. Narayan, S., A. Choyce, R. Linedale, N. A. Saunders, A. Dahler, E. Chan, G. J. Fernando, I. H. Frazer, and G. R. Leggatt. 2009. Epithelial expression of human papillomavirus type 16 E7 protein results in peripheral CD8 T-cell suppression mediated by CD4+CD25+ T cells. *Eur J Immunol* 39: 481-490.

162. Azukizawa, H., H. Kosaka, S. Sano, W. R. Heath, I. Takahashi, X. H. Gao, Y. Sumikawa, M. Okabe, K. Yoshikawa, and S. Itami. 2003. Induction of T-cell-mediated skin disease specific for antigen transgenically expressed in keratinocytes. *Eur J Immunol* 33: 1879-1888.

163. Chang, C. I., B. Zoghi, J. C. Liao, and L. Kuo. 2000. The involvement of tyrosine kinases, cyclic AMP/protein kinase A, and p38 mitogen-activated protein kinase in IL-13-mediated arginase I induction in macrophages: its implications in IL-13-inhibited nitric oxide production. *J Immunol* 165: 2134-2141.

164. Custot, J., C. Moali, J. Brollo , L. Boucher , M. Delaforge , D. Mansuy, J. P. Tenu, J. L. Zimmermann, and e. al. 1997. The New α-Amino Acid Nω-Hydroxy-nor-l-arginine: a High-Affinity Inhibitor of Arginase Well Adapted To Bind to Its Manganese Cluster

J Am Chem So 119: 4086-4087.

165. Aristoteles, L. R., R. F. Righetti, N. M. Pinheiro, R. B. Franco, C. M. Starling, J. C. da Silva, P. A. Pigati, L. C. Caperuto, C. M. Prado, M. Dolhnikoff, M. A. Martins, E. A. Leick, and I. F. Tiberio. 2013. Modulation of the oscillatory mechanics of lung tissue and the oxidative stress response induced by arginase inhibition in a chronic allergic inflammation model. *BMC Pulm Med* 13: 52.

166. Greenacre, S. A., F. A. Rocha, A. Rawlingson, S. Meinerikandathevan, R. N. Poston, E. Ruiz, B. Halliwell, and S. D. Brain. 2002. Protein nitration in cutaneous inflammation in the rat: essential role of inducible nitric oxide synthase and polymorphonuclear leukocytes. *Br J Pharmacol* 136: 985-994.

167. Morris, S. M., Jr. 2009. Recent advances in arginine metabolism: roles and regulation of the arginases. *Br J Pharmacol* 157: 922-930.

168. Laffi, G., M. Foschi, E. Masini, A. Simoni, L. Mugnai, G. La Villa, G. Barletta, P. F. Mannaioni, and P. Gentilini. 1995. Increased production of nitric oxide by neutrophils and monocytes from cirrhotic patients with ascites and hyperdynamic circulation. *Hepatology* 22: 1666-1673.

169. Ding, A. H., C. F. Nathan, and D. J. Stuehr. 1988. Release of reactive nitrogen intermediates and reactive oxygen intermediates from mouse peritoneal macrophages. Comparison of activating cytokines and evidence for independent production. *J Immunol* 141: 2407-2412.

170. Tran le, S., A. S. Bergot, S. R. Mattarollo, D. Mittal, and I. H. Frazer. 2014. Human papillomavirus e7 oncoprotein transgenic skin develops an enhanced inflammatory response to 2,4-dinitrochlorobenzene by an arginase-1-dependent mechanism. *J Invest Dermatol* 134: 2438-2446.

171. Pauleau, A. L., R. Rutschman, R. Lang, A. Pernis, S. S. Watowich, and P. J. Murray. 2004. Enhancer-mediated control of macrophage-specific arginase I expression. *J Immunol* 172: 7565-7573.

172. Modolell, M., I. M. Corraliza, F. Link, G. Soler, and K. Eichmann. 1995. Reciprocal regulation of the nitric oxide synthase/arginase balance in mouse bone marrow-derived macrophages by TH1 and TH2 cytokines. *Eur J Immunol* 25: 1101-1104.

173. Sousa, L. M., M. B. Carneiro, M. E. Resende, L. S. Martins, L. M. Dos Santos, L. G. Vaz, P. S. Mello, D. M. Mosser, M. A. Oliveira, and L. Q. Vieira. 2014. Neutrophils have a protective role during early stages of Leishmania amazonensis infection in BALB/c mice. *Parasite Immunol* 36: 13-31.

174. Usui, F., H. Kimura, T. Ohshiro, K. Tatsumi, A. Kawashima, A. Nishiyama, Y. Iwakura, S. Ishibashi, and M. Takahashi. 2012. Interleukin-17 deficiency reduced vascular inflammation and development of atherosclerosis in Western diet-induced apoE-deficient mice. *Biochem Biophys Res Commun* 420: 72-77.

175. Li, Q., L. Liu, Q. Zhang, S. Liu, D. Ge, and Z. You. 2014. Interleukin-17 Indirectly Promotes M2 Macrophage Differentiation through Stimulation of COX-2/PGE2 Pathway in the Cancer Cells. *Cancer Res Treat* 46: 297-306.

176. Li, L., L. Huang, A. L. Vergis, H. Ye, A. Bajwa, V. Narayan, R. M. Strieter, D. L. Rosin, and M. D. Okusa. 2010. IL-17 produced by neutrophils regulates IFN-gamma-mediated neutrophil migration in mouse kidney ischemia-reperfusion injury. *J Clin Invest* 120: 331-342.

177. Song, C., L. Luo, Z. Lei, B. Li, Z. Liang, G. Liu, D. Li, G. Zhang, B. Huang, and Z. H. Feng. 2008. IL-17-producing alveolar macrophages mediate allergic lung inflammation related to asthma. *J Immunol* 181: 6117-6124.
178. Mizutani, N., T. Nabe, and S. Yoshino. 2014. IL-17A promotes the exacerbation of IL-33-induced airway hyperresponsiveness by enhancing neutrophilic inflammation via CXCR2 signaling in mice. *J Immunol* 192: 1372-1384.
179. Barin, J. G., G. C. Baldeviano, M. V. Talor, L. Wu, S. Ong, F. Quader, P. Chen, D. Zheng, P. Caturegli, N. R. Rose, and D. Cihakova. 2012. Macrophages participate in IL-17-mediated inflammation. *Eur J Immunol* 42: 726-736.
180. Koltsova, E. K., and K. Ley. 2010. The mysterious ways of the chemokine CXCL5. *Immunity* 33: 7-9.
181. Menzies, F. M., F. L. Henriquez, J. Alexander, and C. W. Roberts. 2011. Selective inhibition and augmentation of alternative macrophage activation by progesterone. *Immunology* 134: 281-291.
182. Butcher, M. J., B. N. Gjurich, T. Phillips, and E. V. Galkina. 2012. The IL-17A/IL-17RA axis plays a proatherogenic role via the regulation of aortic myeloid cell recruitment. *Circ Res* 110: 675-687.
183. Kim, H. Y., H. J. Lee, Y. J. Chang, M. Pichavant, S. A. Shore, K. A. Fitzgerald, Y. Iwakura, E. Israel, K. Bolger, J. Faul, R. H. DeKruyff, and D. T. Umetsu. 2014. Interleukin-17-producing innate lymphoid cells and the NLRP3 inflammasome facilitate obesity-associated airway hyperreactivity. *Nat Med* 20: 54-61.
184. Brackett, C. M., J. B. Muhitch, S. S. Evans, and S. O. Gollnick. 2013. IL-17 promotes neutrophil entry into tumor-draining lymph nodes following induction of sterile inflammation. *J Immunol* 191: 4348-4357.
185. Liu, Y., J. Mei, L. Gonzales, G. Yang, N. Dai, P. Wang, P. Zhang, M. Favara, K. C. Malcolm, S. Guttentag, and G. S. Worthen. 2011. IL-17A and TNF-alpha exert synergistic effects on expression of CXCL5 by alveolar type II cells in vivo and in vitro. *J Immunol* 186: 3197-3205.
186. Shi, C., and E. G. Pamer. 2011. Monocyte recruitment during infection and inflammation. *Nat Rev Immunol* 11: 762-774.
187. Kurihara, T., G. Warr, J. Loy, and R. Bravo. 1997. Defects in macrophage recruitment and host defense in mice lacking the CCR2 chemokine receptor. *J Exp Med* 186: 1757-1762.
188. Van Coillie, E., J. Van Damme, and G. Opdenakker. 1999. The MCP/eotaxin subfamily of CC chemokines. *Cytokine Growth Factor Rev* 10: 61-86.

189. Cushing, S. D., J. A. Berliner, A. J. Valente, M. C. Territo, M. Navab, F. Parhami, R. Gerrity, C. J. Schwartz, and A. M. Fogelman. 1990. Minimally modified low density lipoprotein induces monocyte chemotactic protein 1 in human endothelial cells and smooth muscle cells. *Proc Natl Acad Sci U S A* 87: 5134-5138.
190. Okada, M., M. Saio, Y. Kito, N. Ohe, H. Yano, S. Yoshimura, T. Iwama, and T. Takami. 2009. Tumor-associated macrophage/microglia infiltration in human gliomas is correlated with MCP-3, but not MCP-1. *Int J Oncol* 34: 1621-1627.
191. Hengge, U. R., and T. Ruzicka. 2004. Topical immunomodulation in dermatology: potential of toll-like receptor agonists. *Dermatol Surg* 30: 1101-1112.
192. Wack, C., A. Kirst, J. C. Becker, W. K. Lutz, E. B. Brocker, and W. H. Fischer. 2002. Chemoimmunotherapy for melanoma with dacarbazine and 2,4-dinitrochlorobenzene elicits a specific T cell-dependent immune response. *Cancer Immunol Immunother* 51: 431-439.
193. Levis, W. R., K. H. Kraemer, W. G. Klingler, G. L. Peck, and W. D. Terry. 1973. Topical immunotherapy of basal cell carcinomas with dinitrochlorobenzene. *Cancer Res* 33: 3036-3042.
194. Watanabe, H., S. Gehrke, E. Contassot, S. Roques, J. Tschopp, P. S. Friedmann, L. E. French, and O. Gaide. 2008. Danger signaling through the inflammasome acts as a master switch between tolerance and sensitization. *J Immunol* 180: 5826-5832.
195. Romano, M., M. Sironi, C. Toniatti, N. Polentarutti, P. Fruscella, P. Ghezzi, R. Faggioni, W. Luini, V. van Hinsbergh, S. Sozzani, F. Bussolino, V. Poli, G. Ciliberto, and A. Mantovani. 1997. Role of IL-6 and its soluble receptor in induction of chemokines and leukocyte recruitment. *Immunity* 6: 315-325.
196. Chung, Y., S. H. Chang, G. J. Martinez, X. O. Yang, R. Nurieva, H. S. Kang, L. Ma, S. S. Watowich, A. M. Jetten, Q. Tian, and C. Dong. 2009. Critical regulation of early Th17 cell differentiation by interleukin-1 signaling. *Immunity* 30: 576-587.
197. Joseph, S. B., K. T. Miner, and M. Croft. 1998. Augmentation of naive, Th1 and Th2 effector CD4 responses by IL-6, IL-1 and TNF. *Eur J Immunol* 28: 277-289.
198. Feng, Q., H. Wei, J. Morihara, J. Stern, M. Yu, N. Kiviat, I. Hellstrom, and K. E. Hellstrom. 2012. Th2 type inflammation promotes the gradual progression of HPV-infected cervical cells to cervical carcinoma. *Gynecol Oncol* 127: 412-419.
199. Chang, Y. H., C. W. Yu, L. C. Lai, C. H. Tsao, K. T. Ho, S. C. Yang, H. Lee, Y. W. Cheng, T. C. Wu, and M. Y. Shiau. 2010. Up-regulation of interleukin-17 expression

by human papillomavirus type 16 E6 in nonsmall cell lung cancer. *Cancer* 116: 4800-4809.

200. Ma, Y., L. Aymeric, C. Locher, S. R. Mattarollo, N. F. Delahaye, P. Pereira, L. Boucontet, L. Apetoh, F. Ghiringhelli, N. Casares, J. J. Lasarte, G. Matsuzaki, K. Ikuta, B. Ryffel, K. Benlagha, A. Tesniere, N. Ibrahim, J. Dechanet-Merville, N. Chaput, M. J. Smyth, G. Kroemer, and L. Zitvogel. 2011. Contribution of IL-17-producing gamma delta T cells to the efficacy of anticancer chemotherapy. *J Exp Med* 208: 491-503.

201. Nishikawa, K., N. Seo, M. Torii, N. Ma, D. Muraoka, I. Tawara, M. Masuya, K. Tanaka, Y. Takei, H. Shiku, N. Katayama, and T. Kato. 2014. Interleukin-17 Induces an Atypical M2-Like Macrophage Subpopulation That Regulates Intestinal Inflammation. *PLoS One* 9: e108494.

202. Park, H., Z. Li, X. O. Yang, S. H. Chang, R. Nurieva, Y. H. Wang, Y. Wang, L. Hood, Z. Zhu, Q. Tian, and C. Dong. 2005. A distinct lineage of CD4 T cells regulates tissue inflammation by producing interleukin 17. *Nat Immunol* 6: 1133-1141.

203. Ogura, H., M. Murakami, Y. Okuyama, M. Tsuruoka, C. Kitabayashi, M. Kanamoto, M. Nishihara, Y. Iwakura, and T. Hirano. 2008. Interleukin-17 promotes autoimmunity by triggering a positive-feedback loop via interleukin-6 induction. *Immunity* 29: 628-636.

204. Napolitani, G., E. V. Acosta-Rodriguez, A. Lanzavecchia, and F. Sallusto. 2009. Prostaglandin E2 enhances Th17 responses via modulation of IL-17 and IFN-gamma production by memory CD4+ T cells. *Eur J Immunol* 39: 1301-1312.

205. Guerrero, A. R., K. Uchida, H. Nakajima, S. Watanabe, M. Nakamura, W. E. Johnson, and H. Baba. 2012. Blockade of interleukin-6 signaling inhibits the classic pathway and promotes an alternative pathway of macrophage activation after spinal cord injury in mice. *J Neuroinflammation* 9: 40.

206. Ross, R., and A. B. Reske-Kunz. 2001. The role of NO in contact hypersensitivity. *Int Immunopharmacol* 1: 1469-1478.

207. Farhat, S., M. Nakagawa, and A. B. Moscicki. 2009. Cell-mediated immune responses to human papillomavirus 16 E6 and E7 antigens as measured by interferon gamma enzyme-linked immunospot in women with cleared or persistent human papillomavirus infection. *Int J Gynecol Cancer* 19: 508-512.

208. Bajaj-Elliott, M., R. Poulsom, S. L. Pender, N. C. Wathen, and T. T. MacDonald. 1998. Interactions between stromal cell--derived keratinocyte growth factor and

epithelial transforming growth factor in immune-mediated crypt cell hyperplasia. *J Clin Invest* 102: 1473-1480.

209. Zenz, R., R. Eferl, L. Kenner, L. Florin, L. Hummerich, D. Mehic, H. Scheuch, P. Angel, E. Tschachler, and E. F. Wagner. 2005. Psoriasis-like skin disease and arthritis caused by inducible epidermal deletion of Jun proteins. *Nature* 437: 369-375.

210. Frazer, I. H., R. De Kluyver, G. R. Leggatt, H. Y. Guo, L. Dunn, O. White, C. Harris, A. Liem, and P. Lambert. 2001. Tolerance or immunity to a tumor antigen expressed in somatic cells can be determined by systemic proinflammatory signals at the time of first antigen exposure. *J Immunol* 167: 6180-6187.

211. Neumann, S., K. Burkert, R. Kemp, T. Rades, P. Rod Dunbar, and S. Hook. 2014. Activation of the NLRP3 inflammasome is not a feature of all particulate vaccine adjuvants. *Immunol Cell Biol* 92: 535-542.

212. Kashiwagi, Y., M. Maeda, H. Kawashima, and T. Nakayama. 2014. Inflammatory responses following intramuscular and subcutaneous immunization with aluminum-adjuvanted or non-adjuvanted vaccines. *Vaccine* 32: 3393-3401.

213. Mori, A., E. Oleszycka, F. A. Sharp, M. Coleman, Y. Ozasa, M. Singh, D. T. O'Hagan, L. Tajber, O. I. Corrigan, E. A. McNeela, and E. C. Lavelle. 2012. The vaccine adjuvant alum inhibits IL-12 by promoting PI3 kinase signaling while chitosan does not inhibit IL-12 and enhances Th1 and Th17 responses. *Eur J Immunol* 42: 2709-2719.

Appendix – published article 1

ORIGINAL ARTICLE

Human Papillomavirus E7 Oncoprotein Transgenic Skin Develops an Enhanced Inflammatory Response to 2,4-Dinitrochlorobenzene by an Arginase-1-Dependent Mechanism

Le Son Tran[1], Anne-Sophie Bergot[1], Stephen R. Mattarollo[1], Deepak Mittal[1,2,3] and Ian H. Frazer[1,2]

We have shown that the expression of human papillomavirus type 16 E7 (HPV16.E7) protein within epithelial cells results in local immune suppression and a weak and ineffective immune response to E7 similar to that occuring in HPV-associated premalignancy and cancers. However, a robust acute inflammatory stimulus can overcome this to enable immune elimination of HPV16.E7-transformed epithelial cells. 2,4-Dinitrochlorobenzene (DNCB) can elicit acute inflammation and it has been shown to initiate the regression of HPV-associated genital warts. Although the clinical use of DNCB is discouraged owing to its mutagenic potential, understanding how DNCB-induced acute inflammation alters local HPV16.E7-mediated immune suppression might lead to better treatments. Here, we show that topical DNCB application to skin expressing HPV16.E7 as a transgene induces a hyperinflammatory response, which is not seen in nontransgenic control animals. The E7-associated inflammatory response is characterized by enhanced expression of Th2 cytokines and increased infiltration of $CD11b^{+}Gr1^{int}F4/80^{+}Ly6C^{hi}Ly6G^{low}$ myeloid cells, producing arginase-1. Inhibition of arginase with an arginase-specific inhibitor, *N*(omega)-hydroxy-nor-L-arginine, ameliorates the DNCB-induced inflammatory response. Our results demonstrate that HPV16.E7 protein enhances DNCB-associated production of arginase-1 by myeloid cells and consequent inflammatory cellular infiltration of skin.

Journal of Investigative Dermatology (2014) **134,** 2438–2446; doi:10.1038/jid.2014.186; published online 29 May 2014

INTRODUCTION

Persistent infection with oncogenic human papillomaviruses (HPV), particularly HPV16, is associated with selective expression of two virally encoded proteins (E6 and E7). One action of HPV16.E7 protein is to subvert the innate immune system (Frazer *et al.*, 1998) through the downregulation of IFNγ pathways, modulation of antigen presentation, and suppression of Toll-like receptor 9 protein (Bhat *et al.*, 2011).

K14.E7 transgenic mice, which express HPV16.E7 oncoprotein within basal keratinocytes under the control of the keratin 14 transcriptional promoter, have been extensively used as a model of HPV oncoprotein–induced immune suppression associated with human squamous cancers, in which only the *E6* and *E7* genes of the papillomavirus are expressed (Trimble and Frazer, 2009). We have previously shown that skin grafts expressing HPV16.E7 oncoprotein are not spontaneously rejected when transplanted onto syngeneic animals, but they are rejected when certain components of the innate immune system are unavailable, confirming that the expression of HPV16.E7 in the epithelium results in the establishment of a local suppressive environment and the subversion of antigen-specific T cells (Mattarollo *et al.*, 2010; Mittal *et al.*, 2013). Therefore, successful strategies targeting HPV-associated cancer need to circumvent or disrupt the local suppressive environment.

Topical immunotherapy with immunostimulatory agents has been used clinically to treat cancerous lesions including squamous cell and basal cell carcinoma in immunocompetent and immunosuppressed patients (Hengge *et al.*, 2001). Topical application of 2,4-dinitrochlorobenzene (DNCB) is an effective therapy for condylomata acuminata caused by HPV infection. DNCB induced the complete clearance of HPV-associated warts in 13/15 patients (Georgala *et al.*, 1989). The efficacy of this treatment is attributed to the immunostimulatory role of DNCB that might activate cell-mediated

[1]*The University of Queensland Diamantina Institute, Translational Research Institute, Brisbane, Queensland, Australia*

[2]*These authors contributed equally to this work.*

[3]*Current address: QIMR Berghofer Medical Research Institute, Herston 4006, Queensland, Australia.*

Correspondence: Ian H. Frazer, The University of Queensland Diamantina Institute, Translational Research Institute, 37 Kent Street, Woolloongabba, Brisbane, Queensland 4102, Australia. E-mail: i.frazer@uq.edu.au

Abbreviations: CIN, cervical intraepithelial neoplasia; DNCB, 2,4-dinitrochlorobenzene; HPV, human papillomavirus; Nor-NOHA, N^{ω}-hydroxy-nor-L-arginine; mRNA, messenger RNA

Received 23 November 2013; revised 5 March 2014; accepted 21 March 2014; accepted article preview online 14 April 2014; published online 29 May 2014

immunity (Belij *et al.*, 2012). However, the use of DNCB for treatment has been discouraged because of its mutagenic potential (Black *et al.*, 1985). We speculated that understanding how induction of a vigorous acute inflammatory response by DNCB can break the locally immune-suppressive environment and restore the effector function of adaptive immunity might lead to more acceptable treatments for persisting HPV infection.

Arginase, which metabolizes L-arginine to *N*-ornithine and urea, has been identified as a crucial regulator of inflammation. Mammalian cells express two different isoforms, arginase-1 and arginase-2, which are encoded by two distinct genes and are different in their tissue distribution and subcellular localization (Bronte and Zanovello, 2005). Arginase can function as an immunosuppressive factor in the tumor environment (Ochoa *et al.*, 2007), in virus (Tacke *et al.*, 2012), or in parasite infection (Mou *et al.*, 2013). However, this enzyme has also been identified as an important proinflammatory factor in numerous disease models (Kenyon *et al.*, 2008; Zhang *et al.*, 2009; Stoermer *et al.*, 2012). As inflammation decides the fate of HPV infection and arginase is an important regulator of inflammation and immunity, we investigated the interaction between DNCB-induced inflammation and HPV16.E7 protein in induction of arginase in K14.E7 transgenic mice. We show here that K14.E7 transgenic mice exhibit an enhanced local inflammatory response to DNCB treatment, compared with nontransgenic mice, and that myeloid cells express increased arginase-1, which specifically promotes DNCB-induced inflammation.

RESULTS

K14.E7 mice develop a robust inflammation response to DNCB

An inflammatory response was induced in wild-type nontransgenic C57BL/6 and in E7 transgenic K14.E7 mice by applying DNCB topically to the ear skin. The mean increase in ear thickness was monitored as an indicator of inflammatory reaction (Pinto *et al.*, 2010). K14.E7 mice displayed a significantly higher degree of ear swelling than C57BL/6 mice, which peaked at day 3 in response to a single application of DNCB (Figure 1a).

T lymphocytes have been found in several skin inflammation diseases and have an important role in the production of inflammatory cytokines and in the recruitment of innate immune cells (Bromley *et al.*, 2013). They also drive the enhanced inflammatory response seen on repeated exposure to DNCB (Wang *et al.*, 2000). In addition, our previous study showed that lymphocytes are increased in number in K14.E7 skin (Choyce *et al.*, 2013). Therefore, we investigated whether the enhanced inflammatory response to first exposure to DNCB in K14.E7 skin was dependent on local lymphocyte function. K14.E7 mice deficient in lymphocytes ($Rag^{-/-} \times E7$), when exposed to DNCB, exhibited a similar level of ear swelling as K14.E7 mice, and stronger than control $Rag^{-/-}$ mice over 5 days after DNCB treatment (Figure 1a). Thus, DNCB-treated K14.E7 mice exhibit a hyperinflammatory response on first exposure to DNCB, which is independent of an adaptive immune response.

DNCB-treated K14.E7 skin displays an enhanced infiltration of myeloid cells and Th2 cytokine expression

To characterize further the inflammation in DNCB-treated K14.E7 skin, we examined the infiltration of immune cells. Histological examination suggested that the greater ear swelling in K14.E7 mice corresponded to a significant increase in the number of immune cells infiltrating the dermis (Figure 1b). As expected, the thickness of the K14.E7 epidermal layer remained unchanged following DNCB treatment (control: $42.4 \pm 3.7\,\mu m$, DNCB: $40 \pm 3.5\,\mu m$). $Rag^{-/-} \times E7$ mice develop similar ear swelling and inflammatory cell infiltration in the dermis as K14.E7 mice, whereas control $Rag^{-/-}$ mice do not (Figure 1a and b). Thus, the increased ear swelling in K14.E7 in response to DNCB mice was mainly contributed by infiltration of cells of the innate immune system in the dermis, and it was independent of lymphocytes.

Flow cytometry analysis revealed that DNCB-treated K14.E7 ears recruited significantly higher numbers of myeloid cells ($CD45.2^+CD11b^+$) than similarly treated C57BL/6 ears. We observed the same trend when we compared $Rag^{-/-} \times E7$ mice with $Rag^{-/-}$ mice (Figure 2a). In contrast, the number of non-myeloid bone marrow–derived cells ($CD45.2^+CD11b^-$) remained unchanged and was comparable in all four groups following DNCB treatment (Figure 2b). Thus, the expression of HPV16.E7 in the skin mediates the enhanced recruitment of myeloid cells, and this effect is independent of adaptive immunity.

IL-1β and IL-6 are major cytokines secreted from the local inflammation site and promote the recruitment of innate immune cells (Zohlnhofer *et al.*, 2000; Fielding *et al.*, 2008). DNCB treatment resulted in a significant increase in IL-1β messenger RNA (mRNA) expression in both C57BL/6 and K14.E7 skin (Table 1). In addition, IL-6 mRNA expression was significantly increased in DNCB-treated K14.E7 skin but not in nontransgenic skin, suggesting that IL-6 might be responsible for the enhanced recruitment of myeloid cells in K14.E7 skin.

Further, DNCB treatment of K14.E7 mice significantly induced mRNA expression of prostaglandin E2 synthase and Th2 cytokines IL-4 and IL-10. In contrast, there was no significant change in the expression of these factors in DNCB-treated C57BL/6 mice. Th1 cytokines displayed decreased (tumor necrosis factor-α) or unaltered (interferon gamma) expression after DNCB treatment (Table 1).

Together, these results suggest that after a single DNCB treatment to previously unexposed animals, K14.E7 mice mounted an enhanced inflammatory response, which is accompanied by $CD45.2^+CD11b^+$ myeloid cell infiltration and amplified Th2 cytokine expression.

Arginase-1 is specifically induced in DNCB-treated K14.E7 mice

Inflammation and myeloid cell activation can be associated with the induction of arginase (Bronte *et al.*, 2003). We speculated that arginase activity might contribute to enhanced inflammation of K14.E7 skin in response to DNCB. To test this hypothesis, we first investigated arginase activity in the skin of C57BL/6 and K14.E7 mice following DNCB treatment. Arginase activity was comparable in control K14E7 and

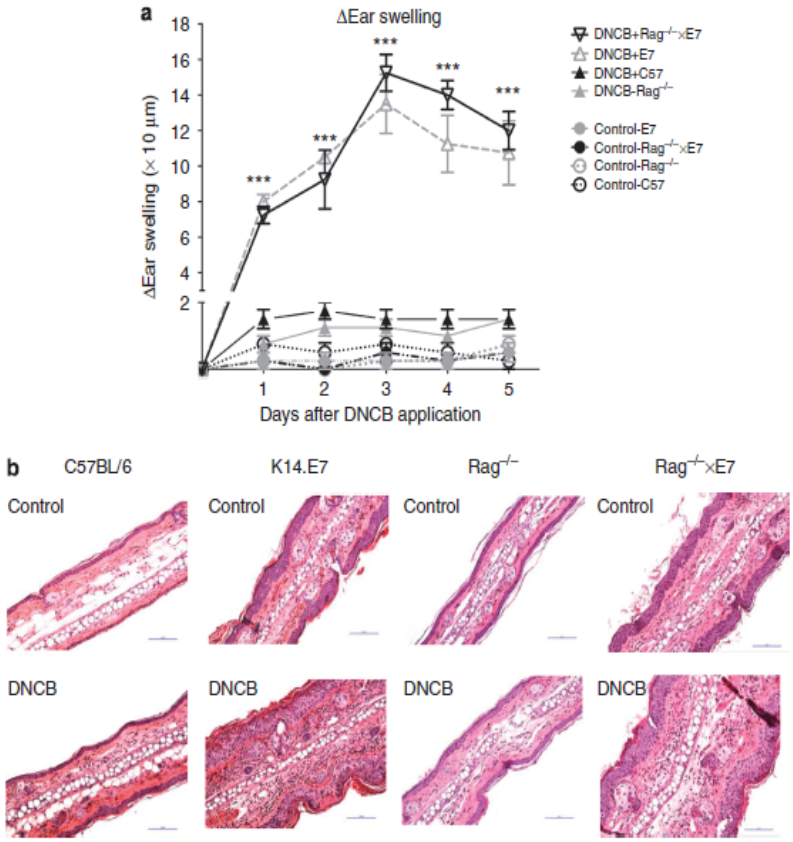

Figure 1. K14.E7 mice exhibit an enhanced inflammatory response to 2,4-dinitrochlorobenzene (DNCB). Ear swelling of C57BL/6, K14.E7, $Rag^{-/-}$, and $Rag^{-/-}$ × E7 mice in response to DNCB or vehicle over 5 consecutive days (**a**) measured by caliper. Data are means ± SEM, and are representative of two independent experiments with four mice per group. ***$P<0.001$. Histology of representative sections from C57BL/6, K14.E7, $Rag^{-/-}$ × E7, and $Rag^{-/-}$ mice (**b**) at 1 day post DNCB or vehicle application. Hematoxylin and eosin stain, original magnification ×200, scale bar = 100 μm (representative of four mice per group).

C57BL/6 ear skin (Figure 3a), as was arginase mRNA expression (Figure 3b and RNAseq data not shown). DNCB-treated K14.E7 skin, however, demonstrated a substantially higher amount of arginase activity than DNCB-treated C57BL/6 skin (Figure 3a). Arginase activity is contributed by two arginase isoforms. Increased arginase activity in K14.E7 mice corresponded to markedly increased (fourfold) arginase-1 mRNA expression. Conversely, the expression of arginase-1 mRNA remained unchanged in DNCB-treated C57BL/6 mice (Figure 3b). In contrast to arginase-1, there was no significant induction of arginase-2 mRNA in either C57BL/6 or K14.E7 skin (Figure 3c).

K14.E7 mice lacking lymphocytes ($Rag^{-/-}$ × E7) not only exhibited a similar level of ear swelling as K14.E7 mice but also of arginase-1 mRNA and arginase activity following DNCB treatment. Notably, Arginase-1 and arginase-2 mRNA expression are not increased in control $Rag^{-/-}$ mice following DNCB treatment (Figure 3b and c). Thus, the induction of arginase in K14.E7 skin is independent of adaptive immunity.

To examine whether the induction of arginase was unique to skin expressing HPV16.E7 oncoprotein as a transgene, K14.hGh and K5.OVA mice expressing human growth hormone or ovalbumin, respectively, under the control of keratin promoters were treated with DNCB. In contrast to K14.E7 mice, there was no change in the level of arginase activity of K14.hGh or K5.OVA mice following DNCB treatment (Figure 3d). Furthermore, the ear swelling of these transgenic mice (K5.OVA: 2.25 ± 0.5 μm; K14.hGh: 1.75 ± 0.5 μm, day 5) was similar to that of C57BL/6 mice (1.75 ± 0.5 μm, day 5) and markedly lower than in K14.E7 mice (19.8 ± 9.9 μm, day 5). Thus, these results suggest that increased arginase activity, likely derived from activated myeloid cells, might be a consequence of exposure of K14.E7-expressing epithelial cells to DNCB.

$CD11b^{+}Gr1^{int}F4/80^{+}Ly6C^{hi}Ly6G^{low}$ cells are the major source of arginase-1 in DNCB-treated K14.E7 mice

Arginase-1 can be induced in myeloid cells including macrophages, dendritic cells, and myeloid-derived suppressive cells

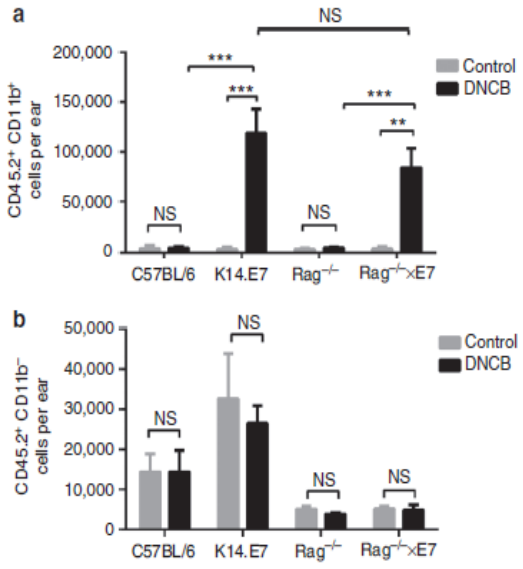

Figure 2. K14.E7 mouse skin has an enhanced myeloid cell infiltration in response to 2,4-dinitrochlorobenzene (DNCB). Absolute counts of leukocyte cells in the skin of C57BL/6 ($n=4$), K14.E7 ($n=6$), $Rag^{-/-}$ ($n=5$), and $Rag^{-/-}$ ×E7 ($n=5$) mice following DNCB treatment. Absolute numbers of $CD45.2^+CD11b^+$ myeloid cells (**a**) and $CD45.2^+CD11b^-$ cells (**b**) were determined by flow cytometry. Data are presented as means ± SEM and are representative of two independent experiments. NS, not significant. $^{**}P<0.01$, $^{***}P<0.001$.

Table 1. Expression of cytokine mRNA in response to DNCB or vehicle in K14E7 and C57 mice

	Expression relative to housekeeping gene *RPL32*				
	C57BL/6		K14.E7		
Cytokine	Vehicle	DNCB	Vehicle	DNCB	*P*
IL-1β (×10⁴)	6.8 ± 0.8	51 ± 4	221 ± 132	1490 ± 900	‡, +, *, ¶
IL-6 (×10⁴)	50 ± 8	55 ± 29	142 ± 103	5310 ± 2870	+, ¶
IL-4 (×10¹¹)	1.3 ± 2.2	3.0 ± 3.1	15.1 ± 14.2	74.5 ± 53.3	+, ¶, *
Ptge2s (×10⁴)	75 ± 74	91 ± 127	158 ± 34	480 ± 124	+, ¶
IL-10 (×10⁴)	0.4 ± 0.3	0.8 ± 0.8	4.0 ± 1.1	7.0 ± 1.6	+, *
IFNγ (×10⁴)	0.2 ± 0.2	0.11 ± 0.12	1.9 ± 1.1	1.1 ± 0.9	*
TNFα (×10⁴)	3.2 ± 2.9	2.7 ± 1.6	41.3 ± 15.2	3.4 ± 2.2	*, ¶

Abbreviations: DNCB, dinitrochlorobenzene; mRNA, messenger RNA; Ptge2s, prostaglandin E2 synthase; TNFα, tumor necrosis factor-α.
‡$P<0.05$ C57 DNCB versus vehicle.
+$P<0.05$ K14E7 DNCB versus vehicle.
*$P<0.05$ K14E7 vehicle versus C57 vehicle.
¶$P<0.05$ change in expression for DNCB-treated K14E7 versus DNCB-treated C57.

in response to a wide range of stimuli (Sindrilaru *et al.*, 2011; Chang *et al.*, 2013). These myeloid cells express surface CD11b (Hammad and Lambrecht, 2008). To confirm whether myeloid cells were the source of DNCB-induced arginase-1 in K14.E7 skin, $CD45.2^+CD11b^-$ and $CD45.2^+CD11b^+$ cells (Supplementary Figure S1 online) were isolated from DNCB-treated C57BL/6 and K14.E7 mice and analyzed for arginase activity and arginase-1 mRNA expression. $CD11b^+$ myeloid cells from DNCB-treated K14.E7 mice produced significantly higher levels of arginase activity per cell compared with $CD11b^-$ cells, and compared with $CD11b^+$ myeloid cells from DNCB-treated C57BL/6 mice (Figure 4a). In addition, arginase-1 mRNA expression was substantially detected in $CD45.2^+CD11b^+$ cells in DNCB-treated K14.E7 mice, but not in $CD11b^-$ or $CD11b^+$ cells from C57BL/6 mice (Figure 4b). Although arginase-2 mRNA was also detected in $CD45.2^+CD11b^+$ cells in K14.E7 skin, arginase-2 mRNA expression was 10 times lower than arginase-1 (Figure 4b). Thus, DNCB-activated myeloid cells ($CD45.2^+CD11b^+$) produce the increased arginase-1 observed in DNCB-treated K14.E7 skin.

CD11b is expressed on different myeloid subsets including macrophages/monocytes and granulocytes. To further define which cell subset expresses arginase-1 in DNCB-treated K14.E7 mice, we examined the expression level of arginase-1 in different populations of $CD11b^+$ cells based on the expression of macrophage marker F4/80 and granulocyte marker Gr1. We found that $F4/80^+Gr1^{int}$ cells expressed significantly higher levels of arginase-1 than other cell populations (Figure 4c). Furthermore, arginase-1 was abundantly expressed in inflammatory monocytes that express $Ly6C^{hi}Ly6G^{low}$ but not in $Ly6C^{low}Ly6G^{hi}$ granulocytes (Figure 4d).

Suppression of arginase ameliorates the ear swelling of inflamed K14.E7 skins

Arginase can be paradoxically involved in the upregulation or downregulation of inflammatory responses. *N*(omega)-hydroxy-nor-L-arginine (nor-NOHA), which is an intermediate in the L-arginine/NO pathway, is widely used as a specific, reversible inhibitor of arginase both *in vitro* and *in vivo* (Tenu *et al.*, 1999; Bratt *et al.*, 2009). To understand whether arginase promoted or suppressed the inflammatory response of K14.E7 mice to DNCB, we administered nor-NOHA or saline buffer to K14.E7 mice 1 day before DNCB treatment and daily for 4 days.

Ear tissue was harvested after 24 hours of DNCB treatment with or without arginase inhibitor, and the expression and activity of arginase were determined. Nor-NOHA, as expected, did not suppress the transcription of arginase-1 gene (Figure 5a), but reduced arginase activity in DNCB-treated K14.E7 skin (Figure 5b).

Furthermore, swelling of DNCB-treated K14.E7 skin was reduced in animals treated with arginase inhibitor (Figure 5c). Consistent with the ear swelling data, arginase inhibition decreased the number of infiltrating cells in the dermis of DNCB-treated K14.E7 mice (Figure 5d and e). These results demonstrate that arginase-1 induced by DNCB in K14.E7 transgenic ear skin, but not in C57BL/6 ear skin, itself contributes to exacerbated inflammatory response to DNCB in K14.E7 skin by recruitment of further inflammatory cells.

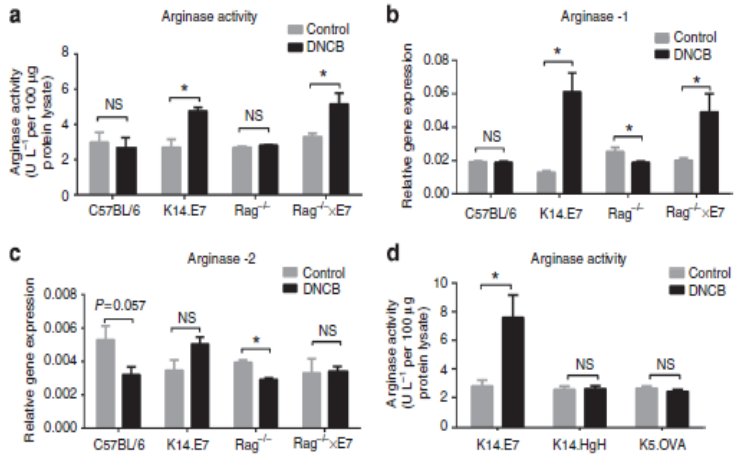

Figure 3. Arginase-1, but not arginase-2, is induced in K14.E7 mice following 2,4-dinitrochlorobenzene (DNCB) treatment, and this regulation is lymphocyte independent. Arginase activity was measured by determining the release of urea product from 100 µg of protein lysate per sample. Protein lysates were prepared from ear tissues of DNCB or vehicle-treated C57BL/6, K14.E7, $Rag^{-/-}$, $Rag^{-/-} \times$ E7, K14.HgH, and K5.OVA ear tissues. Relative gene expression levels of (**b**) arginase-1 and (**c**) arginase-2 messenger RNAs were determined by real-time PCR in the skin of C57BL/6, K14.E7, $Rag^{-/-}$, and $Rag^{-/-} \times$E7 mice 1 day following DNCB treatment, normalized against the housekeeping gene *RPL32*. Data are presented as means ± SEM and are representative of two independent experiments ($n = 4$ mice per group). NS, not significant. $^*P < 0.05$.

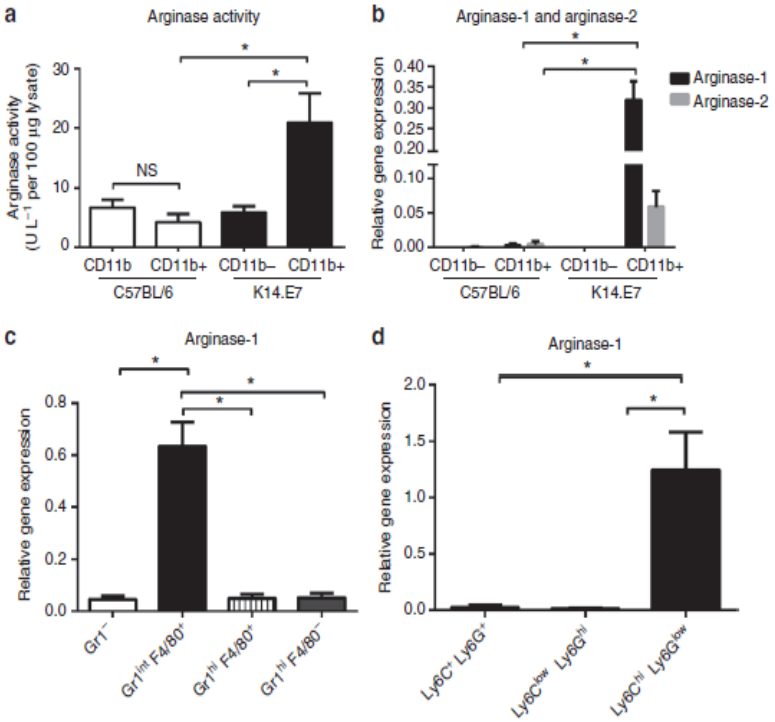

Figure 4. $CD11b^+$ $Gr1^{int}$ $F4/80^+$ $Ly6G^{low}Ly6C^{hi}$ cells produce arginase in 2,4-dinitrochlorobenzene (DNCB)-treated K14.E7 skin. Arginase activity produced by $CD45.2^+CD11b^+$ and $CD45.2^+CD11b^-$ populations from DNCB-treated C57BL/6 and K14.E7 mice (**a**) was determined as described in Materials and Methods. Arginase-1 and arginase-2 mRNA expression (**b**) levels were determined by real-time PCR. Arginase-1 messenger RNA (mRNA) expression levels in $Gr1^-F4/80^+$; $Gr1^{int}F4/80^+$; $Gr1^{hi}F4/80^+$; and $Gr1^-F4/80^-$ subsets from DNCB-treated K14.E7 mice were determined (**c**) by real-time PCR. Real-time PCR analysis of arginase-1 mRNA expression in different cell subsets (**d**) was based on the expression of Ly6C and Ly6G antigens. Data were pooled from four independent experiments. In each experiment, six C57BL/6 and two K14.E7 mice were treated with DNCB or vehicle. Means ± SEM. NS, not significant. $^*P < 0.05$.

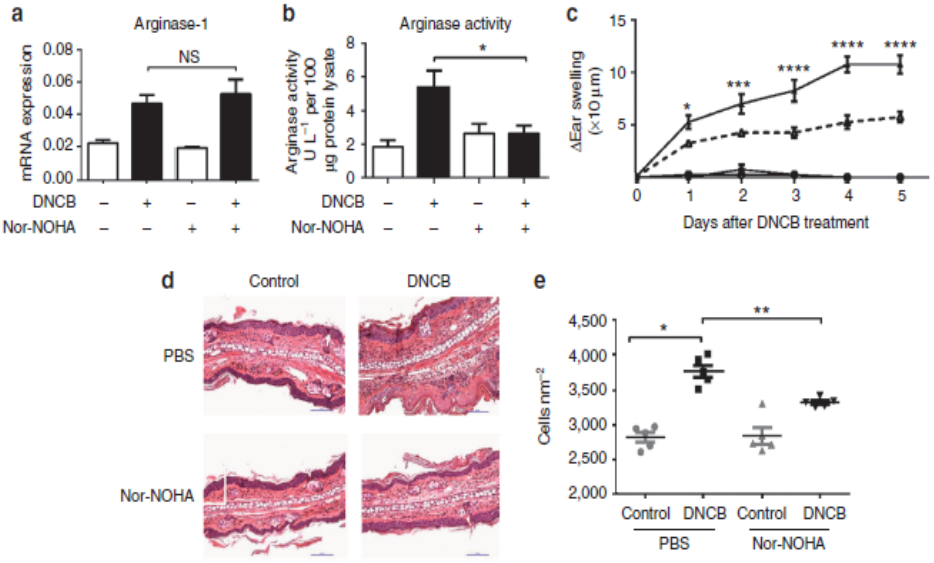

Figure 5. Inhibition of arginase ameliorates the ear swelling of dinitrochlorobenzene (DNCB)-treated K14.E7 mice. Mice were injected with 500 µg of arginase inhibitor (N^{ω}-hydroxy-nor-L-arginine (nor-NOHA)) or saline buffer 1 day before DNCB treatment and daily for 5 days. Arginase-1 messenger RNA (mRNA) expression (**a**) and arginase activity (**b**) in saline or nor-NOHA-treated K14.E7 mice after 24 hours of exposure to DNCB, determined by real-time PCR and arginase assay, respectively. Ear swelling of K14.E7 mice treated with saline (solid line) or nor-NOHA (dashed line) monitored during 5 days after DNCB treatment (**c**). Histological sections (**d**) and quantification of cell numbers infiltrating into the dermis from Nor-NOHA or saline-treated K14.E7 skins 1 day following DNCB application (**e**). Means ± SEM, data show results from two independent experiments ($n=5$). NS, not significant; PBS, phosphate-buffered saline. *$P<0.05$, **$P<0.01$, ***$P<0.001$, ****$P<0.0001$.

DISCUSSION

DNCB triggers a T-cell–independent inflammatory response through the activation of the NALP-3 inflammasome in keratinocytes (Schuepbach-Mallepell *et al.*, 2013), and it has been used to treat HPV-associated genital warts. Despite its efficacy, this chemical is potentially mutagenic and carcinogenic (Black *et al.*, 1985). Therefore, we sought to understand the influence of the expression of the major oncogenic protein of HPV16, E7, on the inflammatory mechanism induced by DNCB using mice transgenic for the E7 protein expressed in keratinocytes. Here, we show that the acute response to DNCB in previously unexposed mice is significantly higher in K14.E7 transgenic mice than in nontransgenic mice. In response to DNCB-induced inflammasome activation, keratinocytes have been shown to produce a wide range of proinflammatory cytokines including IL-6 and IL-1β (Enk and Katz, 1992; Rambukkana *et al.*, 1996), which are known to be responsible for the recruitment of polymorphonuclear cells (Zohlnhofer *et al.*, 2000; Fielding *et al.*, 2008). We indeed found an increased number of inflammatory myeloid cells in the dermis and enhanced mRNA expression levels of IL-6 and IL-1β, in DNCB-treated K14E7 transgenic mice, and show further that DNCB-induced IL-1β and IL-6 production was greatly enhanced in K14E7 skin when compared with nontransgenic skin. We could not detect significant induction of IL-6 in nontransgenic skin. Therefore, we hypothesize that this cytokine might be a regulator of inflammatory cell infiltration in K14.E7 skin and its ear swelling. Premalignant skin of HPV16.E7 transgenic mice is characterized by hyperplastic epidermis and infiltration of innate immune cells of myeloid origin. The presence of these cells in K14.E7 skin might be responsible for the marked inflammatory response to short-term DNCB treatment and inflammasome activation. Interestingly, we were not able to detect these responses to DNCB in other transgenic skin including K14.hGh and K5.OVA, suggesting that they are unique to K14.E7 mice, a consequence of the presence of HPV.E7 oncoprotein in the skin.

DNCB treatment of K14.E7 mice significantly induced mRNA expression of Th2 cytokines IL-4 and IL-10, when compared with wild-type mice. This finding is consistent with the finding in a mouse model of allergic skin inflammation, in which Th2 cytokines are responsible for the amplification and chronicity of allergic skin inflammation (Masuoka *et al.*, 2012), and with a study in which IL-4-deficient mice displayed an impaired ear swelling response to DNCB application (Traidl *et al.*, 1999). Furthermore, we show that DNCB-treated K14.E7 skin exhibited an accumulation of $CD11b^{+}$ myeloid cells, but not of non-myeloid bone marrow–derived cells, which are mainly lymphocytes. Th2 cytokines induce arginase activity in myeloid cells including macrophages and dendritic cells (Munder *et al.*, 1999; Barron *et al.*, 2013). Arginase-2 can be expressed by macrophages, and it has structural and enzyme characteristics similar to arginase-1 (Khallou-Laschet *et al.*, 2010), but it remained unchanged in K14.E7 skin. Thus, the higher level of arginase activity

in DNCB-treated K14.E7 mice is mainly contributed by arginase-1, and is promoted possibly by higher levels of Th2 cytokines and by accumulation of myeloid cells.

One predicted source of enhanced Th2 cytokine production in DNCB-treated K14E7 skin would be Th2 $CD4^+$ lymphocytes. Indeed, K14E7 skin has a large number of $CD4^+$ lymphocytes (Choyce *et al.*, 2013). However, we demonstrate here that the induction of arginase-1 and enhanced ear swelling response of K14.E7 skin are independent of lymphocytes. Th2 cytokines, which induce arginase-1 expression and hyperinflammatory response in DNCB-treated K14.E7, might therefore be derived from innate immune cells (Bradding *et al.*, 1992; Kuroda *et al.*, 2009) or epithelial cells (Balato *et al.*, 2012). We also detected the induction of prostaglandin E2 synthase in DNCB-treated K14.E7 skin. Our data are consistent with a previous study that HPV16.E7 oncoprotein induced cyclooxygenase 2 transcription and prostaglandin E2 synthase production (Subbaramaiah and Dannenberg, 2007). Furthermore, the cyclooxygenase 2–Pteg2s synthase axis has been shown to induce arginase-1 in myeloid cells in a tumor environment (Rodriguez *et al.*, 2005). However, further studies are needed to address the induction mechanism of arginase-1 in DNCB-treated K14.E7 skin.

Cells producing arginase-1 in K14.E7 skin were positive for F4/80 and Ly6C antigen, and express Gr1 at the intermediate level. This population has been defined as monocytic myeloid suppressive cells or inflammatory monocytes, which appear to adopt an immune stimulatory or suppressive function depending on the local environment (Kallberg *et al.*, 2012). Indeed, $CD11b^+Gr1^+$ cells during the early phase of polymicrobial sepsis exhibit proinflammatory phenotypes, whereas this cell population becomes immature and immune suppressive in the late phase (Brudecki *et al.*, 2012).

To understand the role of arginase in the hyperinflammation in K14.E7 skin, we used the compound nor-NOHA, which efficiently suppresses arginase-1 and arginase-2 activity in *in vitro* and *in vivo* studies (Tenu *et al.*, 1999; Bratt *et al.*, 2009). Nor-NOHA abrogates the function of arginase by modifying the structure of the enzyme, and it does not affect the transcription of the arginase gene, consistent with an unaltered arginase mRNA level (Krotova *et al.*, 2010). Arginase inhibitor treatment decreased the arginase activity and the level of leukocyte infiltrate and ear swelling in DNCB-treated K14.E7 mice. This suggests that enhanced arginase activity is critically required for the strong and sustained inflammatory response and that arginase inhibitor alleviates DNCB-induced inflammation by decreasing the recruitment of leukocytes in the skin. Arginase efficiently competes with inducible nitric oxide synthase for the common substrate L-arginine, leading to the inhibition of inducible nitric oxide synthase expression and NO production. As endothelium-derived NO is reported to suppress the expression of adhesion molecules such as vascular cell adhesion molecule-1 and intercellular adhesion molecule-1 (Peng *et al.*, 1998), limiting of NO bioavailability through arginase results in enhanced vascular inflammation (White *et al.*, 2006). In a mouse model of atherogenesis, arginase-2 but not arginase-1 enhances monocyte adhesion to endothelial cells and triggers the production of proinflammatory cytokines through mitochondrial reactive oxygen species (Ming *et al.*, 2012). Liu *et al.* (2013) show that infiltrating myeloid cells produce arginase-1, which promotes angiogenesis and further recruitment of monocytes in a laser-induced injury murine model.

Taken together, our findings demonstrate that HPV16.E7 oncoprotein–expressing skin develops a hyperinflammatory response to DNCB via an arginase-1-dependent mechanism. These findings provide insights into the proinflammatory role of arginase-1 in HPV16.E7-expressing skin in response to immunostimulation by DNCB.

MATERIALS AND METHODS

Mice

K14.HPV16E7 (K14.E7) mice were generated from inbred strain C57BL/6 (Narayan *et al.*, 2009). K14.E7, K14.HgH, and $Rag^{-/-}$, all on a C57BL/6 background, were purchased from Animal Resources Center (Perth, Australia). K5.mOVA mice on a C57BL/6 background were kindly provided by H. Azukizawa (Azukizawa *et al.*, 2003). $Rag^{-/-} \times$ E7 mice were generated by crossing male K14.E7 with female $Rag1^{-/-}$ knockout C57BL/6 mice; heterozygous K14E7 mice were crossed and then backcrossed with homozygous $Rag1^{-/-}$ mice to an F2 generation (Narayan *et al.*, 2009). All mice were maintained under specific pathogen-free conditions at Princess Alexandra Hospital Biological Research Facility. Experimental mice were sex-matched and used at 6–9 weeks of age. All animal procedures complied with guidelines approved by the University of Queensland Animal Ethics Committee.

DNCB treatment

DNCB (Sigma, Sydney, New South Wales, Australia) was dissolved in vehicle (acetone: olive oil (4:1)) immediately before use. Six- to nine-week-old mice were treated with 20 µl of 1% DNCB or vehicle on the left ear and right ear, respectively. After 24 hours, the ear tissues were collected for mRNA and protein analysis. Ear thickness was measured by using the digital caliper, and change in ear swelling was determined by calculating the mean increase in ear thickness compared with untreated ears.

Histological analysis

Ear tissues were fixed using 4% paraformaldehyde. Tissues were embedded in paraffin and 7-µm sections were prepared and stained with hematoxylin and eosin. Immune cell infiltration was evaluated by light microscopy and quantified by using the Nis-elements Br 3.2 software (Nikon Instruments, New York, NY).

Real-time PCR

RNA was isolated from homogenized tissues by using the RNaeasy Mini kit (Qiagen, Melbourne, Victoria, Australia). RNA extracts were quantified using absorption of light at 260 and 280 nm (A260/280). Details of the procedures and primers used for the quantitative real-time PCR are described in Supplementary Methods online.

Arginase activity

Arginase activity was measured by colorimetric determination of urea formed from L-arginine, as previously described (Chang *et al.*, 2000). Details of the procedures are desbribed in Supplementary Methods online.

Flow cytometry and cell sorting

Flow cytometry staining was performed as previously described (Mattarollo *et al.*, 2010). Details of flow cytometry and cell sorting are described in Supplementary Methods online.

Statistical analysis

Each data point represents the mean ± SEM and is representative of two independent experiments with at least four mice per group. Prism (Graph pad Software, La Jolla, CA) was used for graphs and statistical analysis: *$P<0.05$; **$P<0.01$; ***$P<<0.001$; ****$P<0.0001$. Multiple comparisons of ear swelling data were derived by two-way analysis of variance. For other data, statistically significantly differences between groups were analyzed by nonparametric *t*-test (Mann–Whitney test).

CONFLICT OF INTEREST

The authors state no conflict of interest.

ACKNOWLEDGMENTS

This work was supported by grants from the National Institutes of Health (5U01CA141583), National Health and Medical Research Council of Australia (569938), Australian Research Council, Cancer Council Queensland, and Australian Cancer Research Foundation. Tran is a recipient of University of Queensland fellowship for international students. We thank the staff of the Biological Research Facility at Princess Alexandra Hospital for excellent technical assistance with animal care.

SUPPLEMENTARY MATERIAL

Supplementary material is linked to the online version of the paper at http://www.nature.com/jid

REFERENCES

Azukizawa H, Kosaka H, Sano S *et al.* (2003) Induction of T-cell-mediated skin disease specific for antigen transgenically expressed in keratinocytes. *Eur J Immunol* 33:1879–88

Balato A, Lembo S, Mattii M *et al.* (2012) IL-33 is secreted by psoriatic keratinocytes and induces pro-inflammatory cytokines via keratinocyte and mast cell activation. *Exp Dermatol* 21:892–4

Barron L, Smith AM, El Kasmi KC *et al.* (2013) Role of arginase 1 from myeloid cells in th2-dominated lung inflammation. *PLoS One* 8:e61961

Belij S, Popov A, Zolotarevski L *et al.* (2012) Systemic immunomodulatory effects of topical dinitrochlorobenzene (DNCB) in rats. Activity of peripheral blood polymorphonuclear cells. *Environ Toxicol Pharmacol* 33:168–80

Bhat P, Mattarollo SR, Gosmann C *et al.* (2011) Regulation of immune responses to HPV infection and during HPV-directed immunotherapy. *Immunol Rev* 239:85–98

Black HS, Castrow FF 2nd, Gerguis J (1985) The mutagenicity of dinitrochlorobenzene. *Arch Dermatol* 121:348–9

Bradding P, Feather IH, Howarth PH *et al.* (1992) Interleukin 4 is localized to and released by human mast cells. *J Exp Med* 176:1381–6

Bratt JM, Franzi LM, Linderholm AL *et al.* (2009) Arginase enzymes in isolated airways from normal and nitric oxide synthase 2-knockout mice exposed to ovalbumin. *Toxicol Appl Pharmacol* 234:273–80

Bromley SK, Larson RP, Ziegler SF *et al.* (2013) IL-23 induces atopic dermatitis-like inflammation instead of psoriasis-like inflammation in CCR2-deficient mice. *PLoS One* 8:e58196

Bronte V, Serafini P, Mazzoni A *et al.* (2003) L-arginine metabolism in myeloid cells controls T-lymphocyte functions. *Trends Immunol* 24:302–6

Bronte V, Zanovello P (2005) Regulation of immune responses by L-arginine metabolism. *Nat Rev Immunol* 5:641–54

Brudecki L, Ferguson DA, McCall CE *et al.* (2012) Myeloid-derived suppressor cells evolve during sepsis and can enhance or attenuate the systemic inflammatory response. *Infect Immun* 80:2026–34

Chang CI, Zoghi B, Liao JC *et al.* (2000) The involvement of tyrosine kinases, cyclic AMP/protein kinase A, and p38 mitogen-activated protein kinase in IL-13-mediated arginase I induction in macrophages: its implications in IL-13-inhibited nitric oxide production. *J Immunol* 165:2134–41

Chang J, Thangamani S, Kim MH *et al.* (2013) Retinoic acid promotes the development of Arg1-expressing dendritic cells for the regulation of T-cell differentiation. *Eur J Immunol* 43:967–78

Choyce A, Yong M, Narayan S *et al.* (2013) Expression of a single, viral oncoprotein in skin epithelium is sufficient to recruit lymphocytes. *PLoS One* 8:e57798

Enk AH, Katz SI (1992) Early molecular events in the induction phase of contact sensitivity. *Proc Natl Acad Sci USA* 89:1398–402

Fielding CA, McLoughlin RM, McLeod L *et al.* (2008) IL-6 regulates neutrophil trafficking during acute inflammation via STAT3. *J Immunol* 181:2189–95

Frazer IH, Fernando GJ, Fowler N *et al.* (1998) Split tolerance to a viral antigen expressed in thymic epithelium and keratinocytes. *Eur J Immunol* 28:2791–800

Georgala S, Danopoulou I, Katsarou A (1989) Dinitrochlorobenzene treatment of condylomata acuminata. *Australas J Dermatol* 30:103–5

Hammad H, Lambrecht BN (2008) Dendritic cells and epithelial cells: linking innate and adaptive immunity in asthma. *Nat Rev Immunol* 8:193–204

Hengge UR, Benninghoff B, Ruzicka T *et al.* (2001) Topical immunomodulators–progress towards treating inflammation, infection, and cancer. *Lancet Infect Dis* 1:189–98

Kallberg E, Stenstrom M, Liberg D *et al.* (2012) CD11b+Ly6C++Ly6G− cells show distinct function in mice with chronic inflammation or tumor burden. *BMC Immunol* 13:69

Kenyon NJ, Bratt JM, Linderholm AL *et al.* (2008) Arginases I and II in lungs of ovalbumin-sensitized mice exposed to ovalbumin: sources and consequences. *Toxicol Appl Pharmacol* 230:269–75

Khallou-Laschet J, Varthaman A, Fornasa G *et al.* (2010) Macrophage plasticity in experimental atherosclerosis. *PLoS One* 5:e8852

Krotova K, Patel JM, Block ER *et al.* (2010) Endothelial arginase II responds to pharmacological inhibition by elevation in protein level. *Mol Cell Biochem* 343:211–6

Kuroda E, Ho V, Ruschmann J *et al.* (2009) SHIP represses the generation of IL-3-induced M2 macrophages by inhibiting IL-4 production from basophils. *J Immunol* 183:3652–60

Liu J, Copland DA, Horie S *et al.* (2013) Myeloid cells expressing VEGF and arginase-1 following uptake of damaged retinal pigment epithelium suggests potential mechanism that drives the onset of choroidal angiogenesis in mice. *PLoS One* 8:e72935

Masuoka M, Shiraishi H, Ohta S *et al.* (2012) Periostin promotes chronic allergic inflammation in response to Th2 cytokines. *J Clin Invest* 122:2590–600

Mattarollo SR, Rahimpour A, Choyce A *et al.* (2010) Invariant NKT cells in hyperplastic skin induce a local immune suppressive environment by IFN-gamma production. *J Immunol* 184:1242–50

Ming XF, Rajapakse AG, Yepuri G *et al.* (2012) Arginase II promotes macrophage inflammatory responses through mitochondrial reactive oxygen species, contributing to insulin resistance and atherogenesis. *J Am Heart Assoc* 1:e000992

Mittal D, Kassianos AJ, Tran LS *et al.* (2013) Indoleamine 2,3-dioxygenase activity contributes to local immune suppression in the skin expressing human papillomavirus oncoprotein e7. *J Invest Dermatol* 133:2686–94

Mou Z, Muleme HM, Liu D *et al.* (2013) Parasite-derived arginase influences secondary anti-Leishmania immunity by regulating programmed cell death-1-mediated CD4+ T cell exhaustion. *J Immunol* 190:3380–9

Munder M, Eichmann K, Moran JM *et al.* (1999) Th1/Th2-regulated expression of arginase isoforms in murine macrophages and dendritic cells. *J Immunol* 163:3771–7

Narayan S, Choyce A, Linedale R *et al.* (2009) Epithelial expression of human papillomavirus type 16 E7 protein results in peripheral CD8 T-cell suppression mediated by CD4+CD25+ T cells. *Eur J Immunol* 39:481–90

Ochoa AC, Zea AH, Hernandez C *et al.* (2007) Arginase, prostaglandins, and myeloid-derived suppressor cells in renal cell carcinoma. *Clin Cancer Res* 13:721s–6s

Peng HB, Spiecker M, Liao JK (1998) Inducible nitric oxide: an autoregulatory feedback inhibitor of vascular inflammation. *J Immunol* 161: 1970–6

Pinto NB, Morais TC, Carvalho KM *et al.* (2010) Topical anti-inflammatory potential of Physalin E from Physalis angulata on experimental dermatitis in mice. *Phytomedicine* 17:740–3

Rambukkana A, Pistoor FH, Bos JD *et al.* (1996) Effects of contact allergens on human Langerhans cells in skin organ culture: migration, modulation of cell surface molecules, and early expression of interleukin-1 beta protein. *Lab Invest* 74:422–36

Rodriguez PC, Hernandez CP, Quiceno D *et al.* (2005) Arginase I in myeloid suppressor cells is induced by COX-2 in lung carcinoma. *J Exp Med* 202:931–9

Schuepbach-Mallepell S, Philippe V, Bruggen MC *et al.* (2013) Antagonistic effect of the inflammasome on thymic stromal lymphopoietin expression in the skin. *J Allergy Clin Immunol* 132:1348–57

Sindrilaru A, Peters T, Wieschalka S *et al.* (2011) An unrestrained proinflammatory M1 macrophage population induced by iron impairs wound healing in humans and mice. *J Clin Invest* 121:985–97

Stoermer KA, Burrack A, Oko L *et al.* (2012) Genetic ablation of arginase 1 in macrophages and neutrophils enhances clearance of an arthritogenic alphavirus. *J Immunol* 189:4047–59

Subbaramaiah K, Dannenberg AJ (2007) Cyclooxygenase-2 transcription is regulated by human papillomavirus 16 E6 and E7 oncoproteins: evidence of a corepressor/coactivator exchange. *Cancer Res* 67:3976–85

Tacke RS, Lee HC, Goh C *et al.* (2012) Myeloid suppressor cells induced by hepatitis C virus suppress T-cell responses through the production of reactive oxygen species. *Hepatology* 55:343–53

Tenu JP, Lepoivre M, Moali C *et al.* (1999) Effects of the new arginase inhibitor N(omega)-hydroxy-nor-L-arginine on NO synthase activity in murine macrophages. *Nitric Oxide* 3:427–38

Traidl C, Jugert F, Krieg T *et al.* (1999) Inhibition of allergic contact dermatitis to DNCB but not to oxazolone in interleukin-4-deficient mice. *J Invest Dermatol* 112:476–82

Trimble CL, Frazer IH (2009) Development of therapeutic HPV vaccines. *Lancet Oncol* 10:975–80

Wang B, Fujisawa H, Zhuang L *et al.* (2000) CD4+ Th1 and CD8+ type 1 cytotoxic T cells both play a crucial role in the full development of contact hypersensitivity. *J Immunol* 165:6783–90

White AR, Ryoo S, Li D *et al.* (2006) Knockdown of arginase I restores NO signaling in the vasculature of old rats. *Hypertension* 47:245–51

Zhang W, Baban B, Rojas M *et al.* (2009) Arginase activity mediates retinal inflammation in endotoxin-induced uveitis. *Am J Pathol* 175:891–902

Zohlnhofer D, Brand K, Schipek K *et al.* (2000) Adhesion of monocyte very late antigen-4 to endothelial vascular cell adhesion molecule-1 induces interleukin-1beta-dependent expression of interleukin-6 in endothelial cells. *Arterioscler Thromb Vasc Biol* 20:353–9